

บทบาทของ Pd ต่อตัวเร่งปฏิกิริยา Cu/HZSM-5 สำหรับปฏิกิริยารีดักชันแบบเลือกเกิดของ

แก๊สไนตริกออกไซด์ด้วยนอร์มัลออกเทนภายใต้ภาวะรุนแรง



นาย จักรกฤษ รั้งสิมานพ

วิทยานิพนธ์นี้เป็นส่วนหนึ่งของการศึกษาตามหลักสูตรปริญญาวิศวกรรมศาสตรมหาบัณฑิต

สาขาวิชาวิศวกรรมเคมี ภาควิชาวิศวกรรมเคมี

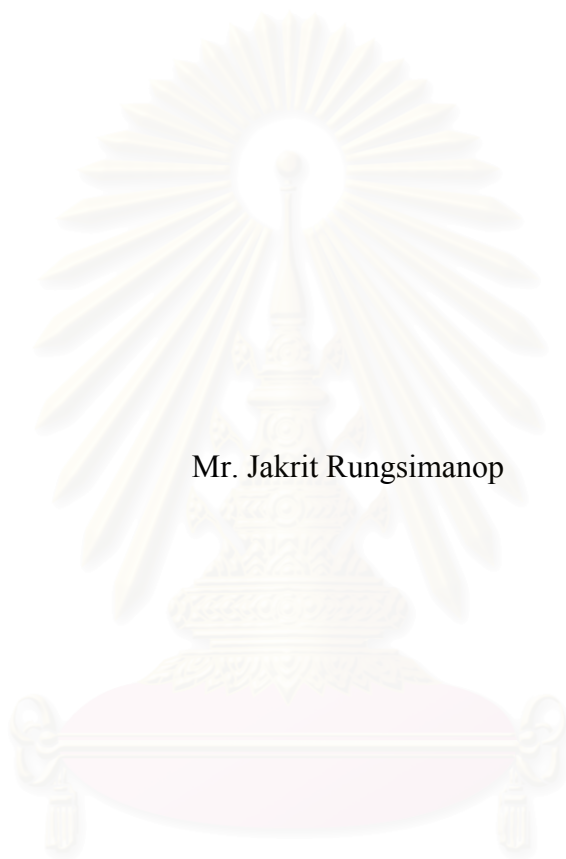
คณะวิศวกรรมศาสตร์ จุฬาลงกรณ์มหาวิทยาลัย

ปีการศึกษา 2543

ISBN 974-346-070-5

ลิขสิทธิ์ของจุฬาลงกรณ์มหาวิทยาลัย

ROLE OF Pd ON Cu/HZSM-5 FOR SELECTIVE CATALYTIC REDUCTION
OF NITRIC OXIDE USING n-OCTANE UNDER SEVERE CONDITION



Mr. Jakrit Rungsimanop

สถาบันวิทยบริการ
จุฬาลงกรณ์มหาวิทยาลัย

A Thesis Submitted in Partial Fulfillment of the Requirements
for the Degree of Master of Engineering in Chemical Engineering

Department of Chemical Engineering

Faculty of Engineering

Chulalongkorn University

Academic Year 2000

ISBN 974-346-070-5

Thesis Title Role of Pd on Cu/HZSM-5 for selective catalytic reduction of
nitric oxide using n-octane under severe condition
By Mr. Jakrit Rungsimanop
Department Chemical Engineering
Thesis advisor Professor Piyasan Prasertdam, Dr. Ing.

Accepted by the Faculty of Engineering, Chulalongkorn University in Partial
Fulfillment of the Requirements for the Master's Degree

.....Dean of Faculty of Engineering
(Professor Somsak Panyakeow, Dr.Eng.)

Thesis Committee

..... Chairman
(Professor Wiwut Tanthapaichakoon, Ph.D.)

..... Thesis Advisor
(Professor Piyasan Prasertdam, Dr. Ing.)

..... Member
(Assistant Professor Tharathon Mongkhonsi, Ph.D.)

..... Member
(Dr. Suphot Phatanasri, Dr. Eng.)

จักรกฤษ รัชสิมานพ : บทบาทของแพลเลเดียมต่อตัวเร่งปฏิกิริยา ZSM-5 ที่มีการแลกเปลี่ยนไอออนทองแดงสำหรับปฏิกิริยารีดักชันแบบเลือกเกิดของแก๊สไนตริกออกไซด์ด้วยนอร์มัลออกเทนภายใต้ภาวะรุนแรง. (ROLE OF Pd ON Cu/HZSM-5 FOR SELECTIVE CATALYTIC REDUCTION OF NITRIC OXIDE USING n-OCTANE UNDER SEVERE CONDITION) อ. ที่ปรึกษา : ศ.ดร.ปิยะสาร ประเสริฐธรรม, 93 หน้า ISBN 947-346-070-5.

งานวิจัยนี้ทำการศึกษาผลของแพลเลเดียมต่อความว่องไวและความเสถียรของตัวเร่งปฏิกิริยา ZSM-5 ที่มีการแลกเปลี่ยนไอออนทองแดง สำหรับปฏิกิริยาการกำจัดแก๊สไนตริกออกไซด์ด้วยนอร์มัลออกเทนภายใต้ภาวะรุนแรง ซึ่งตัวเร่งปฏิกิริยา ZSM-5 ที่มีการแลกเปลี่ยนไอออนทองแดงจะไม่เสถียรและเกิดการเสื่อมอย่างรวดเร็วเมื่ออยู่ในภาวะที่อุณหภูมิสูงและมีไอน้ำอยู่ด้วย ดังนั้นจึงมีการใส่โลหะแพลเลเดียมบนตัวเร่งปฏิกิริยา ZSM-5 ที่มีการแลกเปลี่ยนไอออนทองแดงเพื่อปรับปรุงความว่องไวต่อปฏิกิริยาและความเสถียรของตัวเร่งปฏิกิริยา พบว่าปริมาณ 0.3 เปอร์เซ็นต์โดยน้ำหนักของแพลเลเดียมจะช่วยปรับปรุงความเสถียรและความว่องไวของตัวเร่งปฏิกิริยา การสูญเสียความว่องไวและความเสถียรของตัวเร่งปฏิกิริยา Cu/ZSM-5 ภายใต้ภาวะรุนแรง ซึ่งเกิดจากการเคลื่อนที่ของอะลูมินาจากโครงสร้างของตัวเร่งปฏิกิริยา ซึ่งเป็นผลทำให้เกิดการเคลื่อนที่ของไอออนทองแดงชนิด 2+ ไปยังตำแหน่งที่ไม่ว่องไวต่อปฏิกิริยา

จากผลของ XRD ²⁷Al-NMR TEM และ ESR พบว่าการแลกเปลี่ยนไอออนแพลเลเดียมชนิด 2+ สามารถยับยั้งการเคลื่อนที่ของอะลูมินาจากโครงสร้าง การเคลื่อนที่ของคอปเปอร์ การรวมตัวกันเป็นกลุ่มก้อนของโลหะออกไซด์ ช่วยเสถียรไอออนทองแดงชนิด 2+ และยังคงมีความว่องไวต่อปฏิกิริยาการกำจัดแก๊สไนตริกออกไซด์ภายใต้ภาวะรุนแรง

ภาควิชา.....วิศวกรรมเคมี.....

สาขาวิชา.....วิศวกรรมเคมี.....

ปีการศึกษา 2543

ลายมือชื่อนิสิต.....

ลายมือชื่ออาจารย์ที่ปรึกษา.....

ลายมือชื่ออาจารย์ที่ปรึกษาร่วม.....

#4170248021 : MAJOR CHEMICAL ENGINEERING

KEY WORD: Cu/HZSM-5 / Pd/Cu/ZSM-5 / DeNO_x / hydrothermal pretreatment

JAKRIT RUNGSIMANOP: ROLE OF Pd ON Cu/HZSM-5 FOR SELECTIVE CATALYTIC REDUCTION OF NITRIC OXIDE USING n-OCTANE UNDER SEVERE CONDITION. THESIS ADVISOR: PROF. PIYASAN PRASERTHDAM, Dr.Eng., 93 pp. ISBN 974-346-070-5.

The effect of palladium on the activity and stability of Cu/HZSM-5 catalysts for selective catalytic reduction of NO by n-octane under severe condition has been studied. Cu/HZSM-5 catalyst is easily deactivated at high temperature, especially in steam. Loss of activity and stability on hydrothermal treatment is due to framework dealumination of the zeolite, which causes migration of Cu²⁺ to inactive site. The Pd modification of the Cu/HZSM-5 resulted in improved stability against the hydrothermal treatment with the presence of Pd loading amount approximately 0.3 wt.%

From XRD, ²⁷Al-NMR, TEM and ESR results it reveals that Pd²⁺ ion exchanged Cu/HZSM-5 inhibits the dealumination, the migration of Cu²⁺ and the agglomeration of metal oxide, stabilizes most of the active Cu²⁺ species and allows the catalyst to retain high activity and N₂ selective under severe condition.

สถาบันวิทยบริการ
จุฬาลงกรณ์มหาวิทยาลัย

ภาควิชา.....วิศวกรรมเคมี.....

สาขาวิชา.....วิศวกรรมเคมี.....

ปีการศึกษา 2543

ลายมือชื่อผู้ผลิต.....

ลายมือชื่ออาจารย์ที่ปรึกษา.....

ลายมือชื่ออาจารย์ที่ปรึกษาร่วม.....

ACKNOWLEDGEMENTS

The author would like to express his sincere gratitude to Professor Dr. Piyasan Prasertthdam, his advisor, for his precious suggestion, guidance and encouragement throughout the course of this research. He is grateful to Professor Dr. Wiwut Tanthapanichakoon, chairman of the committee, Assistant Professor Dr. Tharathon Mongkhonsi, and Dr. Suphot Phatanasri, members of the committee for their kind cooperation and encouragement, whose comments have been especially helpful.

His grateful thanks are given to Dr. Tapanee Dangsawai for her kind suggestions and good relationships.

He also would like to thank Mr. Manop Tirarattanasomphot, the technician for ESR analysis, for their valuable help.

Finally, he would like to express his highest gratitude to his parents for their continuous support and encouragement throughout this study.

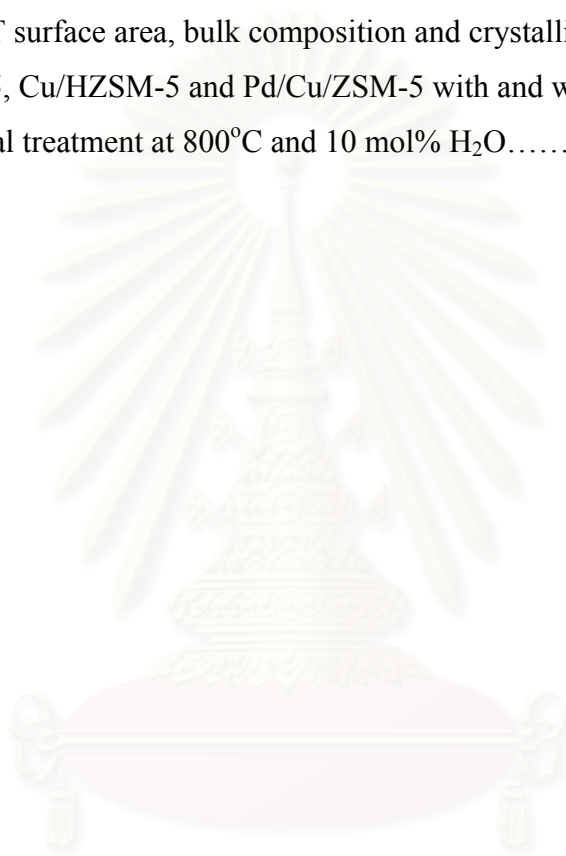
สถาบันวิทยบริการ

CONTENTS

	PAGE
ABSTRACT (IN THAI).....	iv
ABSTRACT (IN ENGLISH).....	v
ACKNOWLEDGEMENTS.....	vi
LIST OF TABLES.....	x
LIST OF FIGURES.....	xi
CHAPTER	
I INTRODUCTION.....	1
II LITERATURE REVIEWS.....	4
III THEORY	
3.1 Selective catalytic reduction (SCR) of NO in the presence of hydrocarbons	13
3.2 Reaction mechanism of NO-SCR.....	14
3.3 ZSM-5 Zeolites.....	15
3.5 Ion Exchange Reaction in Zeolite.....	17
IV EXPERIMENTAL	
4.1 Catalyst preparation.....	21
4.2 Nitric oxide removal.....	22
4.3 Characterizations of catalyst.....	25
V RESULTS AND DISCUSSION.....	29
5.1 Catalyst characterizations.....	29
5.2 Catalytic Performance.....	71
VI CONCLUSIONS AND RECOMMENDATIONS.....	80
6.1 Conclusions.....	80
6.2 Recommendations.....	81
REFERENCES.....	82
APPENDICES	89
APPENDIX A.....	90
APPENDIX B.....	92
VITA.....	93

LIST OF TABLES

TABLE	PAGE
4.1 Operating condition of gas chromatograph.....	24
5.1 Data of BET surface area, bulk composition and crystallinity of H-ZSM-5, Cu/HZSM-5 and Pd/Cu/ZSM-5 with and without hydrothermal treatment at 800°C and 10 mol% H ₂ O.....	31



สถาบันวิทยบริการ
จุฬาลงกรณ์มหาวิทยาลัย

LIST OF FIGURES

FIGURE	PAGE
3.1 Classification of molecular sieve materials indicating extensive variation in composition.....	15
3.2 Three-dimensional structure of silicalite (MFI).....	16
3.3 Diagram of the surface of a zeolite framework.....	18
3.4 Steam dealumination process in zeolite.....	20
3.5 The enhancement of the acid strength of OH groups by their interaction with dislodged aluminum species.....	20
4.1 Schematic diagram of the reaction line for NO and n-octane conversion	26
5.1 XRD patterns of HZSM-5 with hydrothermal treatment.....	32
5.2 XRD patterns of Cu/HZSM-5 with hydrothermal treatment.....	32
5.3 XRD patterns of 0.1%Pd/Cu/HZSM-5 with hydrothermal treatment.....	33
5.4 XRD patterns of 0.2%Pd/Cu/HZSM-5 with hydrothermal treatment.....	33
5.5 XRD patterns of 0.3%Pd/Cu/HZSM-5 with hydrothermal treatment.....	34
5.6 XRD patterns of 0.4%Pd/Cu/HZSM-5 with hydrothermal treatment.....	34
5.7 XRD patterns of 0.6%Pd/Cu/HZSM-5 with hydrothermal treatment.....	35
5.8 XRD patterns of 0.8%Pd/Cu/HZSM-5 with hydrothermal treatment.....	35
5.9 XRD patterns of 1.0%Pd/Cu/HZSM-5 with hydrothermal treatment.....	36

FIGURE	PAGE
5.10 ²⁷ Al MAS NMR spectra of catalysts. (a) fresh H-ZSM-5 (b) severely steamed H-ZSM-5.....	38
5.11 ²⁷ Al MAS NMR spectra of catalysts. (a) fresh Cu/HZSM-5 (b) severely steamed Cu/HZSM-5.....	39
5.12 ²⁷ Al MAS NMR spectra of catalysts. (a) fresh 0.1%Pd/CuHZSM-5 (b) severely steamed 0.1%Pd/Cu/HZSM-5.....	40
5.13 ²⁷ Al MAS NMR spectra of catalysts. (a) fresh 0.2%Pd/CuHZSM-5 (b) severely steamed 0.2%Pd/Cu/HZSM-5.....	41
5.14 ²⁷ Al MAS NMR spectra of catalysts. (a) fresh 0.3%Pd/CuHZSM-5 (b) severely steamed 0.3%Pd/Cu/HZSM-5.....	42
5.15 ²⁷ Al MAS NMR spectra of catalysts. (a) fresh 0.4%Pd/CuHZSM-5 (b) severely steamed 0.4%Pd/Cu/HZSM-5.....	43
5.16 ²⁷ Al MAS NMR spectra of catalysts. (a) fresh 0.6%Pd/CuHZSM-5 (b) severely steamed 0.6%Pd/Cu/HZSM-5.....	44
5.17 ²⁷ Al MAS NMR spectra of catalysts. (a) fresh 0.8%Pd/CuHZSM-5 (b) severely steamed 0.8%Pd/Cu/HZSM-5.....	45
5.18 ²⁷ Al MAS NMR spectra of catalysts. (a) fresh 1.0%Pd/CuHZSM-5 (b) severely steamed 1.0%Pd/Cu/HZSM-5.....	46
5.19 Scanning electron micrograph of catalysts. (a) fresh and (b) severely steamed Cu/HZSM-5.....	48
5.20 Scanning electron micrograph of catalysts. (a) fresh and (b) severely steamed 0.1%Pd/Cu/HZSM-5.....	49
5.21 Scanning electron micrograph of catalysts. (a) fresh and (b) severely steamed 0.2%Pd/Cu/HZSM-5.....	50
5.22 Scanning electron micrograph of catalysts. (a) fresh and (b) severely steamed 0.3%Pd/Cu/HZSM-5.....	51
5.23 Scanning electron micrograph of catalysts. (a) fresh and (b) severely steamed 0.4%Pd/Cu/HZSM-5.....	52
5.24 Scanning electron micrograph of catalysts. (a) fresh and (b) severely steamed 0.6%Pd/Cu/HZSM-5.....	53

FIGURE	PAGE
5.25 Scanning electron micrograph of catalysts. (a) fresh and (b) severely steamed 0.8%Pd/Cu/HZSM-5.....	54
5.26 Scanning electron micrograph of catalysts. (a) fresh and (b) severely steamed 1.0%Pd/Cu/HZSM-5.....	55
5.27 TEM image of severely steamed Cu/HZSM-5.....	57
5.28 TEM image of severely steamed 0.1%Pd/Cu/HZSM-5.....	57
5.29 TEM image of severely steamed 0.2%Pd/Cu/HZSM-5.....	58
5.30 TEM image of severely steamed 0.3%Pd/Cu/HZSM-5.....	58
5.31 TEM image of severely steamed 0.4%Pd/Cu/HZSM-5.....	59
5.32 TEM image of severely steamed 0.6%Pd/Cu/HZSM-5.....	59
5.33 TEM image of severely steamed 0.8%Pd/Cu/HZSM-5.....	60
5.34 TEM image of severely steamed 1.0%Pd/Cu/HZSM-5.....	61
5.35 ESR spectra of high spin Cu ²⁺ of Cu/HZSM-5 with and without hydrothermal treatment at 800 °C 10 mol% H ₂ O a) fresh, b) severe steamed Cu/HZSM-5.....	63
5.36 ESR spectra of high spin Cu ²⁺ of 0.1%Pd/Cu/HZSM-5 with and without hydrothermal treatment at 800 °C 10 mol% H ₂ O a) fresh, b) severe steamed 0.1%Pd/Cu/HZSM-5.....	64
5.37 ESR spectra of high spin Cu ²⁺ of 0.2%Pd/Cu/HZSM-5 with and without hydrothermal treatment at 800 °C 10 mol% H ₂ O a) fresh, b) severe steamed 0.2%Pd/Cu/HZSM-5.....	65
5.38 ESR spectra of high spin Cu ²⁺ of 0.3%Pd/Cu/HZSM-5 with and without hydrothermal treatment at 800 °C 10 mol% H ₂ O a) fresh, b) severe steamed 0.3%Pd/Cu/HZSM-5.....	66
5.39 ESR spectra of high spin Cu ²⁺ of 0.4%Pd/Cu/HZSM-5 with and without hydrothermal treatment at 800 °C 10 mol% H ₂ O a) fresh, b) severe steamed 0.4%Pd/Cu/HZSM-5.....	67
5.40 ESR spectra of high spin Cu ²⁺ of 0.6%Pd/Cu/HZSM-5 with and without hydrothermal treatment at 800 °C 10 mol% H ₂ O a) fresh, b) severe steamed 0.6%Pd/Cu/HZSM-5.....	68

FIGURE	PAGE
5.41 ESR spectra of high spin Cu^{2+} of 0.8%Pd/Cu/HZSM-5 with and without hydrothermal treatment at 800 °C 10 mol% H_2O a) fresh, b) severe steamed 0.8%Pd/Cu/HZSM-5.....	69
5.42 ESR spectra of high spin Cu^{2+} of 1.0%Pd/Cu/HZSM-5 with and without hydrothermal treatment at 800 °C 10 mol% H_2O a) fresh, b) severe steamed 1.0%Pd/Cu/HZSM-5.....	70
5.43 The effect of hydrothermal treatment on activity of NO conversion of Cu/HZSM-5.....	72
5.44 The effect of hydrothermal treatment on activity of n-octane conversion of Cu/HZSM.....	72
5.45 The effect of hydrothermal treatment on activity of NO conversion of 0.1%PdCu/HZSM-5.....	73
5.46 The effect of hydrothermal treatment on activity of n-octane conversion of 0.1%PdCu/HZSM-5.....	73
5.47 The effect of hydrothermal treatment on activity of NO conversion of 0.2%PdCu/HZSM-5.....	74
5.48 The effect of hydrothermal treatment on activity of n-octane conversion of 0.2%PdCu/HZSM-5.....	74
5.49 The effect of hydrothermal treatment on activity of NO conversion of 0.3%PdCu/HZSM-5.....	75
5.50 The effect of hydrothermal treatment on activity of n-octane conversion of 0.3%PdCu/HZSM-5.....	75
5.51 The effect of hydrothermal treatment on activity of NO conversion of 0.4%PdCu/HZSM-5.....	76
5.52 The effect of hydrothermal treatment on activity of n-octane conversion of 0.4%PdCu/HZSM-5.....	76
5.53 The effect of hydrothermal treatment on activity of NO conversion of 0.6%PdCu/HZSM-5.....	77
5.54 The effect of hydrothermal treatment on activity of n-octane conversion of 0.6%PdCu/HZSM-5.....	77

FIGURE	PAGE
5.55 The effect of hydrothermal treatment on activity of NO conversion of 0.8%PdCu/HZSM-5.....	78
5.56 The effect of hydrothermal treatment on activity of n-octane conversion of 0.8%PdCu/HZSM-5.....	78
5.57 The effect of hydrothermal treatment on activity of NO conversion of 1.0%PdCu/HZSM-5.....	79
5.58 The effect of hydrothermal treatment on activity of n-octane conversion of 1.0%PdCu/HZSM-5.....	79

CHAPTER I

INTRODUCTION

The emission of nitrogen oxide (NO_x), both from stationary and automotive sources is environmentally damaging. Among of nitrogen oxides, nitric oxide (NO) is a main composition emitted. NO can be oxidized slowly to NO_2 but rapidly in the condition of sunlight and hydrocarbon from unburned gasoline, contributing to the formation of acid rain and tropospheric ozone [1]. The three-way automotive catalyst has been highly successful in controlling exhaust emission from conventional petrol engines, which operate under stoichiometric condition. However, the exhaust from lean burn and from diesel engines contains over 5% oxygen. Under these net-oxidizing conditions, the 3-way catalyst is no longer effective.

As for NO_x which is produced in the exhaust gas from stationary facilities, a process of selective catalytic reduction (SCR) is adopted commercially [2], using mixed oxide catalysts such as vanadia-tungstine on titania support, and NH_3 is used as the reductant. Although removal of NO can be achieved even under the presence of oxygen, it has still many problems to be overcome such as disadvantages in the transportation and storage of NH_3 , the emission of unreacted NH_3 , the corrosion of equipment and the high equipment cost. Therefore, a process for the removal of NO using more convenient and safe reductants other than NH_3 is strongly demanded.

So far, significant studies on the selective catalytic reduction (SCR) of NO_x using hydrocarbons as reductant in the presence of excess oxygen were reported using zeolitic catalyst [3,4]. Copper ion exchanged H-ZSM-5 is known as an effective catalytic for NO removal even in the presence of excess oxygen when an appropriate reductant is used [5]. It is accepted that copper in the Cu (II) state is important for NO removal under lean burn condition [6]. However, it is also known that Cu/HZSM-5 zeolite is easily deactivated at high temperature, especially in steam, which may occur in practical situations [7]. It is well known that severe hydrothermal treatments induce strong dealumination of zeolite framework, leading to the collapse

of the structure [8]. On the other hand, platinum group metal catalysts have also been studied for NO conversion [9,10] and it is known that platinum group metal catalyst are highly resistant to large amount of steam [11].

As mentioned above, in this research Cu/HZSM-5 and Pd/Cu/HZSM-5 are used as catalyst for the selective catalytic reduction of NO using n-octane under severe condition. The effects of the palladium loading and the maintaining Cu²⁺ species on stability of the catalysts are discussed.

This present work is categorized into 6 chapters. This chapter contains a brief introduction. The literature review is summarized in Chapter II. The theory in this research, studies about the selective catalytic reduction of NO by hydrocarbon oxidation reaction, property of Cu/ZSM-5 catalyst and deactivation of catalysts are presented in chapter III. The experimental systems, the reaction procedures and characterization are described in chapter IV. Chapter V presents the results and discussion of the characterization. Finally, overall conclusions were generally summarized in chapter VI.

1. The Objective of This Study

To study role of palladium on Cu/HZSM-5 for selective catalytic reduction of nitric oxide using n-octane as reducing agent under severe condition.

2. The Scope of This Study

- 2.1 Prepare Cu/HZSM-5 and Pd/Cu/ZSM-5 by using ion exchange method.
- 2.2 Characterization of catalysts by following method.
 - Specific surface area by BET method.
 - Bulk composition by ICP method.
 - Structure and crystallinity of catalysts by X-ray diffraction.

- Morphology on the surface of catalysts by SEM and TEM method.
- The coordination of Al in the framework of zeolite by ^{27}Al MAS NMR.
- High spin Cu^{2+} of catalysts by ESR analysis.

2.3 Reaction test using feed gas composition of NO 1000 ppm, n-octane 1000 ppm, O_2 2%, He balance with a GHSV of $30,000 \text{ h}^{-1}$. The reaction was carried out between 200 and 600°C .

2.4 Study role of palladium on Cu/HZSM-5 for selective catalytic reduction of nitric oxide using n-octane under severe condition. Furthermore, find out the optimum content of Pd promoting high NO conversion.



สถาบันวิทยบริการ
จุฬาลงกรณ์มหาวิทยาลัย

CHAPTER II

LITERATURE REVIEWS

Much attention has been devoted to the possible application of Cu^{2+} ion exchange ZSM-5 zeolite for the selective reduction of NO with hydrocarbon in excess oxygen [12]. However, the most significant problem of Cu/ZSM-5 is deactivation during the catalytic run at high temperature, especially in the presence of water vapor.

This chapter reviews the works about catalytic activity and characterization of Cu/ZSM-5 and metal ion exchange ZSM-5 zeolite. In addition, the effects of water, hydrothermal treatment condition and catalyst preparation on the property of catalysts are demonstrated as follows:

Catalysts containing copper ions exchanged into the zeolite H-ZSM-5 are attracted considerable attention because they are very active both NO decomposition and the selective catalytic reduction (SCR) of nitrogen oxides (NO_x) in the presence of excess oxygen, so-called lean-burn condition.

Iwamoto *et al.* [13-15] and Held *et al.* [16] proposed that copper ion exchanged ZSM-5 catalyst to be active for NO removal by both direct NO decomposition and NO reduction. It is generally accepted that Cu/ZSM-5 prepared via the so-called excessive ion exchange procedure is the most active in both reactions. This preparation procedure was recommended to promote the formation of [Cu (II)-O-Cu (II)] pairs, where the oxygen is either from the zeolite framework or from structural OH group. Cu (II) is very easily reduced to Cu (I), the reduction occurs even in a nitrogen atmosphere at 673 K, and this is associated with oxygen removal. Furthermore, they showed that NO selectively reduced over Cu/ZSM-5 in the presence of O_2 by C_2H_4 , C_3H_6 , and C_3H_8 . Similar to the case of NO- NH_3 reaction [2], oxygen was found to enhance the rate of the NO-hydrocarbon reaction.

Shelef [17] studied the mechanism of nitric oxide decomposition over Cu/ZSM-5. A mechanism was proposed which was based on active sites consisting of coordinatively unsaturated cupric (Cu^{2+}) ions in a square planar configuration. These sites were deposited to chemisorb NO molecules in the gem-dinitrosyl form ($\text{Cu}^{2+} : \text{NO} + \text{NO}_g \rightarrow \text{Cu}^{2+}$), which shifted to the left at higher temperature. The pair of adsorbed NO molecules decomposed as N_2 and O_2 . This mechanism accounted for the experimental behavior in chemisorption and decomposition without invoking a cyclical oxyreduction of the surface sites.

Hamada *et al.* [18,19] reported that H-form of zeolite was active at elevated temperature for the selective catalytic reduction of NO by hydrocarbon. Moreover, other metal ion exchanged zeolite and its relative material have been investigated for NO removal. However, H-ZSM-5 was not recommended to be used in practical because of its sensitivity to hydrothermal environments typical in diesel exhausts.

Campbell and co-workers [20] investigated the effect calcination and hydrothermal treatment on the structure and properties of H-ZSM-5 zeolite with a range of aluminum content. The result of treated zeolite was undertaken with solid state NMR (^{27}Al and ^{29}Si NMR), infrared, nitrogen and water adsorption, X-ray diffraction, X-ray photoelectron spectroscopy, and scanning electron microscopy. Both calcination and hydrothermal treatment were found to cause dealumination of the zeolite lattice and formation of extralattice aluminum species of low symmetry, which remained within the pores of the zeolite. It was found that H-ZSM-5 with low aluminum content had more resistance to dealumination by either method or the degree of dealumination was greater when steam was present in the treatment.

Iwamoto *et al.* [21-23] also reported that the zeolite structure has an effect on the catalytic activity of the NO-hydrocarbon reaction. In addition to ZSM-5, copper was ion exchanged in ferrierite, mordenite and Y type zeolite. Both copper ion exchanged ZSM-5 and mordenite zeolite were the most active catalysts even at such low temperature and high space velocity ($> 10,000 \text{ h}^{-1}$) and Cu-Y is the least active

one. For NO reaction, an appropriate zeolite structure seems to depend on the nature of hydrocarbon used.

Li *et al.* [24] compared the catalytic activities of catalysts for NO decomposition. The order of activity was as follows: Cu/MFI > Ag-Co₃O₄ > La-Sr-Co (Cu)-O > Pt/Al₂O₃ > Y-Ba-Cu-O/MgO. Among metal ion exchanged MFI zeolites observed copper exchanged MFI zeolite was active for NO reduction at low light-off temperature.

Charjar *et al.* [25] studied the activity of Cu/ZSM-5 zeolite prepared by three different procedures: ion exchange, impregnation and precipitation. C₃H₈ was used as a reductant and the oxygen content was higher 0.5 vol%. The activities, measured as turnover frequencies, indicated the following order: Cu/MFI (exchanged) > Cu/MFI (impregnated) > Cu/MFI (precipitated) > CuAl₂O₃. The adsorption of carbon monoxide followed by Fourier Transform Infrared spectroscopy (FT-IR) suggested that copper presented as isolated Cu⁺ ions presented in the catalysts. The dispersion of cuprous ions was the highest for the sample prepared by the exchange process. The catalytic activity appeared related to high dispersion of isolated Cu⁺ ions in the MFI framework.

Campa *et al.* [26] compared the activities for NO decomposition between copper ion exchanged ZSM-5 and copper impregnated ZSM-5. They found that copper ion exchanged promoted activity 10 folds higher than copper impregnated one. This supported the idea that ion exchange is the best technique to prepare the catalyst. For ion exchange method, the levels of metal ion exchanged depended on the amount of aluminium ions in zeolite matrix. It was shown that the degree of exchange for the copper ion affected on the activity for NO removal.

Iwamoto *et al.* [27,28] concluded that the repeated ion exchange of ZSM-5 zeolite with Cu²⁺ solution resulted in excessive loading of copper ions above 100% exchange level and the resulting catalysts were more active for NO decomposition.

Martinez *et al.* [29] suggested that addition of 2 mol% of H₂O in the feed retarded NO conversion reversibly. Unfortunately, Cu/MFI lost its activity enormously (60%) when it was operated at high temperature and steam existence (923K, 10%H₂O). From H₂-TPR characterization not only the reduction band at 240°C (assigned to Cu²⁺ → Cu⁺) and at 350°C (assigned to Cu⁺ → Cu⁰), but also the new bands at ca. 280 and 320°C were found for deactivated Cu/MFI. The band at 320°C was suggested as Cu species interacting with extraframework Al produced during dealumination of zeolite. They suggested that the main reason for the deactivation of Cu/MFI was the mobility of Cu²⁺ in the presence of H₂O rather than MFI dealumination.

Kharas *et al.* [30] also reported that an irreversible deactivation of Cu-ZSM-5 was caused by prolonged exposure to high temperature and wet exhaust gas. The reaction operated at temperatures of 600°C - 800°C resulted in substantial deactivation. These catalytic treatments resulted in substantial losses of micropore volume. Sintering of copper species to CuO and Cu₂O was observable by XRD; sintering to CuO can be discerned from EXAFS analysis.

Abreu *et al.* [31] investigated the deactivation of CuZSM-5 catalysts under NO selective catalytic reduction (SCR) by propane in both the absence and the presence of water as a function of zeolite form, Si/Al ratio and copper content. It was verified that CuMFI deactivation is higher on H-form zeolite comparing to Na-form and decreases when the copper exchange level increases, which can be achieved either by an increasing of the zeolite Si/Al ratio or the copper content. XRD, IR and ²⁷Al NMR spectra of fresh and used catalyst indicative of high crystallinity were detected. From temperature programmed desorption of NO (NO-TPD) and H₂ TPR data indicated that the fresh and used catalyst should have a different copper distribution, which can be suggest that the deactivation of CuMFI catalysts is probably related to the migration of copper species (without formation CuO) to another location.

Kucherov *et al.* [32] concluded that the loss of catalytic activity of Cu/MFI after high temperature treatment in the presence of steam caused by the change in the local topology of the isolated Cu^{2+} sites. Steaming at 620°C or short calcination at 900°C inhibited the chemisorption on the active sites and the reducibility of these sites. These structural rearrangements happened before dealumination and agglomeration of the active metal.

Budi *et al.* [33] investigated the hydrothermal treatment effected on the performance of Cu, Co, and Mn exchanged MFI zeolite catalysts. X-ray diffraction measurements showed that all of the catalysts studied in this work remained crystalline ZSM-5; ie. the losses of activity on steaming are not caused by collapse of the zeolite lattice. From ^{27}Al NMR spectra, the dealumination of zeolite lattice occurred to a lesser extent in the following: H/ZSM-5 > Cu/MFI > Co/MFI > Mn/MFI. The Cu K-edge EXAFES showed growth of a second shell indicating Cu-Cu interactions due to the formation of microcrystalline ensemble of CuO during hydrothermal aging. Furthermore, they reported that the ESR spectra of CuZSM-5 before and after steam treatment did not show any significant change in line shape, however, the intensity of ESR copper signal of the steam treated catalyst was lower than that of the corresponding fresh CuZSM-5 catalyst, consistent with the formation of CuO species in the zeolite matrix. These results indicated that the deterioration of catalyst activity on a steam exposure was due to dealumination of zeolite framework, causing loss of cation exchange capacity and residual Bronsted acidity.

Tanabe *et al.* [34] reported that dealumination caused the deactivation of Cu/ZSM-5. Electron spin resonance (ESR) result indicated that aggregation of copper ion did not occur and copper remained as isolated ions in Cu/ZSM-5. The ESR spectra of dehydrated Cu/ZSM-5 suggested the migration of copper ions in the zeolite after the deactivation to sites where gas molecules like nitric oxide and propene cannot reach them. This migration was triggered by the dealumination of zeolite.

Matsumo *et al.* [35] and Iwamoto *et al.* [36] suggested that the deactivation of Cu/ZSM-5 was due to a change of copper ions to an inactive form. ESR results may be the direct evidence of those inactive copper species. The Cu^{2+} ions migrate to 5-membered oxygen ring sites due to the hydrothermal treatment, which causes the deactivation of the catalyst.

Petunchi and Hall [37] suggested that the aggregation of metal component on the external surface of the zeolite was due to the dealumination of the zeolite framework.

Correa *et al.* [38] investigated the decomposition of nitrous oxide in excess oxygen over Co- and Cu- exchanged MFI zeolites. They reported that Co/MFI was much more resistant than Cu/MFI in excess oxygen. The tolerance of Co/MFI catalysts to the excess oxygen was significant when Co^{2+} stabilized in the zeolite framework. Furthermore, Co/MFI was much more tolerant than Cu/MFI to wet exhaust streams containing N_2O and oxygen.

Amor and Farris [39] and Sano *et al.* [40] studied the hydrothermal stability of Co/MFI comparing with Cu/MFI, MFI as protonated form and MFI as Na form at the condition of 2% H_2O at 750°C . Using XRD characterization, MFI as Na form transformed to cristobalite form indicating the destruction of MFI structure while MFI as H form did not show any substantial loss in surface area, pore volume or $Z\text{-O}_2$ ($Z=\text{Si}$) under similar condition. Cu/MFI loss in surface area and micropore volume more severely than Co/MFI. By observing ^{29}Si and ^{27}Al NMR analysis, MFI as protonated form loss aluminium framework evidently with steaming. The dramatic increment of octahedral non-framework aluminium on Cu/MFI was shown in steam condition. As for Co/MFI, while it was less active than Cu/MFI in the presence of steam at 500°C , it demonstrated more stable performance for 18 h without any further drop of activity during stability test run.

Li et al. [41] investigated the effect of water vapor on the selective reduction of NO with CH₄ in excess oxygen over a Co/ZSM-5 catalyst. The presence of 2 mol% water significantly decreases the NO conversion at $T \leq 450^\circ\text{C}$ but has less of an effect at $T \geq 500^\circ\text{C}$. The selectivity of methane toward NO reduction was enhanced by the presence of water at low temperature and is unchanged at high temperatures. This inhibition is reversible upon eliminating water from the system. The effect of water is dependent on the level of water added, space velocity, reaction temperatures, and level of methane in the feed. The addition of water increases the empirical reaction order with respect to either CH₄ or NO from a fractional order to first order. Temperature programmed desorption studies show that the amount of NO adsorption on Co/ZSM-5 is significantly reduced if it is not fully dried, and the competitive adsorption between H₂O and NO is probably the cause of the inhibition by water addition, Co/ZSM-4 is capable of remove NO and NO and CO simultaneously in either a dry or wet feed.

Iwamoto *et al.* [42] reported that platinum group metal has high resistance for the presence of steam even the large amount of H₂O in the feed gas.

Rokosz *et al.* [43] and Kucherov *et al.* [44] studied the stability of Cu/ZSM-5 for selective catalytic reduction of NO in streams with ca. 10% H₂O which causes dealumination and activity loss. Multivalent Co²⁺, Ni²⁺, Ga²⁺, Al³⁺, La³⁺ and Ce³⁺ ions were tried as stabilizer. The addition of La was proved to be able to retard the high temperature rearrangement of Cu²⁺ site especially the active square-planar Cu²⁺ configuration. The presence of both Cu and La is less effective in the inhibition of the dealumination by steaming than that of La only.

Teraoka *et al.* [45] studied the influence of co-exchange cations on the catalytic activity of Cu/ZSM-5 for the selective catalytic reduction of NO by ethylene. The presence of Ca, Sr, Fe, Co and Ni cations was increase the activity. On the other hand, the presence of the co-exchanged cations appeared to have no effect on temperature of maximum NO reduction. Maximum NO conversion of all catalysts levels at 673 K. With the condition higher and equivalent to 673 K, At and above

this temperature, all co-exchanged systems were more active than Cu/ZSM-5, with CaCu/ZSM-5 system being the most active one.

Budi *et al.* [46] studied the effects of high hydrothermal treatment on the activity and selectivity of CuZSM-5 catalysts for the selective catalytic reduction of NO with propene. The deactivation of the catalysts was monitored using X-ray diffraction, magnetic angle spinning ^{27}Al and ^{29}Si nuclear magnetic resonance, X-ray photoelectron spectroscopy and ion scattering spectroscopy. They propose that the loss of activity and selectivity on steam treatment is due to framework dealumination of the zeolite, which causes Cu migration out of the zeolite pores to the external surface. Pre exchange of the zeolite with La^{3+} cation inhibits the dealumination, preventing Cu migration to the surface allowing the catalyst to retain high activity and N_2 selectivity after steam treatment.

Tapanee [47] investigated the effect of copper content ion exchanged on MFI type zeolite on nitric oxide conversion. It was found that the copper content on MFI catalyst affects the activities of both NO and n-octane conversions. The more copper content on MFI catalysts, the lower the temperature of maximum NO and n-octane conversions: 50%Cu/MFI (T_{max} for NO conversion is about 600°C , T_{max} for n-octane conversion is 600°C) > 100%Cu/MFI (550°C , 550°C) > 200%Cu/MFI (400°C , 400°C). Therefore, it can be concluded that the catalyst with higher copper content exhibited the higher catalytic activity. Due to the higher activity for NO conversion, 200%Cu/MFI is taken into account in the further study. For the effect of water vapor presence on NO conversion was analyzed on 200%Cu/MFI with various amount of water vapor (0-10 mol% H_2O) in the feed gas. It was shown that 200%Cu/MFI can exhibit high activities for both NO and n-octane conversions even the existence of 10% H_2O in the feed gas. This can be suggested that 200%Cu/MFI composes of a large amount of active species preserving high NO conversion. However, it can be identified that the larger amount of water vapor existed in the feed gas, the lower the activity for NO conversion of 200%Cu/MFI. Furthermore, 10% H_2O is practically presented in outlet gas of automobile and stationary sources

Tapanee *et al.* [48] reported that Pd-modification of Cu/H-ZSM-5 improved its stability for NO removal under hydrothermal conditions. The Pd/Cu/H-ZSM-5 showed higher activity for NO conversion than Cu/H-ZSM-5, although there was a decrease in the activity of the Pd/Cu/H-ZSM-5 after pretreatment. The conversion of NO to N₂ on the pretreated Pd/Cu/H-ZSM-5 was twice higher than that on the pretreated Cu/H-ZSM-5. The collapse of the ZSM-5 framework did not play a significant role in catalyst deactivation even after pretreatment at 800°C in a N₂ stream with 10 mol% H₂O. The crucial role of Pd modification is to preserve of active Cu²⁺ species for NO conversion.

From above paper review, a number of catalysts have been studied for the SCR of NO by hydrocarbon, Cu/ZSM-5 seems to be the most active and have been studied extensively. Accordingly, this study concerns the role of Pd on Cu/HZSM-5 for the SCR of NO under severe condition and show that co-exchange of palladium can also stabilize these catalysts. The stabilizing effect of Pd on Cu/HZSM-5 was also noted previously [47,48]. This study is an extension of these investigations.

สถาบันวิทยบริการ
จุฬาลงกรณ์มหาวิทยาลัย

CHAPTER III

THEORY

3.1 Selective catalytic reduction (SCR) of NO in the presence of hydrocarbons

The SCR of NO by hydrocarbons is believed to be the most promising way to eliminate nitrogen oxide. The main advantage of the corresponding reaction is the use of a gas mixture very similar to that found in exhausts. Reduction by hydrocarbons occurs readily in the range 300-500°C, and is favoured by high NO and hydrocarbon concentration.



Copper ion-exchanged zeolite was reported to be a significantly more active catalyst for the direct decomposition of NO than the preceding catalyst such as platinum on alumina and mixed oxides [13-15]. However, its catalytic activity was insufficient, particularly in the presence of oxygen, sulfur oxides or water vapor and at very low concentrations of NO. From literature review, Cu-zeolites were effective when they were applied to real lean burn engines. It was also shown that the reaction did not take place the direct decomposition of NO and reduction of NO by hydrocarbon in the exhaust gas. A number of catalysts were found to be active for this reaction [16,49].

The zeolite catalysts did not exhibit satisfactory activity and durability in the presence of water vapor. Among the carriers of Cu or other transition metals, ZSM-5 and mordenite are very efficient. The negative effects of water vapor on these catalysts are serious. There are two major effects of water [50]:

- reversible retardation due to the competitive adsorption between water and NO or hydrocarbon.
- irreversible deactivation brought about by the dealumination of zeolite and aggregation of metal ions that lead to the degradation of zeolite framework.

3.2 Reaction mechanism of NO-SCR

It is realized that NO-SCR is a very complex reaction comprising many steps. Focusing on the initial step of the NO transformation. The mechanisms are divided into three parts. [50]

(1) NO reacts directly with partially oxidized hydrocarbons (HC-O)



This mechanism is consistent with the fact that the reduction of NO starts at nearly temperature with the oxidation of the hydrocarbon.

(2) In the second mechanism, NO is oxidized to NO₂ adsorbed and then react with HC.



Hamada and coworkers proposed this mechanism for NO reduction over alumina and H-ZSM-5 catalysts [51], based principally on the higher reactivity of NO₂-HC-O₂ than NO-HC-O₂.

(3) The third mechanism is the direct decomposition of NO which forms N₂ and oxidized surface catalyst, the after the catalyst is reduced by hydrocarbon [52]. Pt catalysts possibly follow this mechanism.

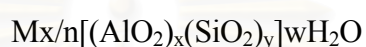


The second mechanism, the NO₂ as the intermediate, probably operates in most cases, including the case of Cu/ZSM-5. But the dominant mechanism depends on kind of the catalyst, the reductant and the reaction condition.

3.3 ZSM-5 Zeolites

Zeolites are highly crystalline, hydrated aluminosilicates structurally based on infinitely extending three dimensional network of AlO_4 and SiO_4 . These networks are linked to each other by sharing all of the oxygens [53,54].

The structural formula of a zeolite is best expressed for the crystallographic unit cell as:



where M is the cation of valence n, w is the number of water molecules and the ratio y/x has usually values of 1-5 depending upon the structure. The sum $(x+y)$ is the total number of tetrahedra in the unit cell [55]. The portion with $[(AlO_2)_x(SiO_2)_y]$ represents the framework composition.

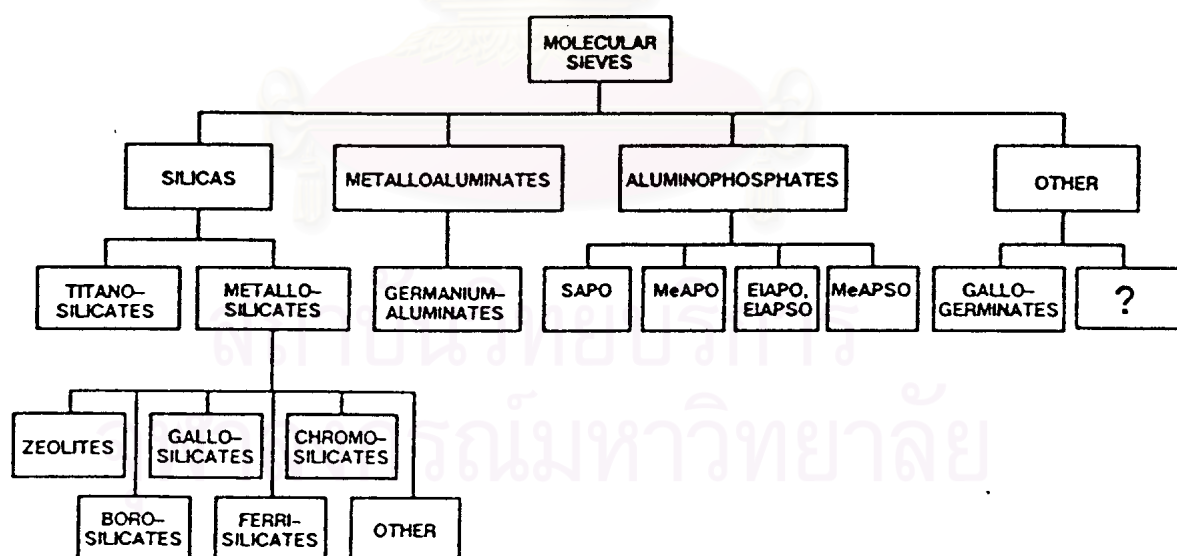


Figure 3.1 Classification of molecular sieve materials indicating extensive variation in composition [55].

ZSM-5 and silicalite have achieved commercial significance. Comparing the properties of the low and intermediate zeolites with those of the high silica zeolites and silica molecular sieves, their resulting properties allow the low and intermediate zeolites to remove water from organic and to carry out separations and catalysis on dry streams. In contrast, the hydrophobic high silica zeolites and silica molecular sieves can remove and recover organic from water streams and carry out separations and catalysis in the presence of water. Therefore, high silica zeolites showed the higher stability of the framework against the water vapor than low silica zeolites.

The ten membered rings with the ca. 0.55 nm in diameter in figure 3.2a are able to access to a network of interesting pores within the crystal. The three dimensional structure of silicalite and ZSM-5 is illustrated in figure 3.2b [56].

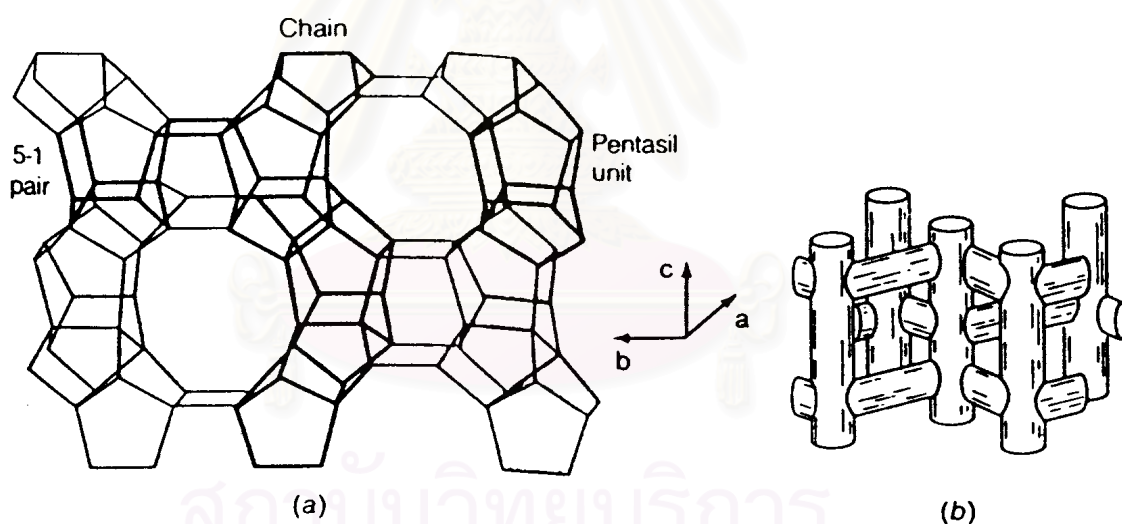


Figure 3.2 Three-dimensional structure of silicalite (MFI) [56]

- (a) Structure formed by stacking of sequences of layers
- (b) Channel network

The pore structure consists of two intersecting channel systems as shown in figure 3.2b; one straight and the other sinusoidal and perpendicular to the former. Small molecules can penetrate into this intracrystalline pore structure, where they may be catalytically converted.

Zeolites are often prepared in the sodium form, and this can be replaced by ion exchange with various other cation including ammonium, or by hydrogen ion, or even by transition metal in order to achieve high activity in specify reaction.

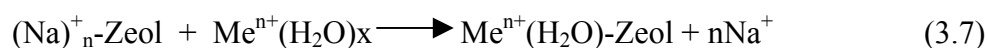
The properties of a zeolite are depended on the structure of zeolite, the size of the free channels, the location, charge and size of the cation within the framework, the presence of faults and occluded material, and the ordering of the T atoms (framework metal atoms) Therefore, structural information is important in understanding the absorptive and catalytic properties of zeolite [57].

3.4 Ion Exchange Reaction in Zeolite

The ease of cation exchange in zeolites and other minerals led to an early interest in ion exchange materials for use as water softening agents. Nowadays, it is found that ion exchanged is the simplest and most important for modifying the properties of zeolite. Zeolite are normally prepared in the Na form, and this can be change to NH₄ form and also following by heat treatment to produce H-form zeolite. The equations of this ion exchange are



The transition metal exchanged zeolite could be prepared as well. The procedure which is certainly the most suitable in introduce cation into the zeolite framework, consist of exchanging the primary cation, such as Na⁺ or NH₄⁺ and so on, with a solution of the metal salt, through conventional ion exchange technique as show in figure 3.3 and equation below: [57]



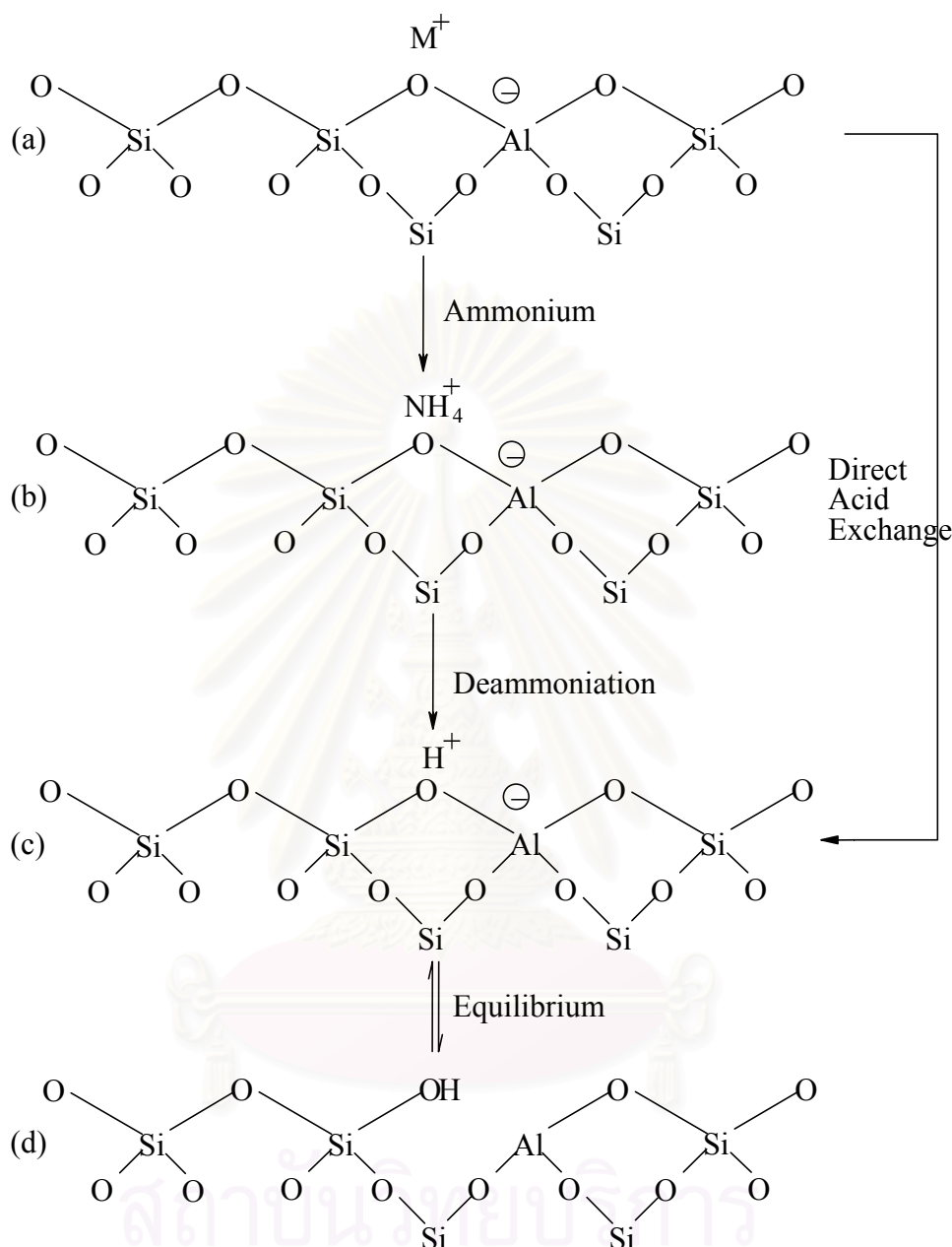


Figure 3.3 Diagram of the surface of a zeolite framework [53].

- In the as-synthesis form M⁺ is either an organic cation or an alkali metal cation.
- Ammonium in exchange produces the NH₄⁺ exchanged form.
- Thermal treatment is used to remove ammonia, producing the H⁺ acid form.
- The acid form in (c) is in equilibrium with the form shown in (d), where there is a silanol group adjacent to tricoordinate aluminum.

The cation exchange behaviour of zeolites depends upon

- 1) the nature of cation species, the cation size, both anhydrous and hydrated, and cation charge
- 2) the temperature
- 3) the concentration of the cation species in solution
- 4) the anion species associated with the cation in solution
- 5) the solvent (most exchange has been carried out in aqueous solutions, although some has been done in organic solvents)
- 6) the structural characteristic of the particular zeolite

Cation selectivities in zeolites do not follow the typical rules that are evidenced by other inorganic and organic exchangers. Zeolite structures have unique features that lead to unusual types of cation selectivity and sieving. The recent structural analyses of zeolites form basis for interpreting the variable cation exchange behaviour of zeolite.

Cation exchange in zeolite is accompanied by dramatic alteration of stability, adsorption behaviour and selectivity, catalytic activity and other important physical properties. Since many of these properties depend upon controlled cation exchange with particular cation species, detailed information on the cation exchange equilibria is important. Extensive studies of the ion exchange processes in some of the more important mineral and synthetic zeolite have been conducted [53].

Dehydroxylation is thought to occur in ZSM-5 zeolite above 500°C and calcination at 800 to 900 °C produces irreversible dehydroxylation which cause deflection in crystal structure of zeolit.

Dealumination is believed to occur during dehydroxylation which may result from the steam generation within the sample. The dealumination is indicated by an increase in the surface concentration of aluminum on the crystal. The dealumination process is expressed in figure 3.4. The extent of dealumination monotonously increases with the partial pressure of steam.

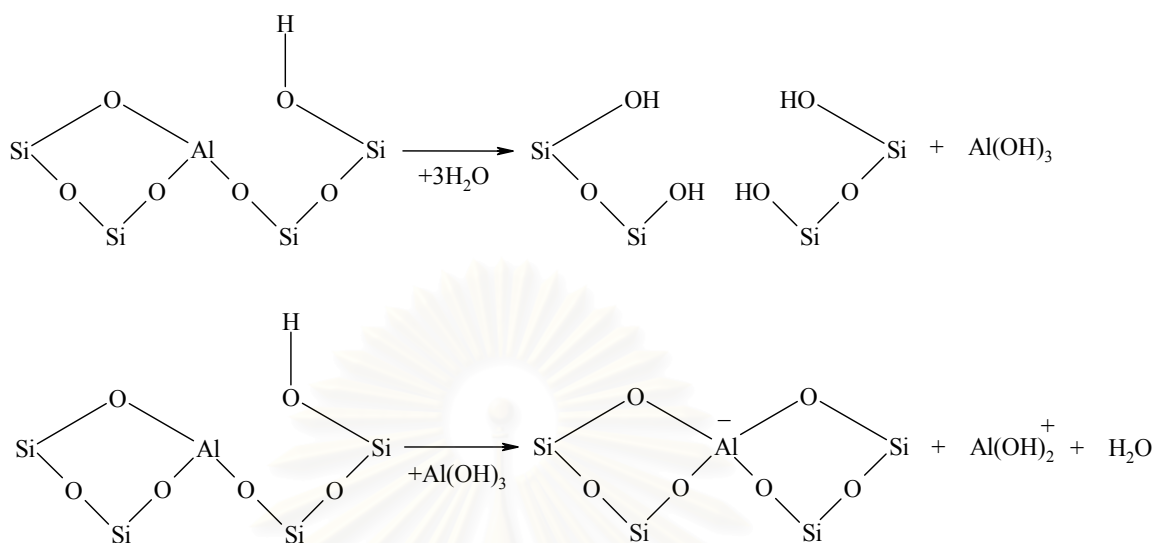


Figure 3.4 Steam dealumination process in zeolite [54].

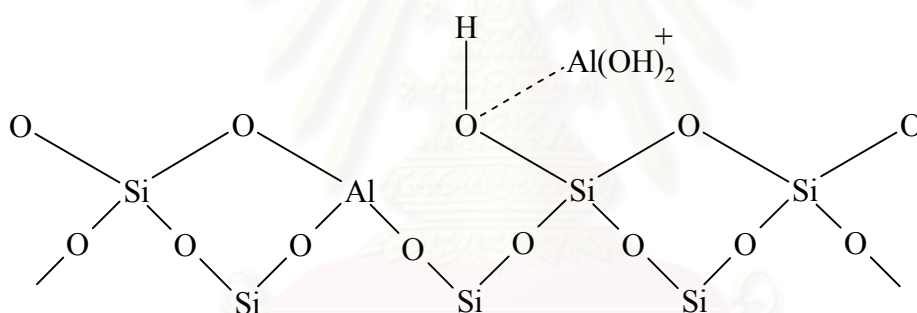


Figure 3.5 The enhancement of the acid strength of OH groups by their interaction with dislodged aluminum species [54].

The enhancement of the acid strength of OH groups is recently proposed to be pertinent to their interaction with those aluminum species sites tentatively expressed in figure 3.5. Partial dealumination might therefore yield a catalyst of higher activity while severe steaming reduces the catalytic activity.

CHAPTER IV

EXPERIMENTAL

4.1 Catalyst preparation

The starting material was Na-ZSM-5 zeolite with Si/Al molar ratio of 50, supplied by ALSI-PENTA ZEOLITE SM-55. Cu/H-ZSM-5 and Pd/Cu/H-ZSM-5 were used for NO removal reaction. The preparation of Cu/H-ZSM-5 and Pd/Cu/H-ZSM-5 were described as follows:

4.1.1 Ammonium ion-exchange

The hydrogen form of ZSM-5 was obtained by ion exchange Na^+ with NH_4^+ in an aqueous solution of 1M NH_4NO_3 at 80°C for 1 h, 50 ml per gram of catalyst and heated on a magnetic stirrer. The mixture was then cooled down to room temperature and repeatedly ion-exchanged twice. The ion-exchanged crystal was washed twice with deionized water using centrifuge separator and dried at $110\text{-}120^\circ\text{C}$ for at least 3 h in an oven. After ammonium ion-exchange, the dried catalyst obtained was NH_4 form of ZSM-5. The $\text{NH}_4/\text{ZSM-5}$ catalyst was calcined up to 540°C for 3.5 h in order to remove NH_3 and nitrocompound species. Therefore, NH_4 form zeolite was transformed into the protonated form designated as H-ZSM-5.

4.1.2 Metal ion exchange

Pd/H-ZSM-5 catalysts were prepared by the ion-exchange method as follows [48]: Approximately 5 g of $\text{NH}_4\text{-ZSM-5}$ was ion-exchanged in an aqueous solution of $[\text{Pd}(\text{NH}_4)_4]\text{Cl}_2\cdot\text{H}_2\text{O}$ as the Pd source. The ion exchange was performed for 24 h at 90°C under the continuous stirring by a magnetic stirrer. After the ion exchange process, the preparation was thoroughly washed with deionized water for 3-5 times to get rid of some ions. The content of palladium was varied in the range 0.1-1 wt.% Pd. The metal ion-exchanged H-ZSM-5 is designated as Me/ZSM-5.

In case of Cu/H-ZSM-5 catalysts were then ion exchanged twice in an aqueous solution of $\text{Cu}(\text{CH}_3\text{COO})_2 \cdot \text{H}_2\text{O}$ at 80°C for 24 h. The mixture was cooled down to room temperature and repeatedly ion-exchanged twice. Afterward, followed by washing with deionized water. The ion exchange level of Cu was ca. 200% on assumption of the exchange of one Al ion for one Cu ion. The Cu loading was controlled by the number of ion exchange repetition. The excessive loading of copper ions lead to the presence not only of Cu^{2+} but also from the presence of Cu^+ in the ZSM-5 zeolite has already been clarified by electron spin resonance (ESR), phosphorescence, and carbon monoxide adsorption techniques [34].

As for Pd/Cu/H-ZSM-5, successive ion exchange of $\text{NH}_4\text{-ZSM-5}$ with palladium first and then copper was followed adopting the same method as mentioned above. The catalysts were dried in an oven at 110°C overnight and then calcined at 540°C for 3.5 h in air to convert it into the protonated form. The catalyst in powder form was tableted using a tablet machine. It was crushed and sieved into 8-16 mesh provide to the reaction.

4.2 Nitric Oxide Removal

4.2.1 Chemical and Reagents

Nitric oxide (1% by vol.) in helium, Oxygen (10% by vol.) in helium, Helium of UHP grade (99.999%) provided by Thai Industrial Gases Limited and n-octane (99.99%), analytical grade supplied by Carlo Erba were used in these experiment.

4.2.2 Instrument and Apparatus

A flow diagram of the steady state nitric oxide reduction system is shown in Figure 4.1. The system consists of a reactor, an automation temperature controller, an electrical furnace, a gas control system and a saturator. The instruments used in this system is listed and explained below:

1. Reactor: The NO reduction reactor is a conventional microreactor made from a quartz tube with 6 mm inside diameter. The reaction was carried out under ordinary gas flow and atmospheric pressure. The effluent gas was sampled and analyzed by on-line gas chromatography.

2. Automatic Temperature controller: This consists of a magnetic switch connected to a variable transformer and a RKC temperature controller series REX-C900 with to a thermocouple attached to the catalyst bed in reactor. A dial setting establishes a set point at any temperature within the range between 0 °C to 999 °C.

3. Electrical furnace: This supplied the required heating to the reactor for the NO reduction reaction. The reactor can be operated from room temperature up to 600°C at a maximum voltage of 220 volts.

4. Gas control system: Nitric oxide, oxygen and helium cylinder; each cylinder equipped with a pressure regulator (0-120 psig), a set of needle valves was used to adjust the flow rate of gases. A sampling valve was used to take sample of effluent gas into a gas chromatograph analyzer.

5. Saturator: The contain for liquid phase material that was used in this study for water vaporization and steam passing by hot flue gas to the microreactor.

6. Gas Chromatography: The apparatus consist of thermal conductivity detector equipped gas chromatographs, SHIMADZU GC-8ATP and SHIMADZU GC-8AIT. Operating condition used in this study are given in table 4.1

Table 4.1 Operating condition of gas chromatograph

Gas Chromatograph	SHIMADZU GC-8ATP	SHIMADZU GC-8AIT
Detector	TCD	TCD
Packed column	MS-5A	PORAPAK-Q
Carrier gas	He (UHP)	He (UHP)
Flow rate of carrier gas	40 ml/min	80 ml/min
Column temperature	70 °C	90 °C
Detector temperature	100 °C	100 °C
Injector temperature	100 °C	100 °C
Analyzed gas	O ₂ , N ₂ , CO	CO ₂

4.2.3 Hydrothermal treatment

In order to investigate the stability of the catalyst under severe condition, the catalysts were packed in quartz fixed-bed reactor and heated to the desired temperature in flowing helium. The standard hydrothermal procedure was set with 10 mol% H₂O and the temperature was controlled at 800°C for 12-24 h [44,46,48]. The reactor was heated from ambient temperature to 600°C with the heating rate of 9.6 °C/min and then it was heated up to 800°C with the heating rate of approximately 1.67°C/min. Water vapor was admitted by passing helium through a saturator heated in water bath controller at 60°C. The stream line was heated to prevent water condensation.

4.2.4 Reaction Procedure

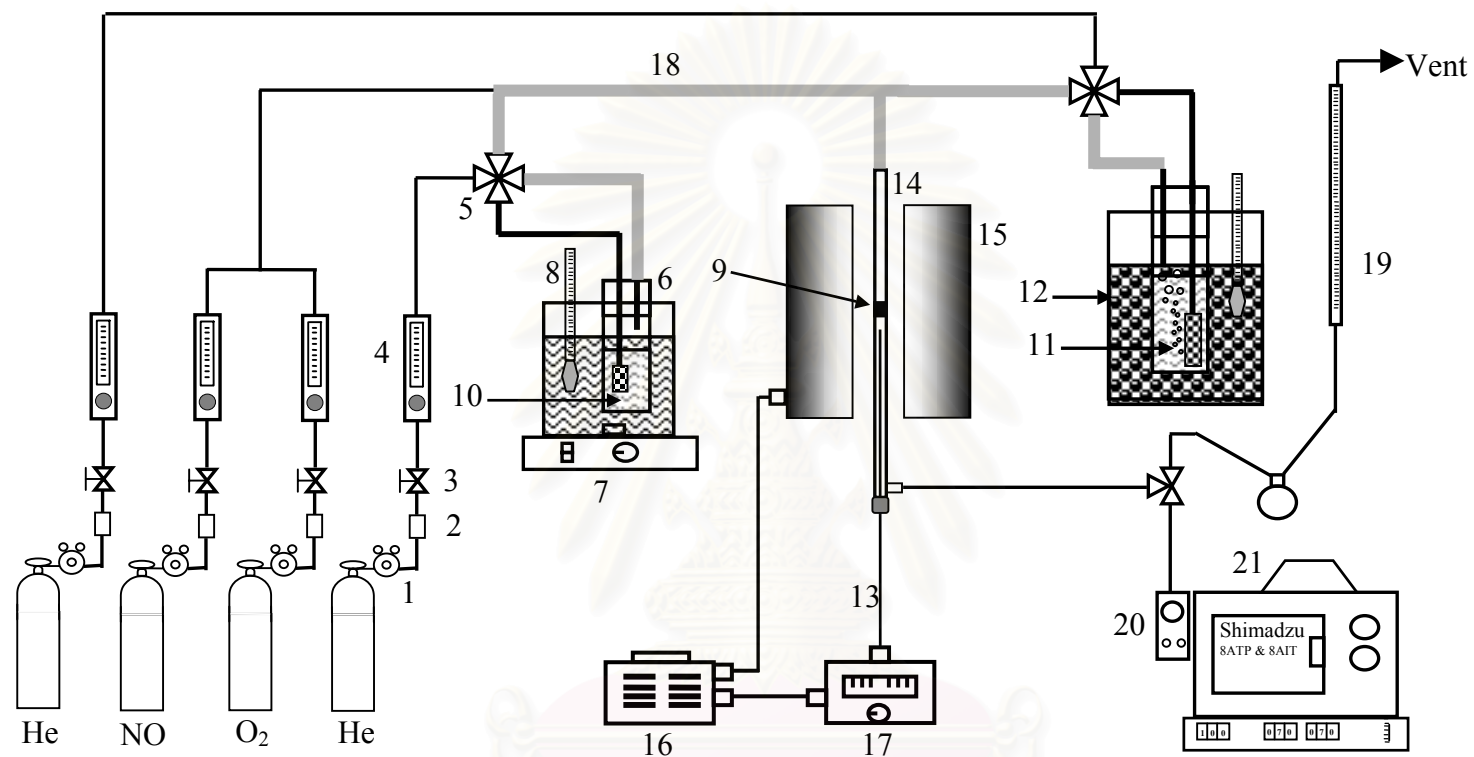
The catalytic reaction was carried out using an ordinary flow microreactor under atmospheric pressure. To avoid pressure drop during the reaction test, the catalyst as powder form was tabletted, crushed, and sieved into 8 - 16 mesh prior to use.

A 0.25 g catalyst was packed into the quartz tube reactor of 6 mm inner diameter. In order to investigate the activity for NO removal, catalyst was heated up to 600°C under He flow at a constant heating rate of 10°C/min and maintained at this temperature for 30 min. After that, a feed gas which composed 1,000 ppm NO, 1,000 ppm, n-octane, 2 mol% O₂, 10 mol% H₂O balanced with He was allowed to flow with a GHSV of 30,000 h⁻¹. Water vapor was admitted by passing He through a saturator containing water that was heated using water bath at 60°C. The reactant stream line was heated at 100°C to avoid water condensation. Every 30 min after feed gas introducing to ensure the steady state of catalytic activity, the reactants and products were analyzed by gas chromatographs (SHIMADZU GC-8ATP, and SHIMADZU GC-8AIT MS-5A and porapak Q respectively) equipped with integrators. The reaction test was undertaken every 50°C diminishing from 600°C to 200°C followed the same procedure as mentioned above. The catalytic activity of nitric oxide reduction and n-octane combustion were investigated as the amount of N₂ and carbon oxides (CO_x; CO₂+CO) produced, respectively. Figure 4.1 illustrated the reaction scheme for NO and n-octane conversion.

4.3 Characterization of Catalyst

4.3.1 X-ray diffraction (XRD) analysis

The crystallinity and structure of the catalyst can be analyzed using X-ray diffraction analysis. The XRD patterns of the catalysts were performed by E-ray diffraction spectroscopy D5000, SIEMENS using CuK α radiation with Ni filter in the 2 θ range of 4 to 60°



- | | | | |
|----------------------------|------------------|-----------------------|----------------------------------|
| 1. Pressure Regulator | 2. Gas Filter | 3. On - Off Valve | 4. Flow meter |
| 5. 4 - way Valve | 6. Saturator | 7. Magnetic Stirrer | 8. Thermometer |
| 9. Catalyst Bed | 10. Water | 11. n-Octane | 12. Ice |
| 13. Thermocouple | 14. Reactor | 15. Furnace | 16. Variable Voltage Transformer |
| 17. Temperature Controller | 18. Heating Tape | 19. Bubble Flow Meter | 20. Sampling Valve |
| 21. Gas Chromatography | | | |

Figure 4.1 Schematic diagram of the reaction line for NO and n-octane conversion analyzing by gas chromatograph consisting of molecular sieve-5A and porapak Q columns

4.3.2 BET surface area

BET method was applied to measure the specific surface area of catalyst. Macromeritics model ASAP 2000 using liquid nitrogen as a probe molecule was operated in this study. This unit is located at Analysis Centre of Department of Chemical Engineering, Faculty of Engineering, Chulalongkorn University. The operating condition are listed as follows:

Sample weight:	0.3 g
Degas temperature:	150°C
Vacuum pressure:	< 10 μ Hg
Pressure table :	5 points

4.3.3 Inductively Coupled Plasma analysis (ICP)

The bulk metal composition of catalysts were analyzed by Inductively Coupled Plasma analysis, JOBIN YVON model JY 2000S was applied in this study. The unit is located at Thailand Institute of Science and Technology Research.

4.3.4 Scanning electron micrograph (SEM) analysis

The surface morphology of the catalyst was studied by using Scanning Electron Microscope model JEOL JSM-35 CF (SEM) at the Scientific and Technology Research Equipment Centre, Chulalongkorn University (STREC).

4.3.5 Transmission Electron Microscopy (TEM) technique

TEM micrographs were obtained by direct observation of the fresh and steamed sample by a transmission electron microscopy model JEOL JEM-200CX with an acceleration energy of 100 kV at the Scientific and Technology Research Equipment Centre, Chulalongkorn University (STREC).

4.3.6 ^{27}Al magnetic angle spinning nuclear magnetic resonance (^{27}Al MAS NMR)

Quantitative analysis of alumina tetrahedral in zeolites was conducted by Al-Nuclear magnetic Resonance (^{27}Al – NMR). The ^{27}Al MAS-NMR spectra were obtained using a BRUKER DPX-300 spectroscopy operating at 78.2 MHz., at National Metal and Materials Technology Centre (MTEC) Rammer VI Road, Bangkok. The signal of alumina tetrahedral could be detected at around 50 ppm.

4.3.7 Electron spinning resonance (ESR) analysis

Electron spinning resonance (ESR) analysis was chosen to study the presence or absence of the specie component which has unpaired electron. In this study it is worth to investigate high spin Cu^{2+} on the catalyst using X-band JEOL mode JES-RE 2X spectrometer equipped with a JEOL microwave power 0.1 mW at the Scientific and Technology Research Equipment Centre, Chulalongkorn University (STREC). The sample was tested in liquid nitrogen temperature. Before ESR analysis, the sample was calcined at 500°C for 2 h to remove adsorbed species.

CHAPTER V

RESULTS AND DISCUSSION

This chapter, is separated in to two parts, which are the characterization of prepared catalysts and the activity of catalysts for NO removal.

5.1 Catalyst characterizations

5.1.1 Physical Properties

Table 5.1 shows the data expressing bulk composition, specific surface area and crystallinities of catalysts analyzed by Inductively Coupled Plasma analysis, BET method and X-ray diffraction method, respectively.

In this study, crysallinity and crystal structure of the catalyst are analyzed by X-ray diffraction technique. Crystallinity, as determined by XRD profiles, is calculated using the intensity of diffraction line at $23.3^\circ 2\theta$, which is compared with that of H-ZSM-5 as a reference. X-ray diffraction lines of H-ZSM-5, Cu/HZSM-5 and Pd/Cu/HZSM-5 with and without hydrothermal treatment are depicted in figures 5.1 to 5.9.

From table 5.1, it can be shown that the content of metal loaded in these catalysts did not disappeared with hydrothermal treatment indicated by the similar Cu/Al and Pd/Al ratios of both with and without hydrothermal treatment. This indicated that there is no significant loss of metal species such as evaporation of metal (CuO , CuOH , Cu^0 , Cu^{2+} , PdO , Pd^0 and Pd^{2+}) due to the hydrothemal treatment.

H-ZSM-5 and Cu/HZSM-5 considerably lost their crystallinity after pretreatment due to the structure collapse. Such tendency of lost in crystallinity and BET surface area is reduced with the presence of Pd and no significant lost of crystallinity was observed on Pd/Cu/HZSM-5 catalysts with amount of Pd up to

0.2 wt. % or more. This suggests the stabilization effect of Pd on ZSM-5 framework structure. It should be noted that some loss of structure occurred after pretreatment particularly the catalyst without Pd.

Cilambelli et al. noticed that CuO formed after passing a feed stream over an over-exchanged Cu/ZSM-5 could be observed by XRD [58]. Descorme et al. reported that the formation of agglomerated palladium particles (PdO) was observed by XRD on Pd ion exchanged zeolite after steam treatment at 800°C [59]. However, CuO and PdO are not detected in this study.



สถาบันวิทยบริการ
จุฬาลงกรณ์มหาวิทยาลัย

Table 5.1 Data of BET surface area , bulk composition and crystallinity of H-ZSM-5, Cu/HZSM-5 and Pd/Cu/ZSM-5 with and without hydrothermal treatment at 800°C and 10 mol% H₂O

Catalyst	BET surface area (m ² /g catalyst)		Me/Al atomic ratio				Crystallinity (%)	
			Cu/Al		Pd/Al			
	fresh	severely steamed	fresh	severely steamed	fresh	severely steamed	fresh	severely steamed
H-ZSM-5	350	295	-	-	-	-	100	48
Cu/HZSM-5	326	286	0.911	0.913	-	-	100	85
0.1% Pd/Cu/HZSM-5	310	275	0.89	0.892	0.012	0.012	99	87
0.2% Pd/Cu/HZSM-5	310	289	0.901	0.892	0.023	0.022	99	97
0.3% Pd/Cu/HZSM-5	302	290	0.865	0.863	0.035	0.034	99	98
0.4% Pd/Cu/HZSM-5	300	289	0.864	0.86	0.042	0.048	98	98
0.6% Pd/Cu/HZSM-5	298	280	0.849	0.85	0.072	0.074	97	98
0.8% Pd/Cu/HZSM-5	298	288	0.827	0.824	0.088	0.089	97	97
1.0% Pd/Cu/HZSM-5	298	286	0.821	0.821	0.112	0.11	98	97

^a Intensity are reference to diffraction line at 23.3° 2θ

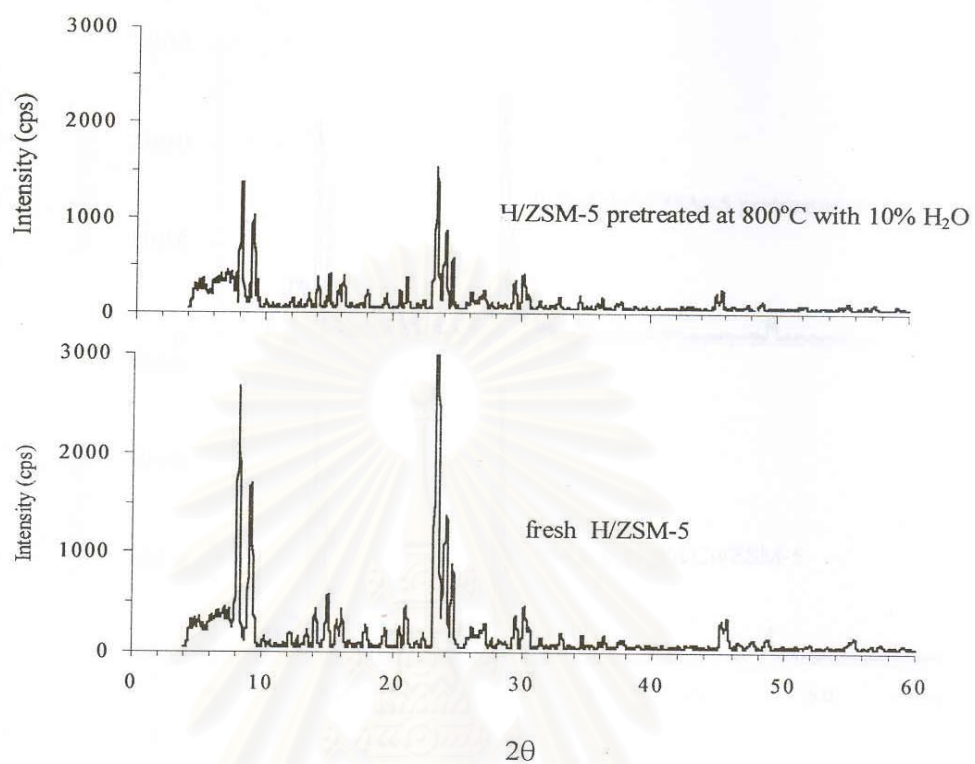


Figure 5.1 XRD patterns of HZSM-5 with hydrothermal treatment

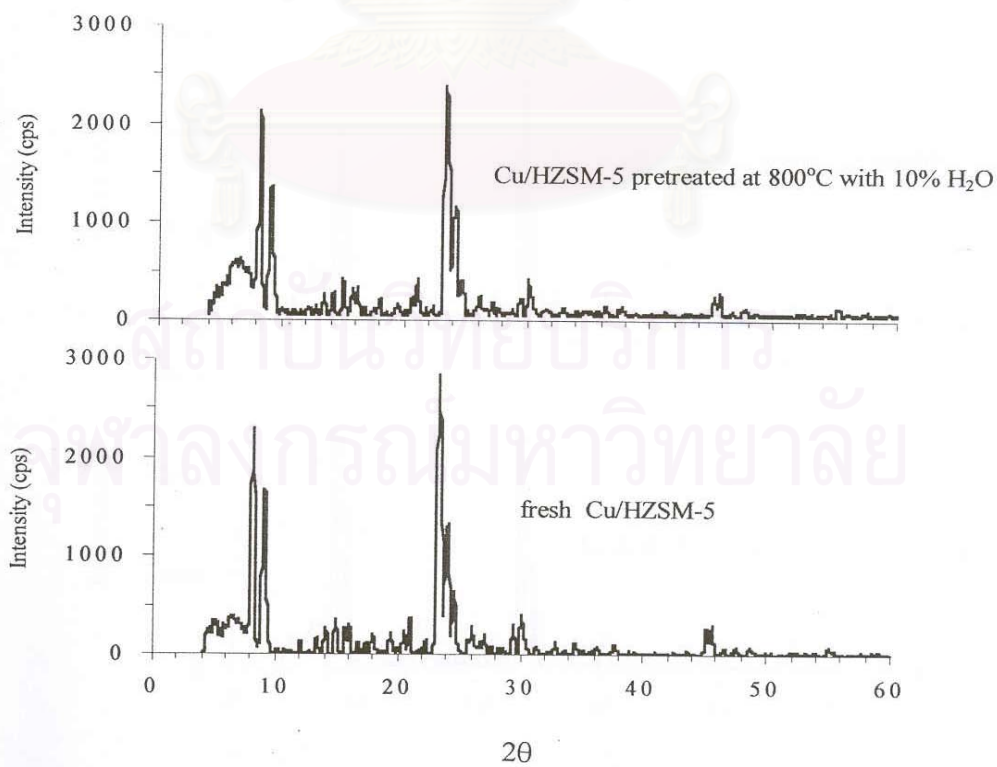


Figure 5.2 XRD patterns of 200%Cu/HZSM-5 with hydrothermal treatment

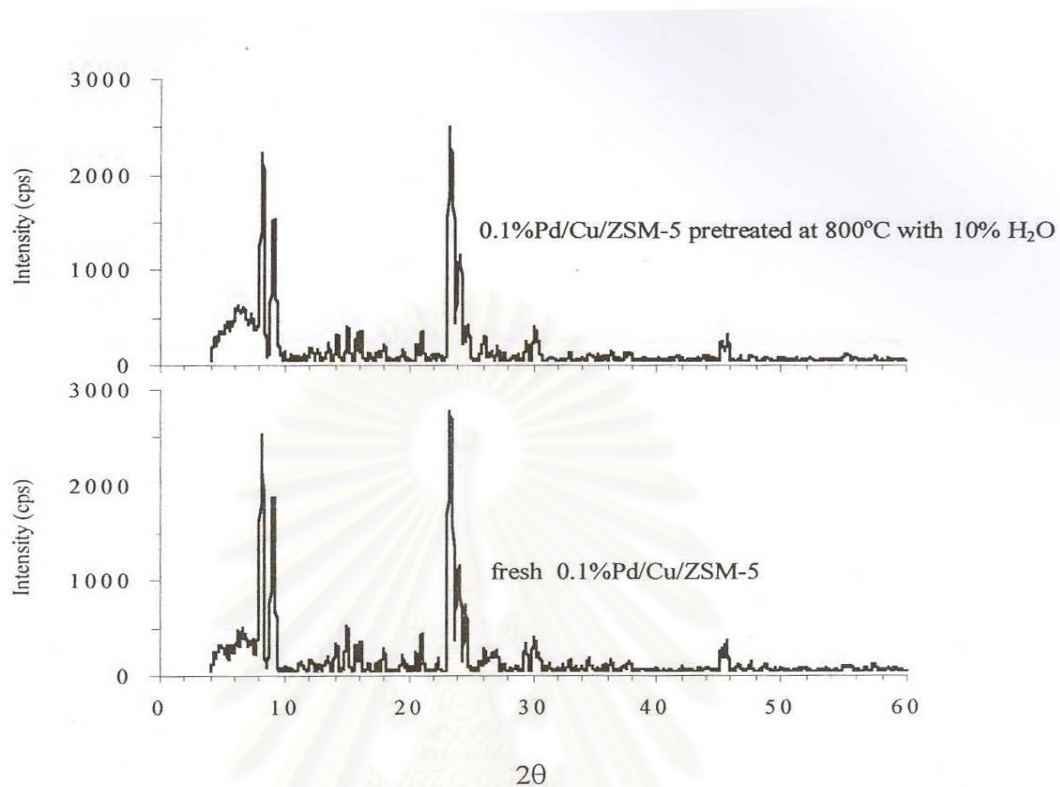


Figure 5.3 XRD patterns of 0.1%Pd/Cu/HZSM-5 with hydrothermal treatment

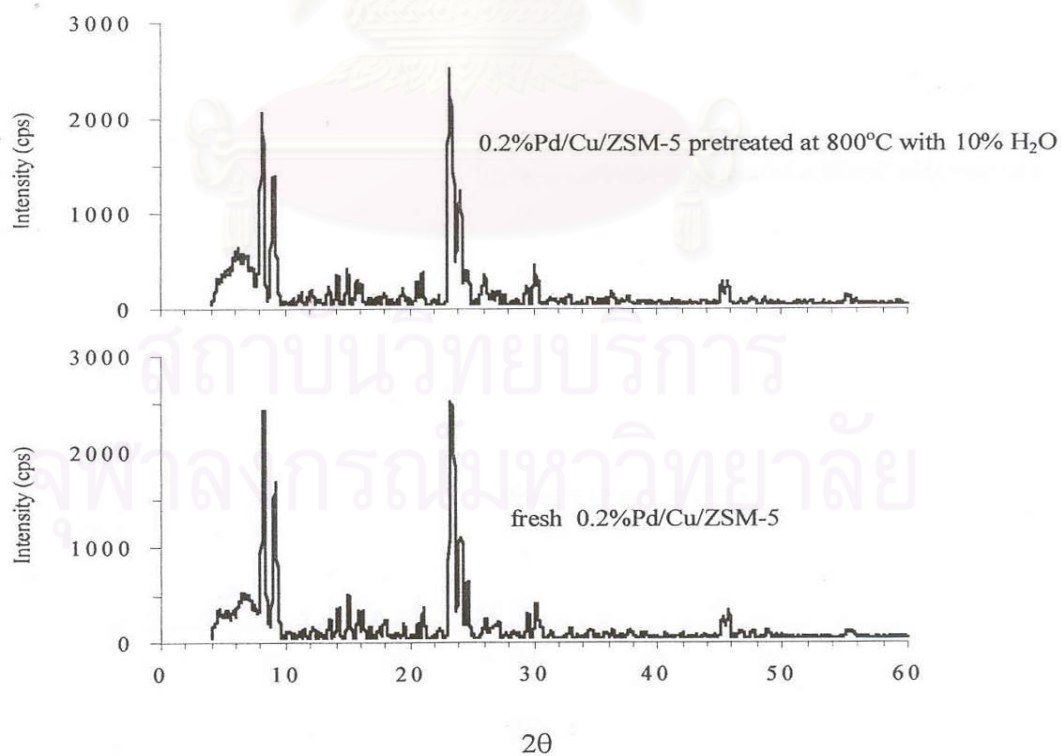


Figure 5.4 XRD patterns of 0.2%Pd/Cu/HZSM-5 with hydrothermal treatment

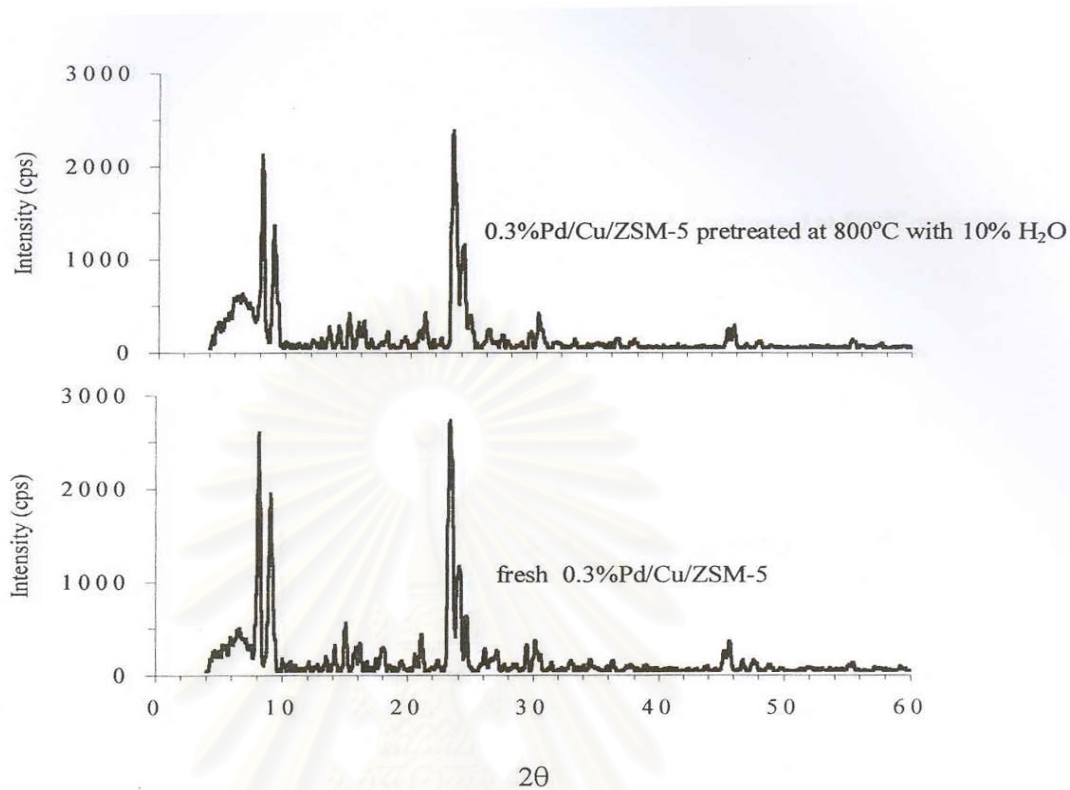


Figure 5.5 XRD patterns of 0.3%Pd/Cu/HZSM-5 with hydrothermal treatment

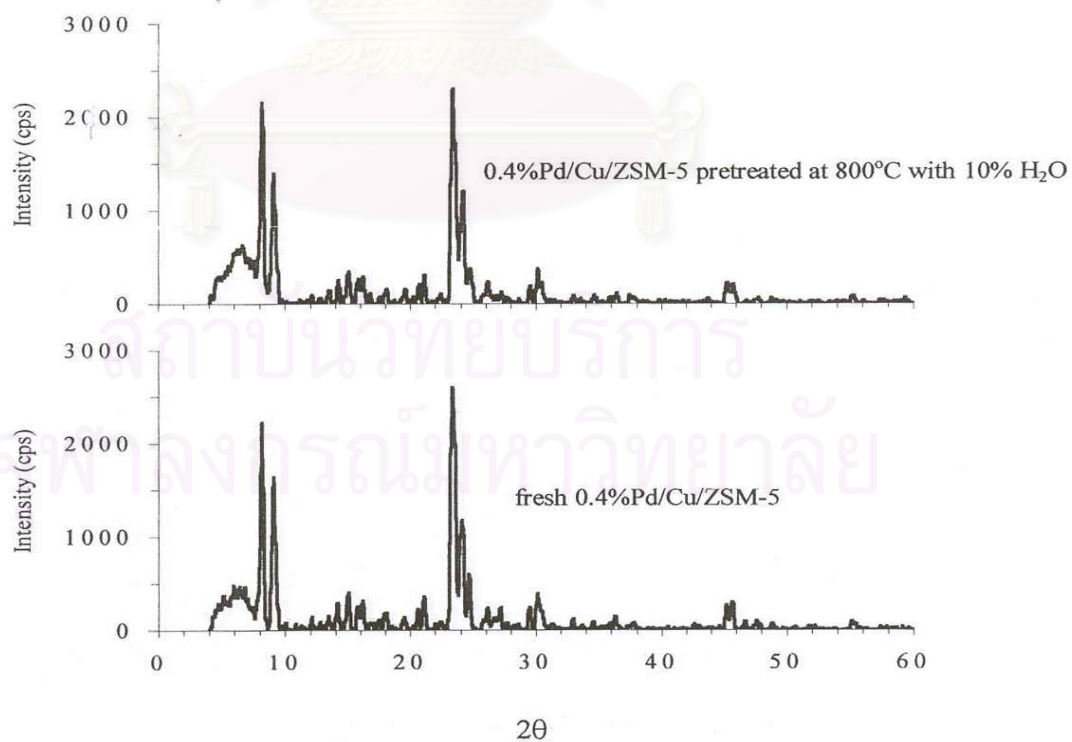


Figure 5.6 XRD patterns of 0.4%Pd/Cu/HZSM-5 with hydrothermal treatment

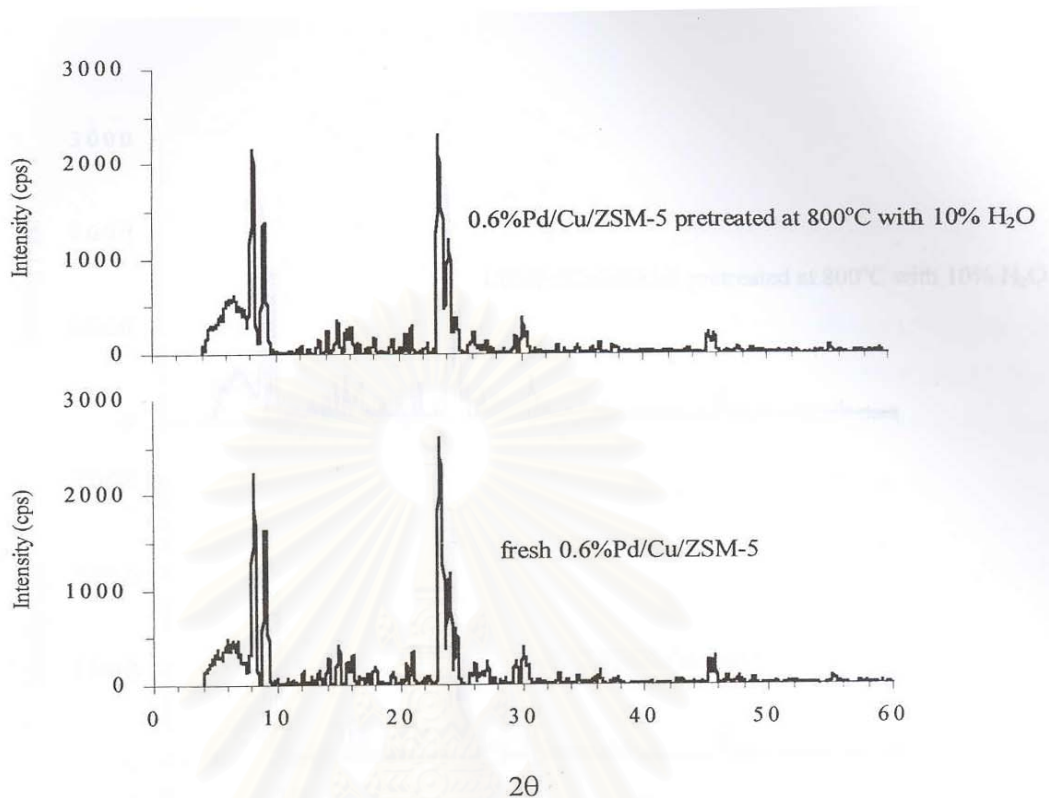


Figure 5.7 XRD patterns of 0.6%Pd/Cu/HZSM-5 with hydrothermal treatment

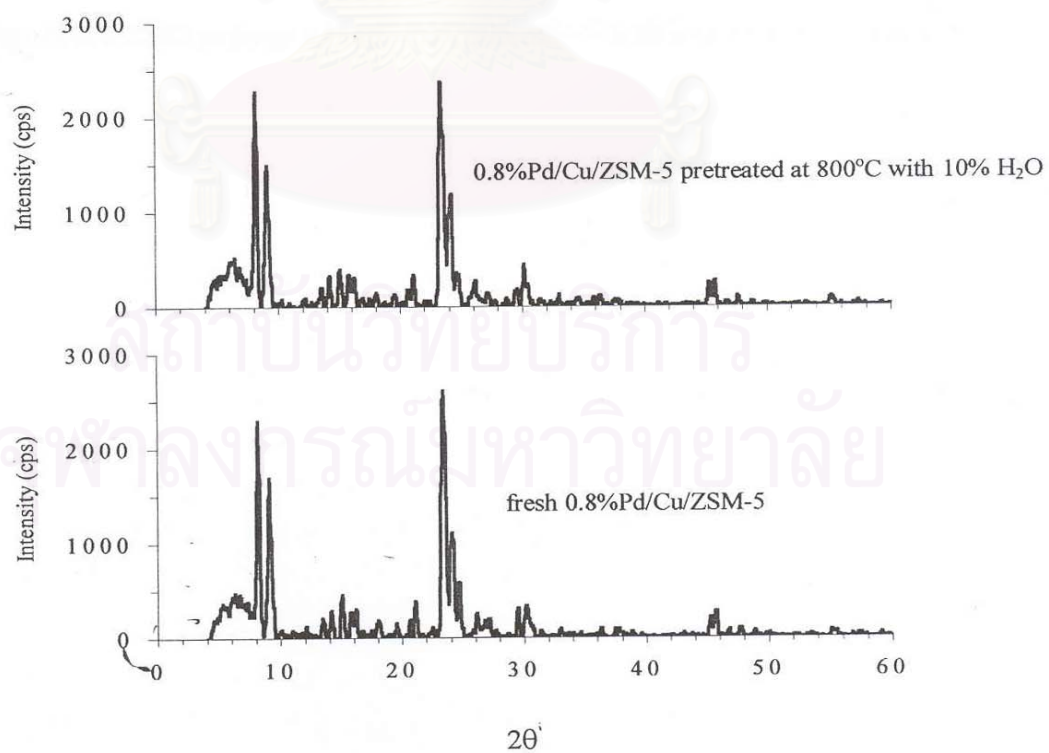


Figure 5.8 XRD patterns of 0.8%Pd/Cu/HZSM-5 with hydrothermal treatment

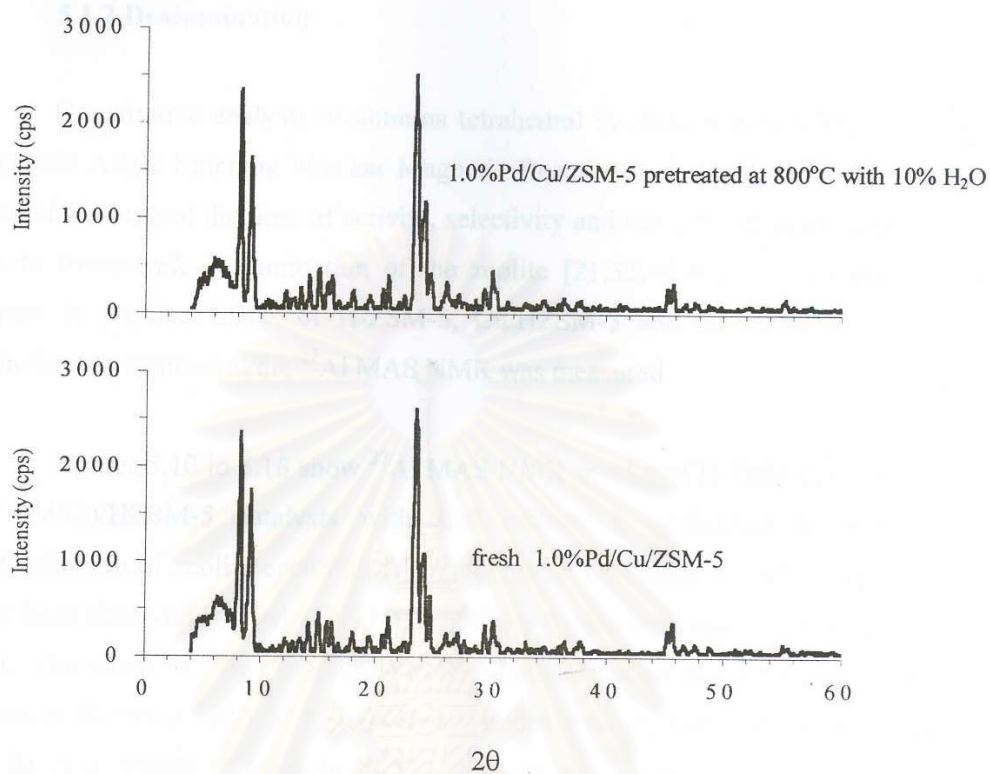


Figure 5.9 XRD patterns of 1.0%Pd/Cu/HZSM-5 with hydrothermal treatment

สถาบันวิทยบริการ
จุฬาลงกรณ์มหาวิทยาลัย

5.1.2 Dealumination

Quantitative analysis of alumina tetrahedral in zeolites is conducted by ^{27}Al Magnetic Angle Spinning Nuclear Magnetic Resonance (^{27}Al MAS NMR). Many researchers suggest that loss of activity, selectivity and stability on steam treatment is due to framework dealumination of the zeolite [21,32,44,46]. To investigate the change in physical states of H-ZSM-5, Cu/HZSM-5 and Pd/Cu/HZSM-5 by the hydrothermal treatment, the ^{27}Al MAS NMR was measured.

Figures 5.10 to 5.18 show ^{27}Al MAS NMR spectra of H-ZSM-5, Cu/HZSM-5 and Pd/Cu/HZSM-5 catalysts with and without hydrothermal treatment. If dealumination of zeolite occurred, Al in octahedral coordination with oxygen would have been observed by ^{27}Al MAS NMR at about 0 ppm as supported by Tanabe et al. [60]. The result of ^{27}Al MAS NMR of the catalysts before and after pretreatment is shown in figures 5.10 to 5.18. The fresh catalysts exhibited only one sharp signal at ca. 50 ppm, which is assigned to the tetrahedral aluminum in the zeolite lattice [34,46,60]. Hydrothermal treatment of H-ZSM-5, Cu/HZSM-5 and 0.1%Pd/Cu/HZSM-5 at 800°C and 10 mol% H₂O caused the appearance of new ^{27}Al MAS NMR signal at 0 ppm assigned to extra framework Al atom in octahedral coordination [34,35,46,60]. These results indicated that dealumination occurs in pretreated H-ZSM-5 and Cu/HZSM-5 zeolite lattice. This is consistent with the report of loss in activity and stability after steam pretreatment due to framework dealumination of the zeolite. However, only one signal of ^{27}Al MAS NMR at around 50 ppm is observed on Pd/Cu/HZSM-5 with the amount of 0.3 wt. % or higher even after pretreatment and no peak relating to octahedral aluminum is noticed. This suggests that the presence of a certain amount of Pd, approximately 0.3 wt. % loading as observed in this study, could stabilize the MFI framework structure by preventing the occurrence of dealumination.

Extensive dealumination of the Cu/HZSM-5 lattice with hydrothermal treatment could destroy the sites for ion exchanging and also alter the nature and location of copper species in the catalyst.

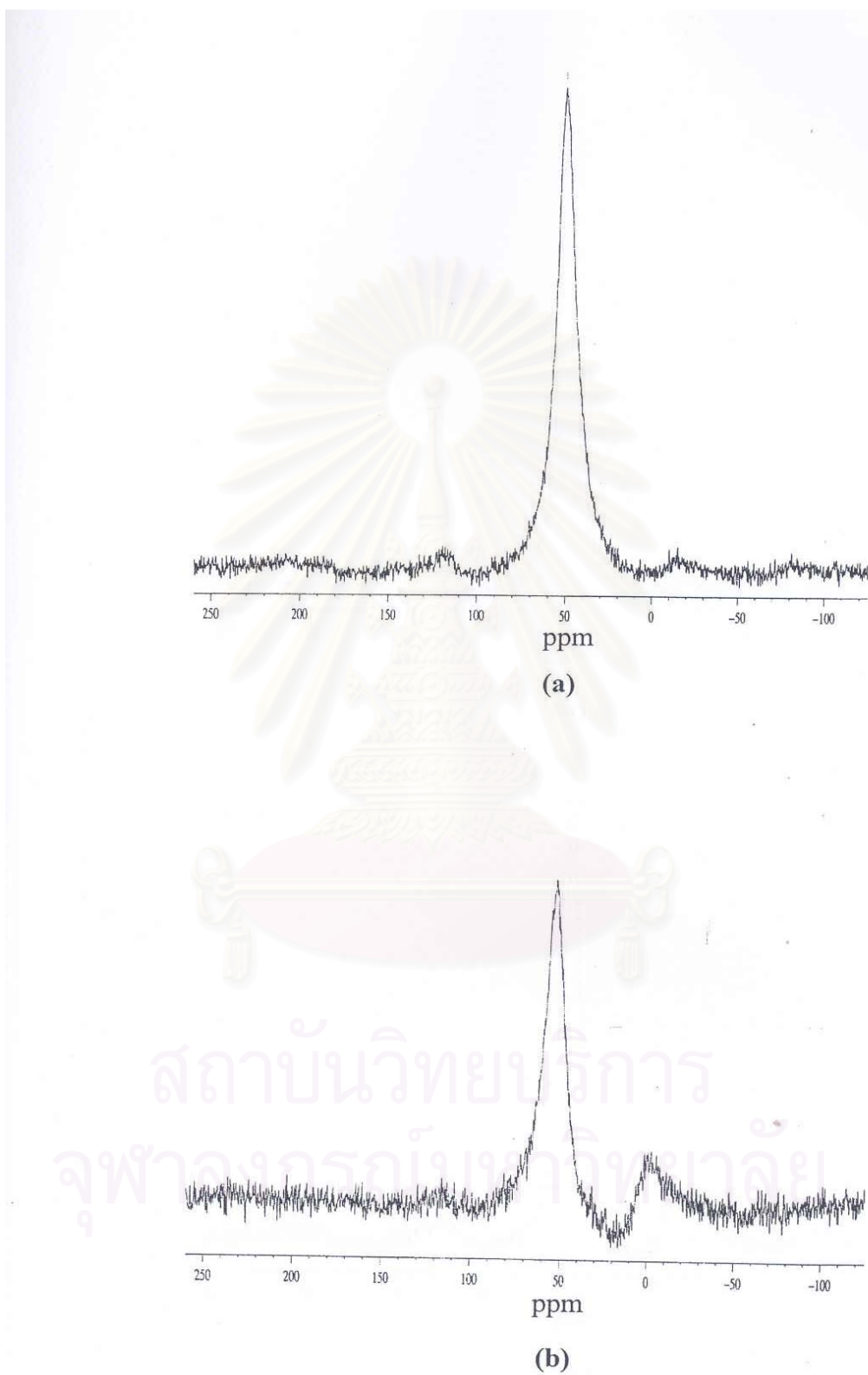


Figure 5.10 ^{27}Al MAS NMR spectra of catalysts. (a) fresh H-ZSM-5 (b) severely steamed H-ZSM-5

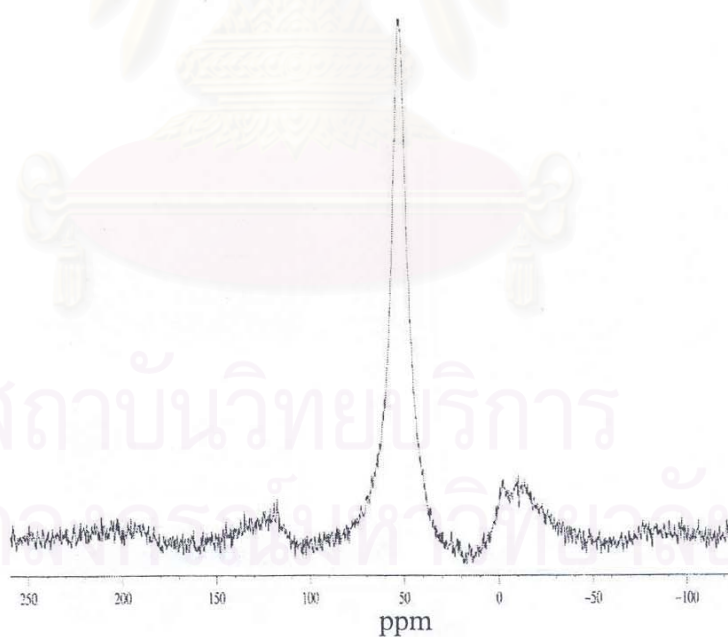
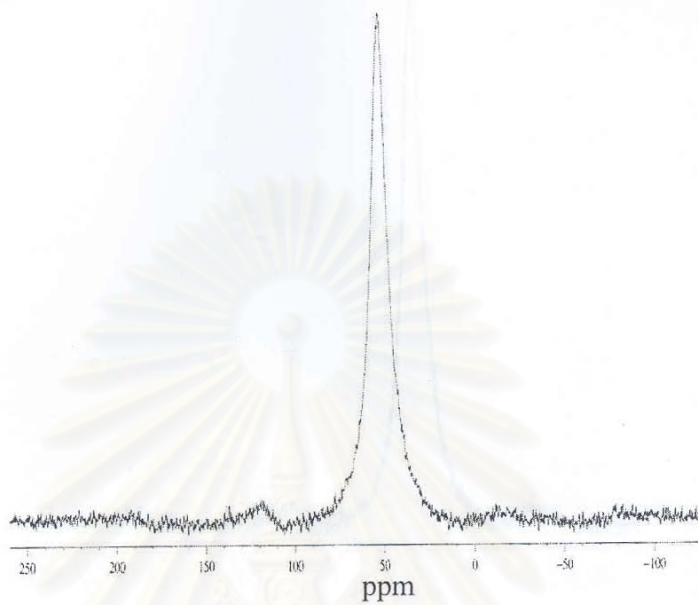


Figure 5.11 ^{27}Al MAS NMR spectra of catalysts. (a) fresh Cu/HZSM-5 (b) severely steamed Cu/HZSM-5

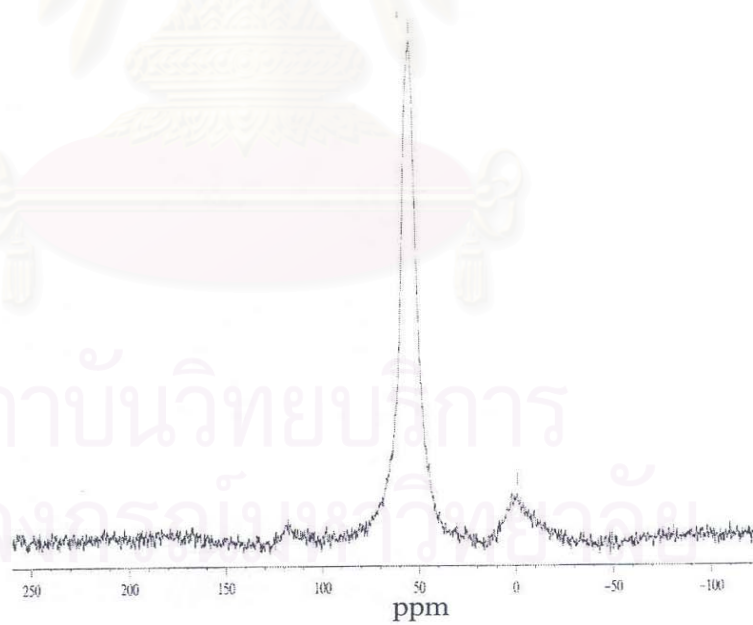
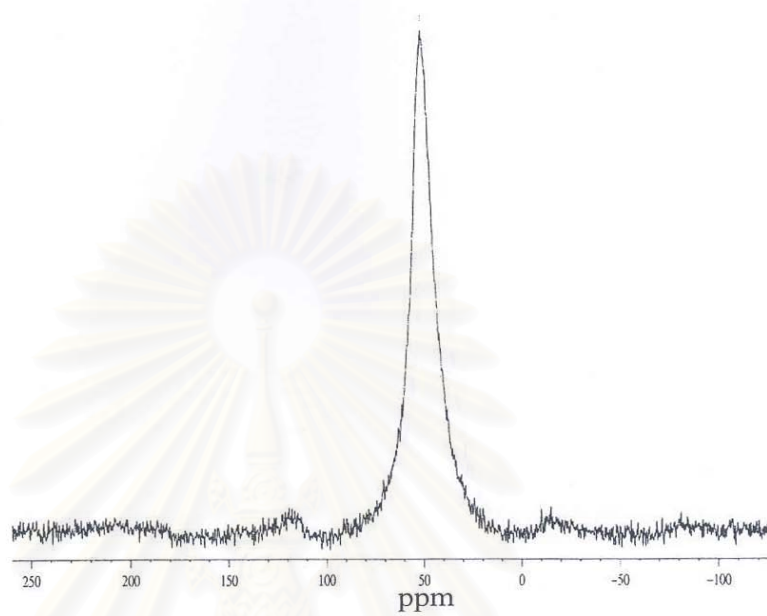


Figure 5.12 ^{27}Al MAS NMR spectra of catalysts. (a) fresh 0.1% PdCu/HZSM-5
(b) severely steamed 0.1% PdCu/HZSM-5

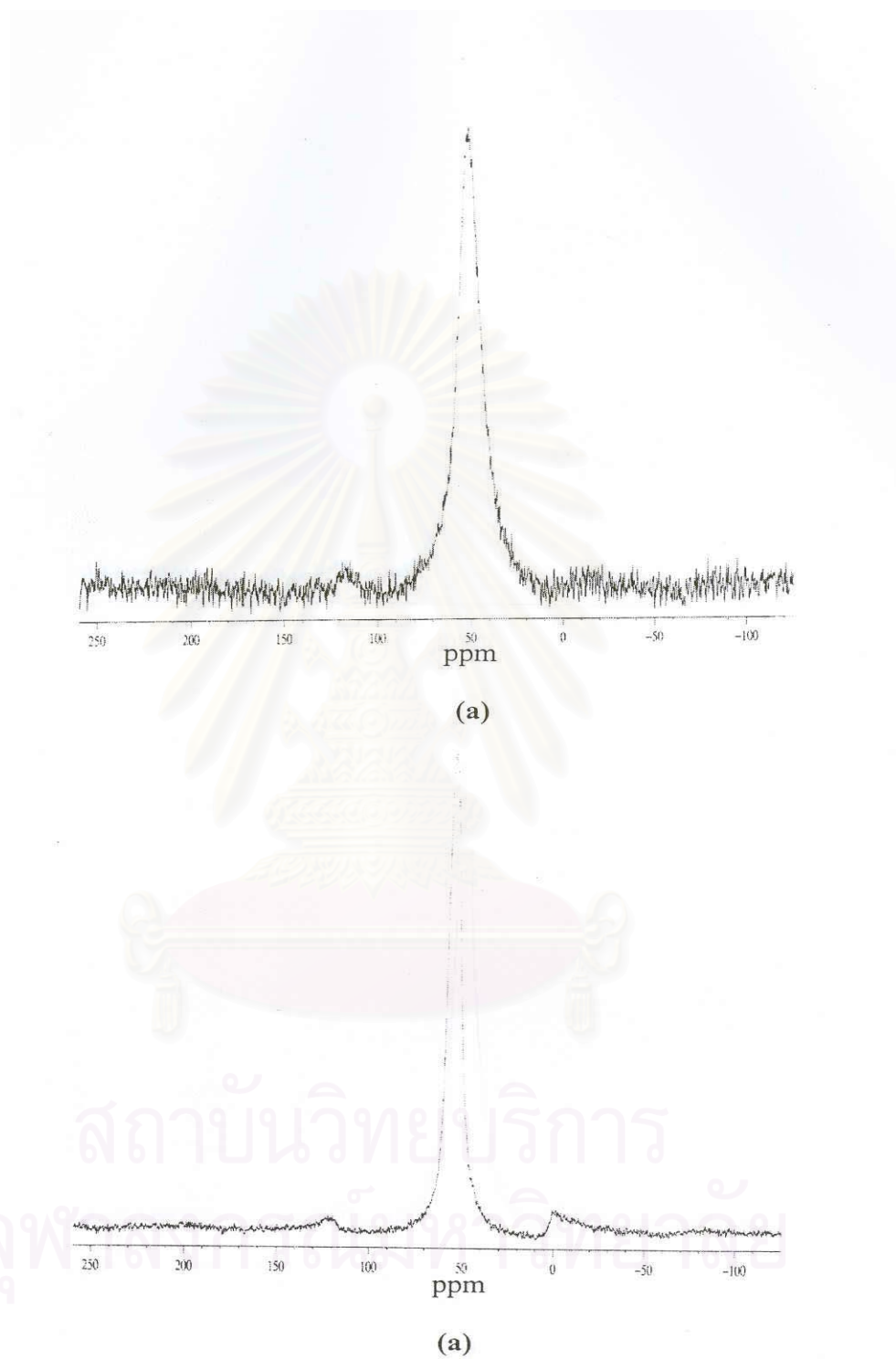
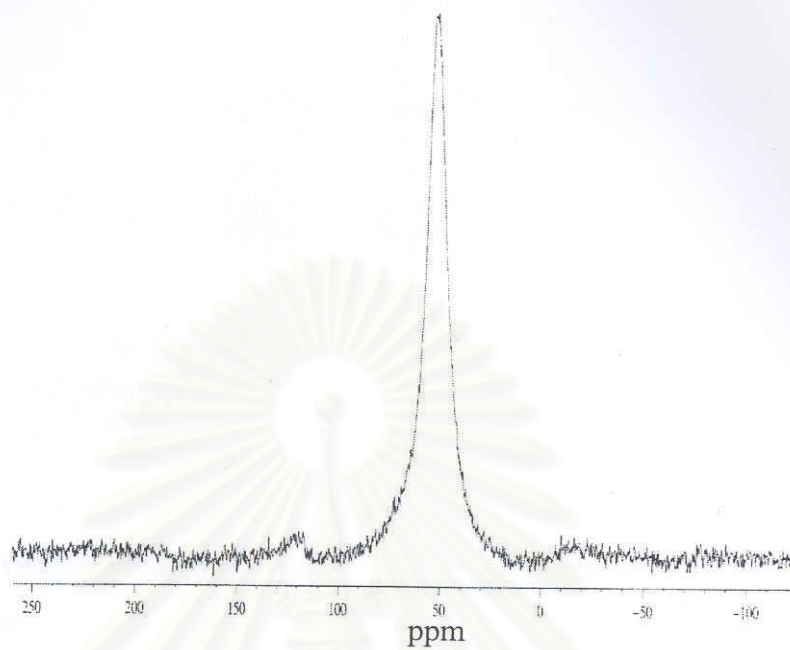
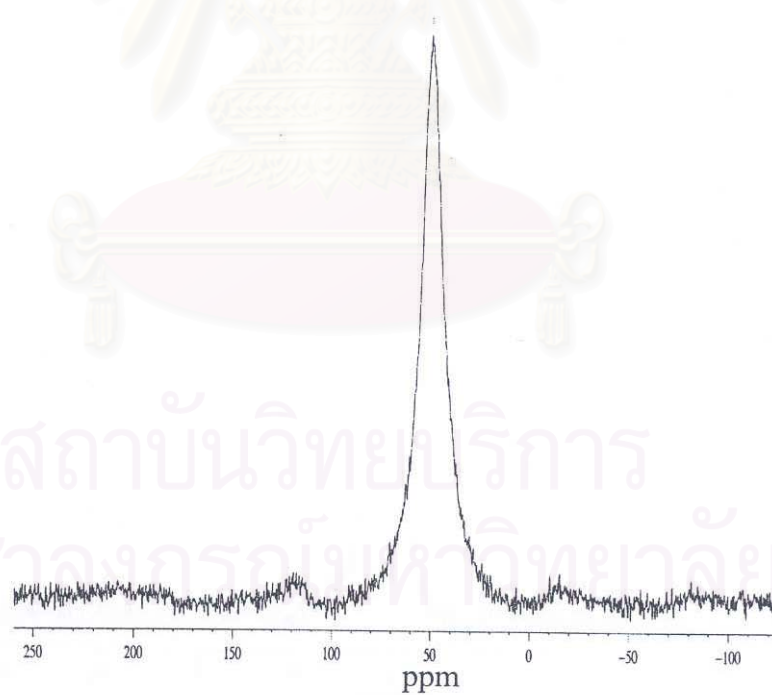


Figure 5.13 ^{27}Al MAS NMR spectra of catalysts. (a) fresh 0.2% PdCu/HZSM-5
(b) severely steamed 0.2% PdCu/HZSM-5



(a)



(a)

Figure 5.14 ^{27}Al MAS NMR spectra of catalysts. (a) fresh 0.3% PdCu/HZSM-5
(b) severely steamed 0.3% PdCu/HZSM-5

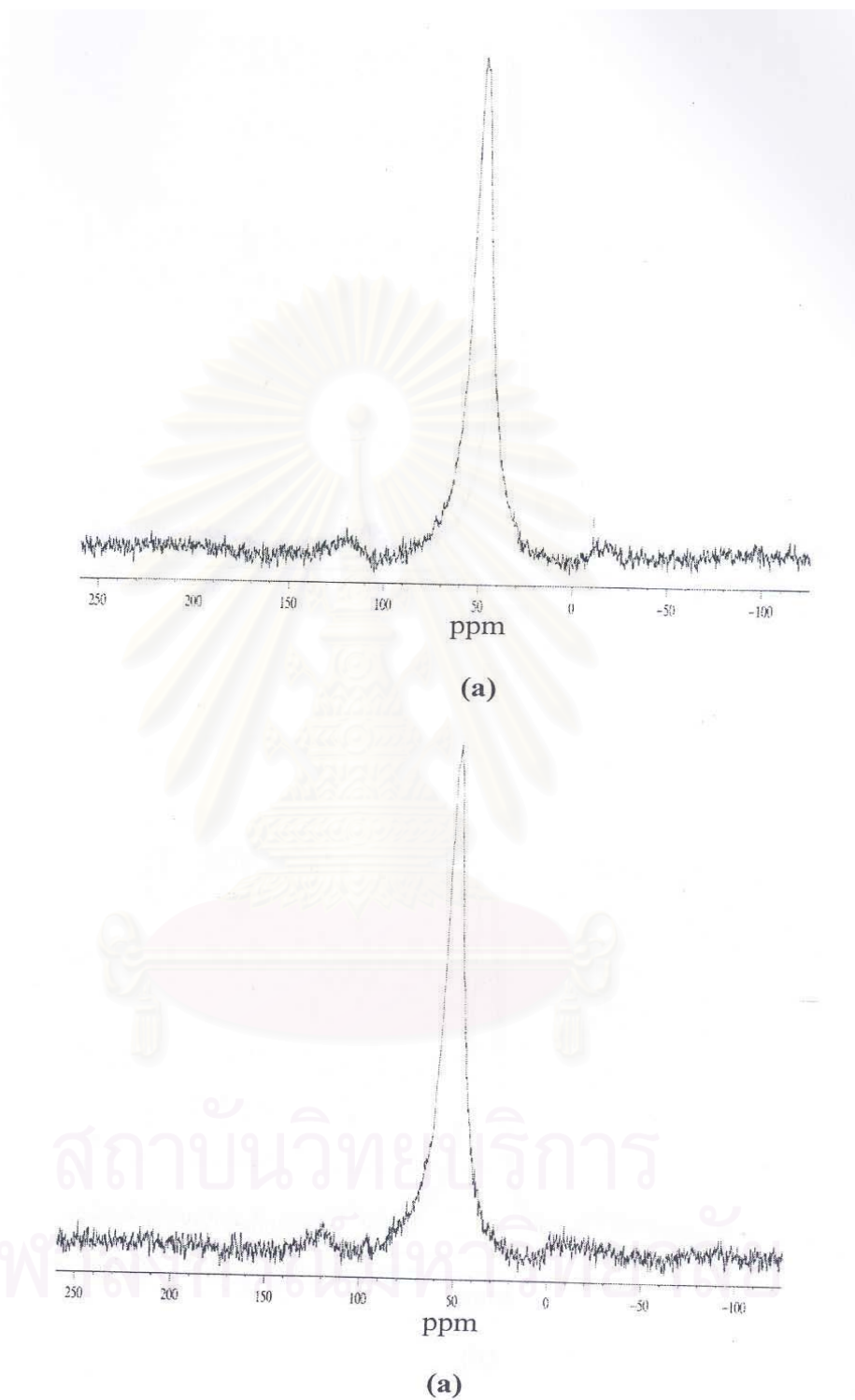


Figure 5.15 ^{27}Al MAS NMR spectra of catalysts. (a) fresh 0.4% PdCu/HZSM-5
(b) severely steamed 0.4% PdCu/HZSM-5

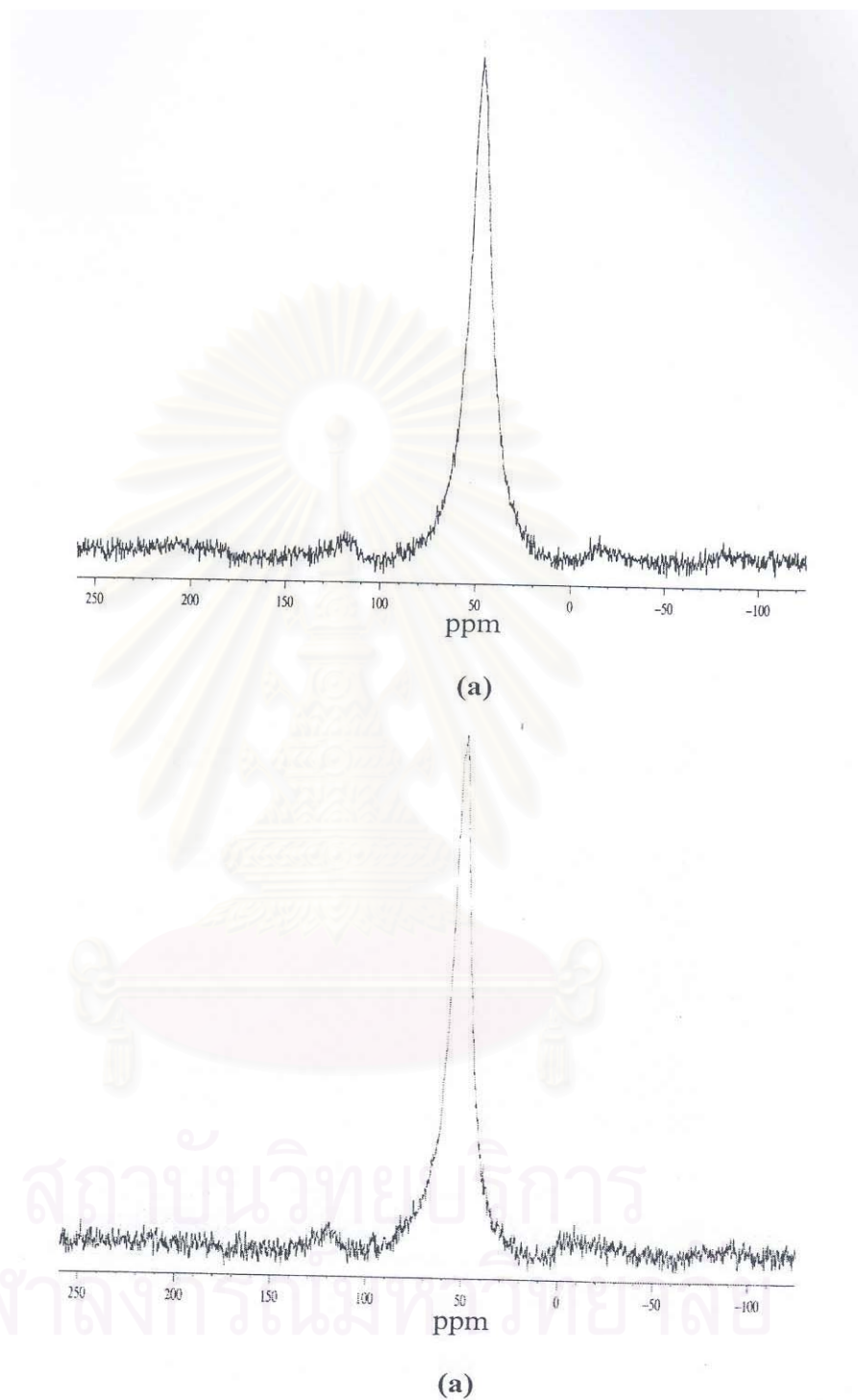


Figure 5.16 ^{27}Al MAS NMR spectra of catalysts. (a) fresh 0.6% PdCu/HZSM-5
(b) severely steamed 0.6% PdCu/HZSM-5

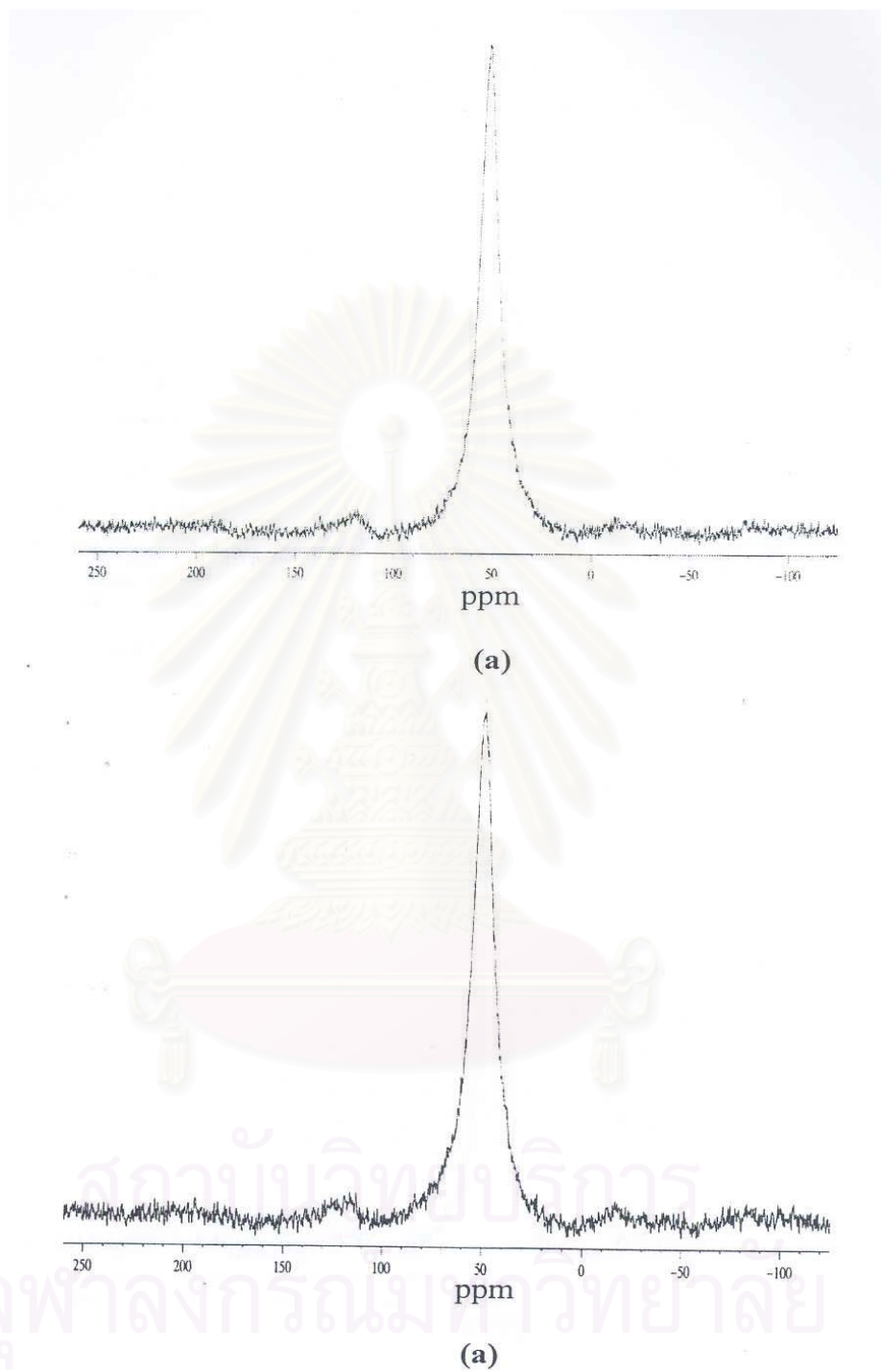


Figure 5.17 ^{27}Al MAS NMR spectra of catalysts. (a) fresh 0.8% PdCu/HZSM-5
(b) severely steamed 0.8% PdCu/HZSM-5

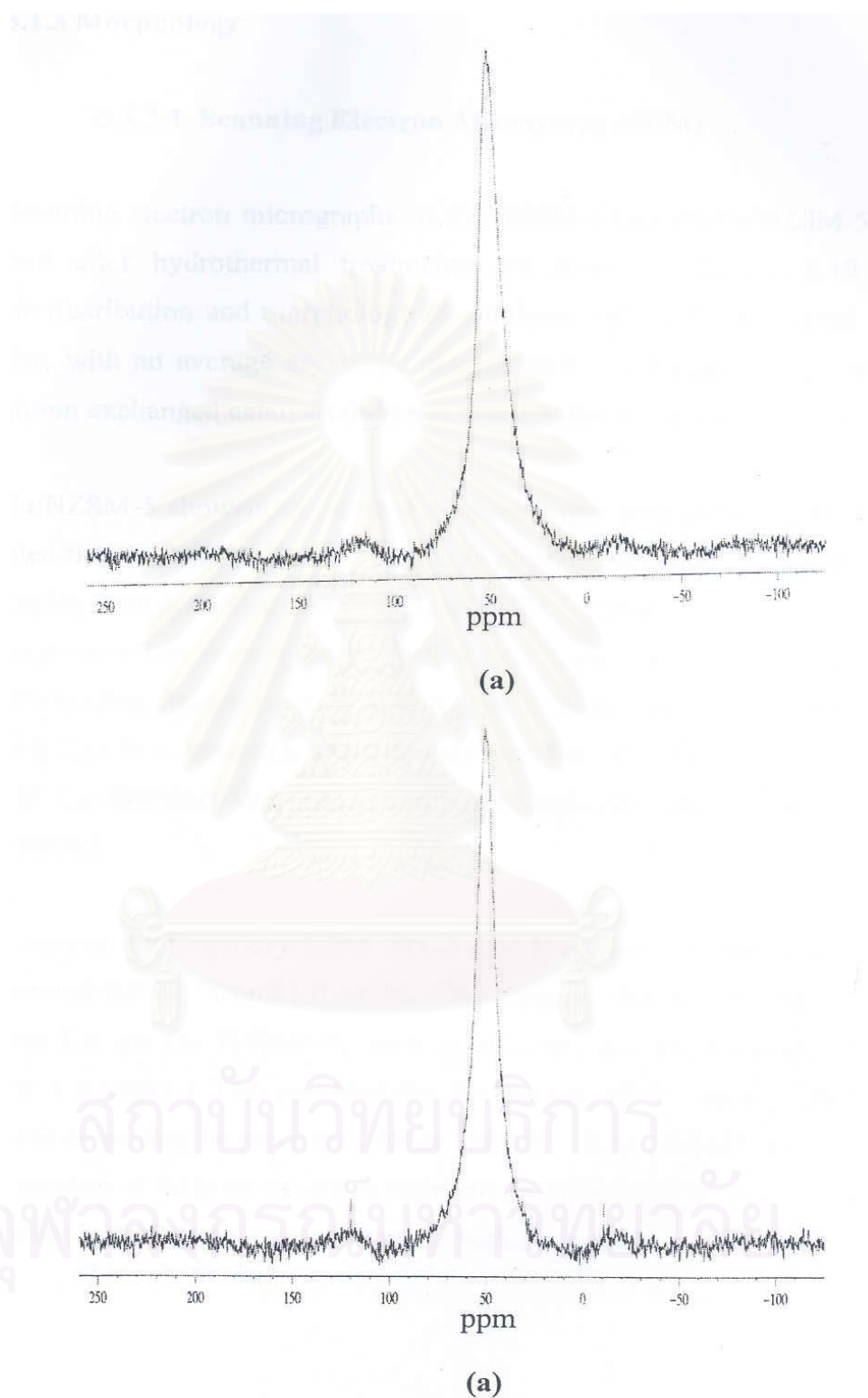


Figure 5.18 ^{27}Al MAS NMR spectra of catalysts. (a) fresh 1.0% PdCu/HZSM-5
(b) severely steamed 1.0% PdCu/HZSM-5

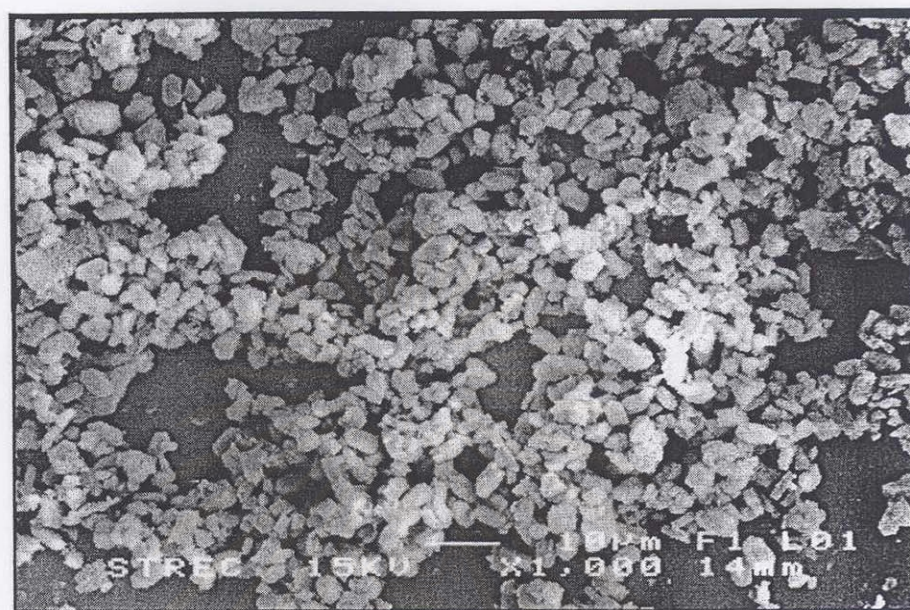
5.1.3 Morphology

5.1.3.1 Scanning Electron Microscopy (SEM)

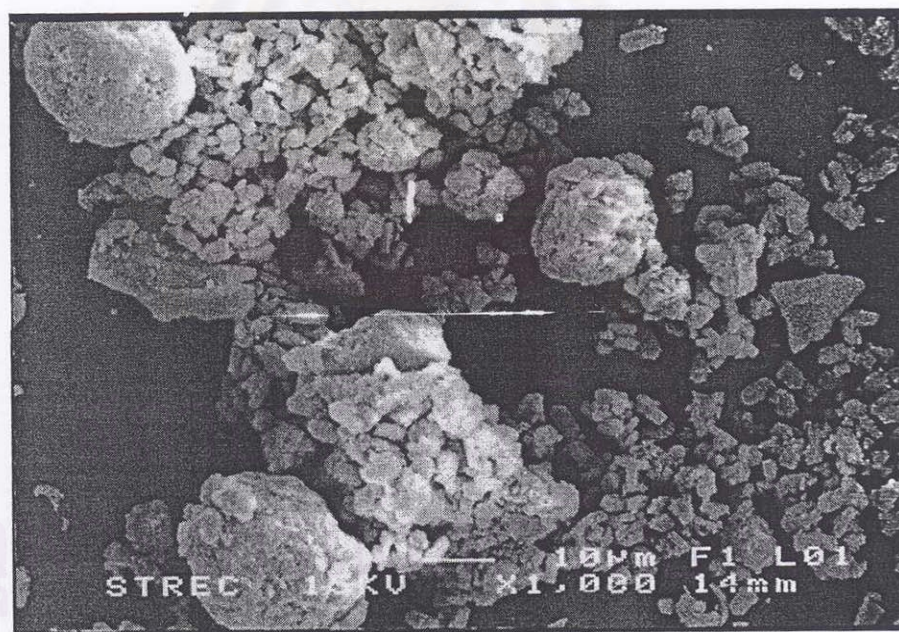
Scanning electron micrographs of Cu/HZSM-5 and Pd/Cu/HZSM-5 catalysts before and after hydrothermal treatments are shown in figures 5.19 to 5.26. Crystallite distribution and morphology of catalysts without hydrothermal treatment are similar, with an average crystallite size diameter of 5 μm . It is observed that palladium ion exchanged catalysts does not greatly alter the shape of crystal.

Cu/HZSM-5 showed an obvious agglomeration after pretreatment. This can be indicated that Cu/HZSM-5 easily forms its cluster and further growth by sintering accompanying with gathering unit particle of ZSM-5 material. As for Pd/Cu/HZSM-5, such agglomeration seem to be prevented considerably especially for the samples with the Pd loading amount ranging from 0.3 wt. % to 0.6 wt. %. It means that the Pd part, which has less tendency toward sintering than Cu has, would interfere the progress of Cu sintering, and consequently, the agglomeration of ZSM-5 particle is largely retarded.

However, the larger crystallite size is clearly observed on the catalysts with Pd loading amount 0.8 wt. % and 1.0 wt. %. This suggests that there could be change in the Pd and Cu on the H-ZSM-5, such as alloying and metal oxide, due to the hydrothermal treatment. This provided that the amount of Pd present is higher than a certain level according to previous studies [59,63]. It is interesting to note that an optimum amount of Pd is necessary to stabilize the crystal morphology of Cu/HZSM-5 subjected to hydrothermal treatment at the high temperature.

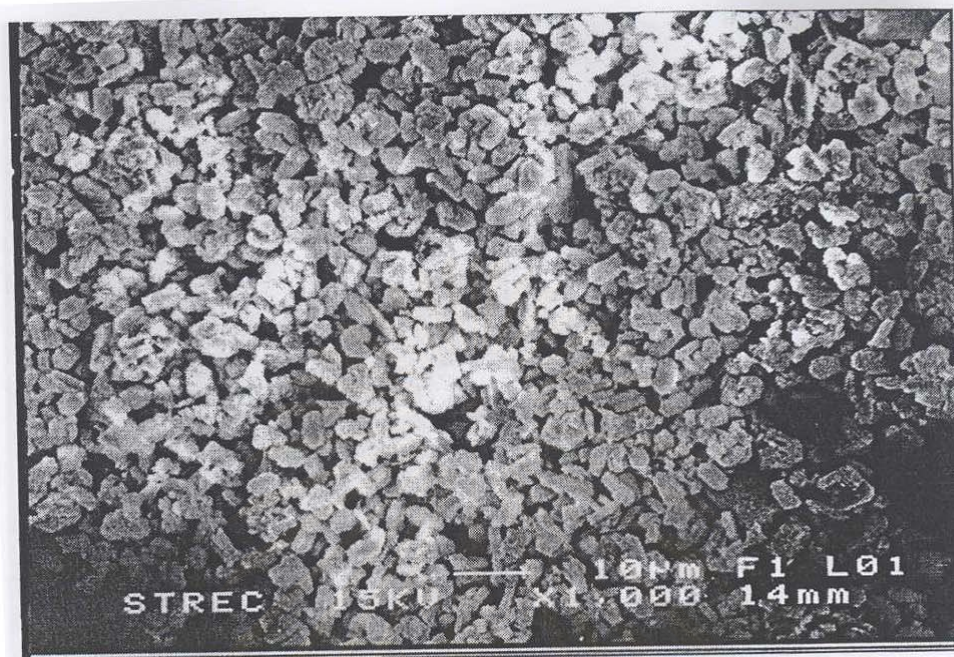


(a)

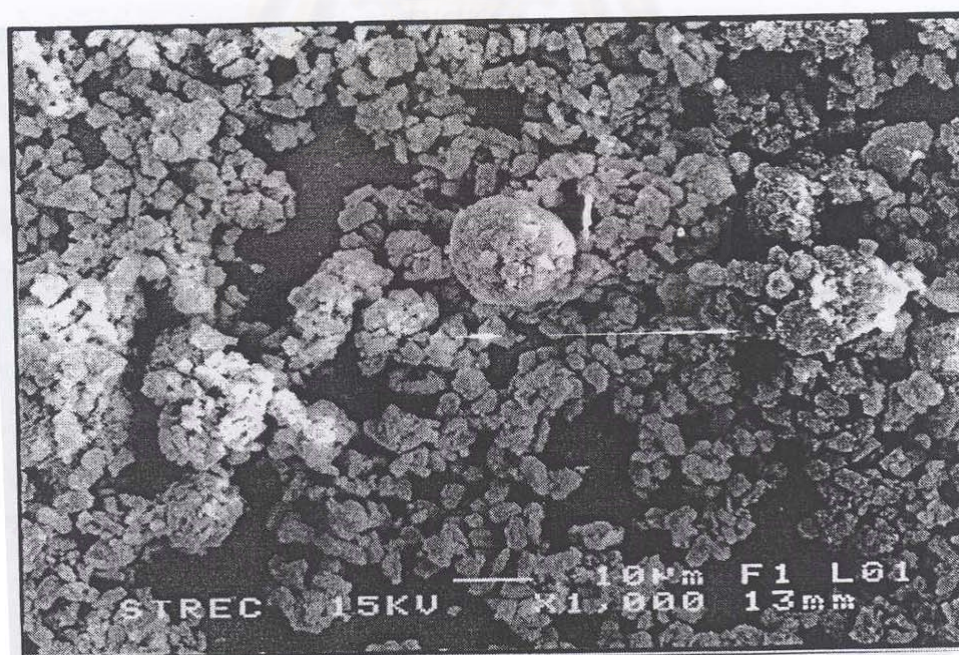


(b)

Figure 5.19 Scanning electron micrograph of catalysts. (a) fresh Cu/HZSM-5, (b) severely steamed Cu/HZSM-5,

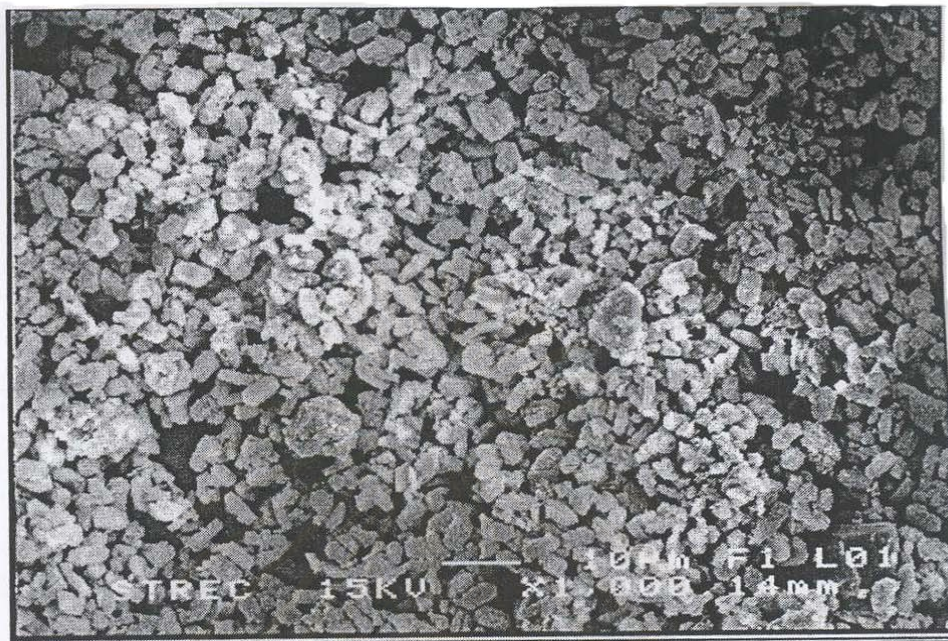


(a)

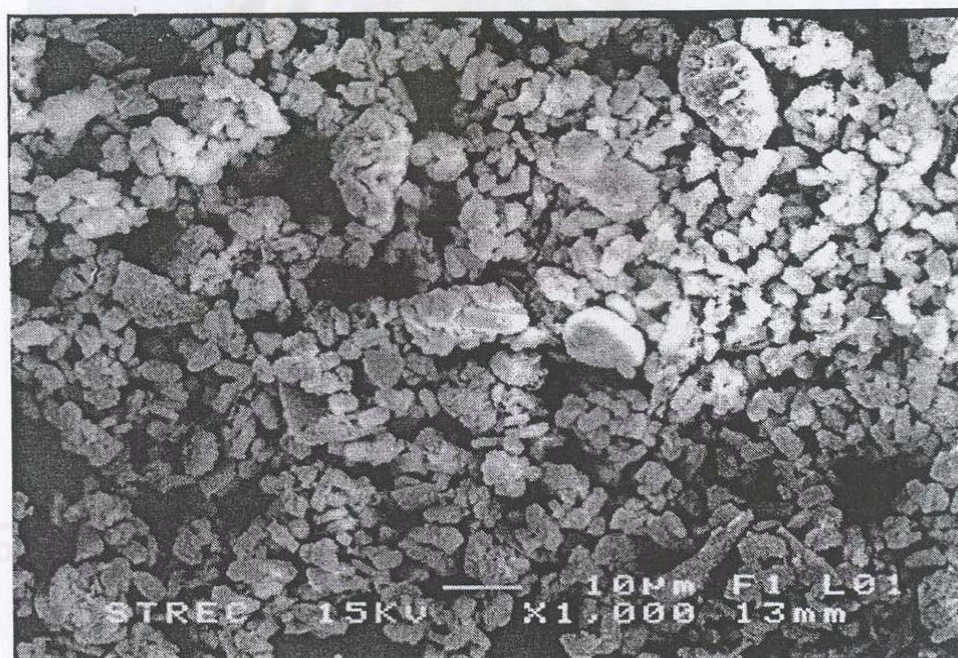


(b)

Figure 5.20 Scanning electron micrograph of catalysts. (a) fresh 0.1%Pd/Cu/HZSM-5, (b) severely steamed 0.1%Pd/Cu/HZSM-5,

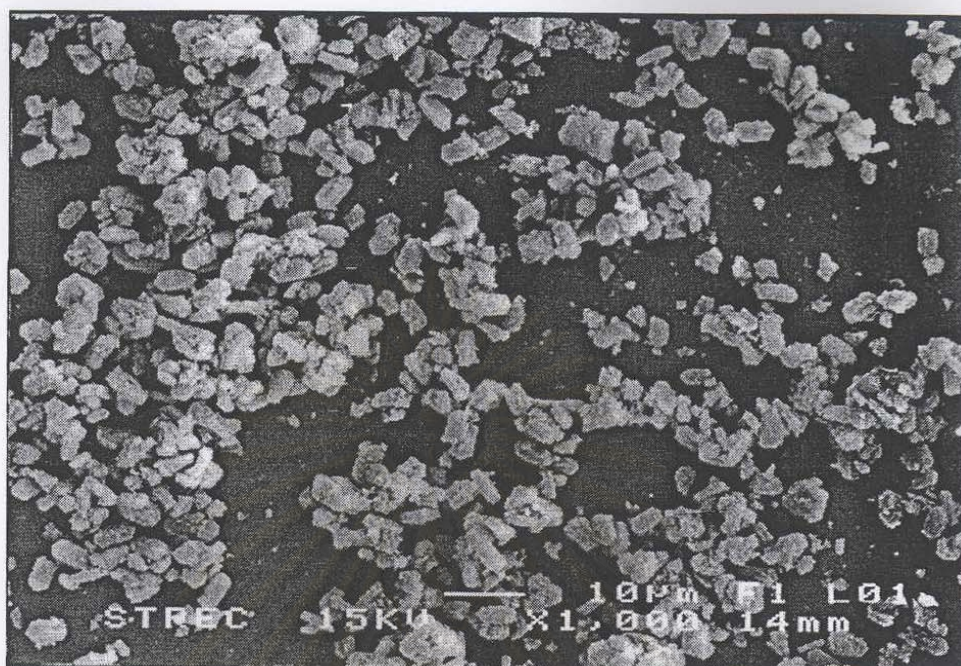


(a)



(b)

Figure 5.21 Scanning electron micrograph of catalysts. (a) fresh 0.2% Pd/Cu/HZSM-5, (b) severely steamed 0.2%Pd/Cu/HZSM-5,

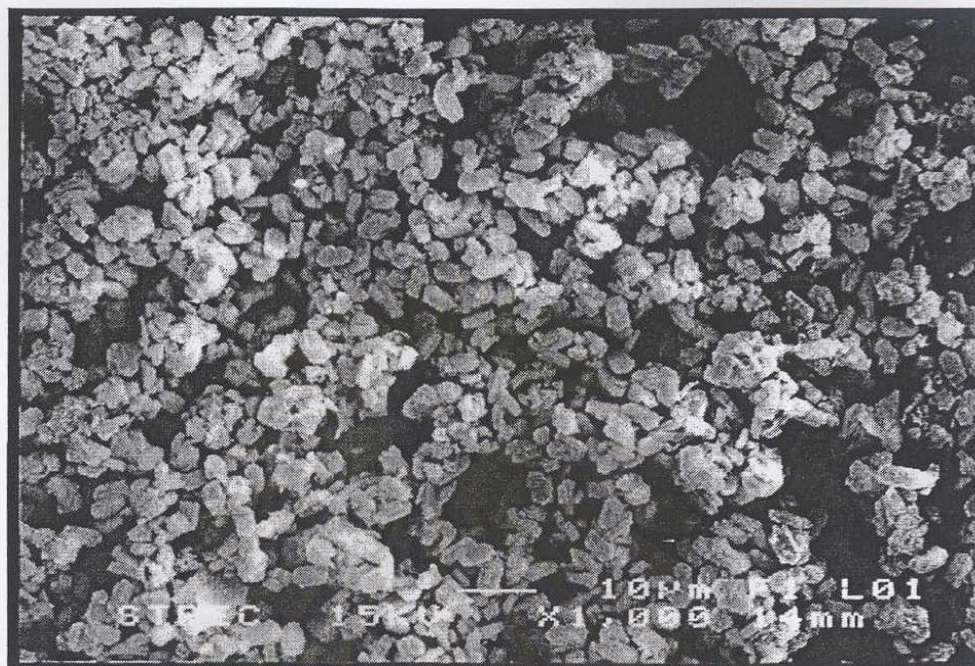


(a)

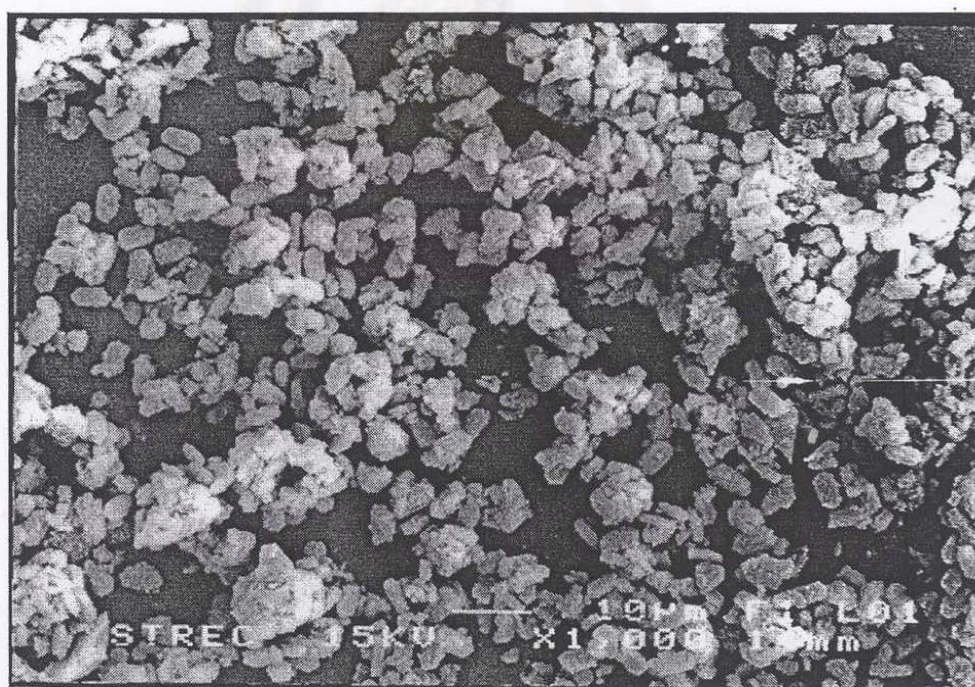


(b)

Figure 5.22 Scanning electron micrograph of catalysts. (a) fresh 0.3%Pd/Cu/HZSM-5, (b) severely steamed 0.3%Pd/Cu/HZSM-5,

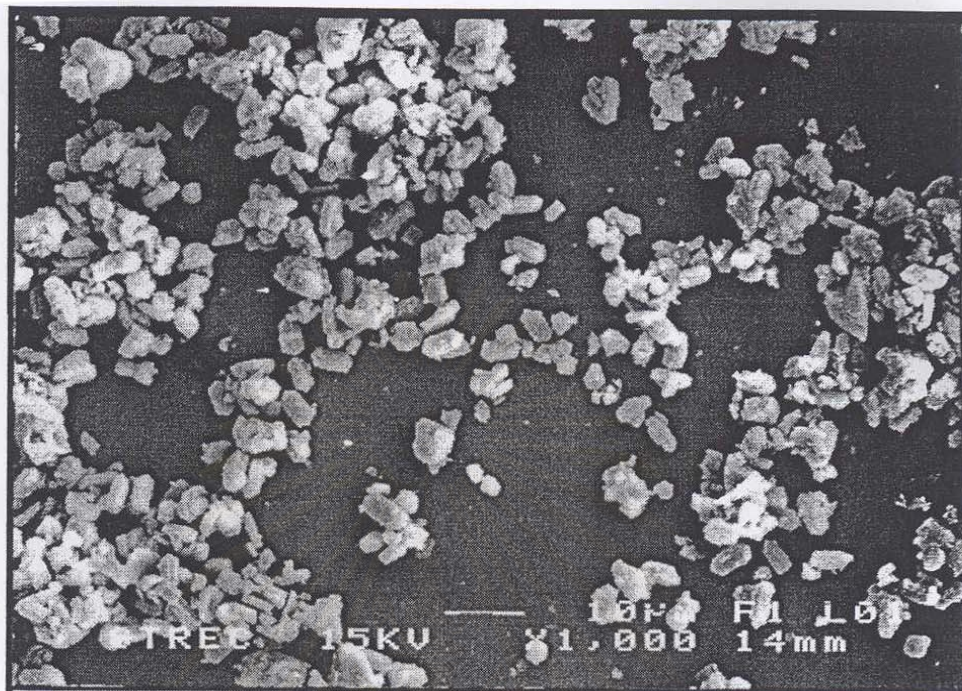


(a)

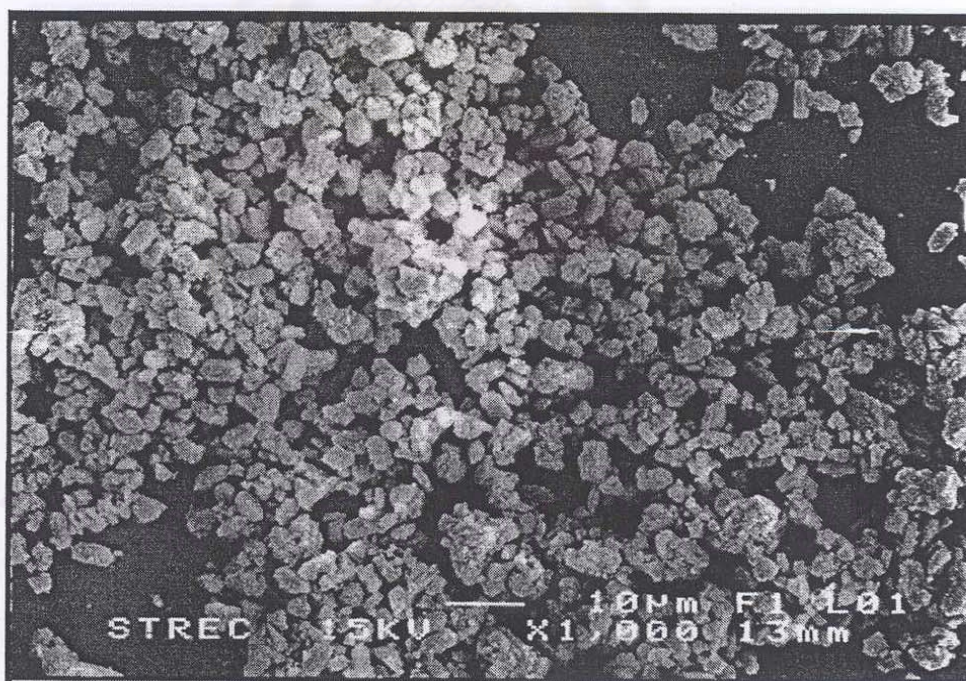


(b)

Figure 5.23 Scanning electron micrograph of catalysts. (a) fresh 0.4%Pd/Cu/HZSM-5, (b) severely steamed 0.4%Pd/Cu/HZSM-5,

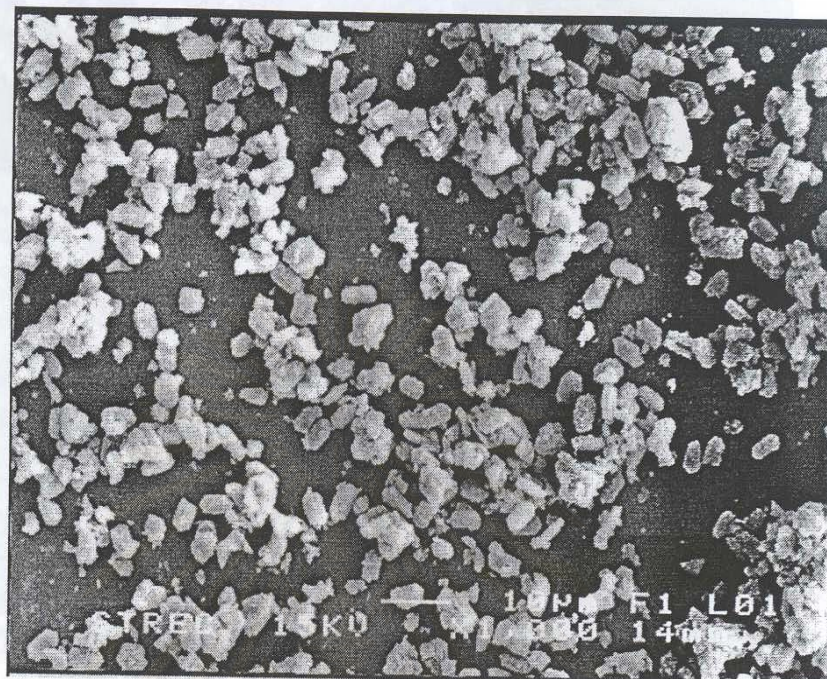


(a)

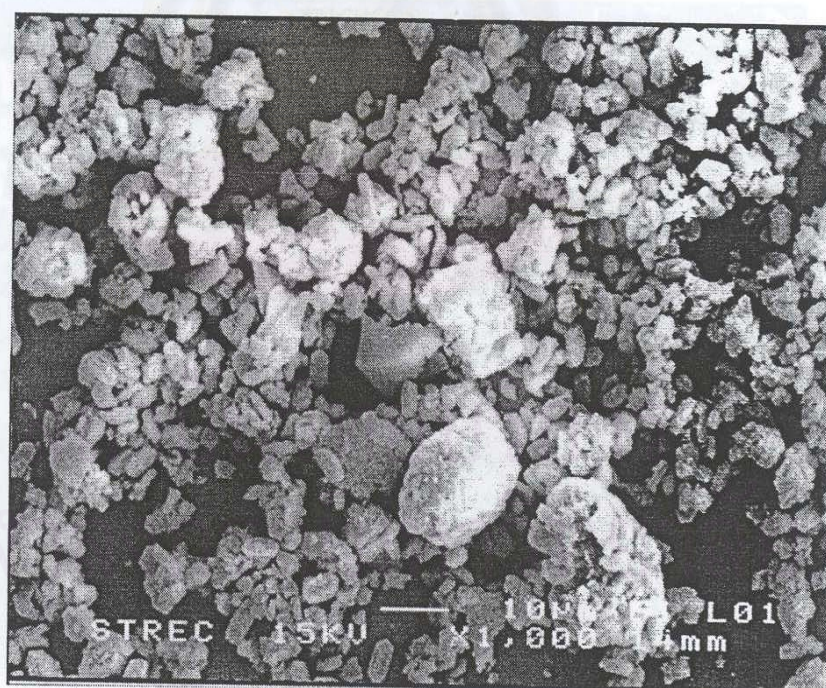


(b)

Figure 5.24 Scanning electron micrograph of catalysts. (a) fresh 0.6%Pd/Cu/HZSM-5, (b) severely steamed 0.6%Pd/Cu/HZSM-5,



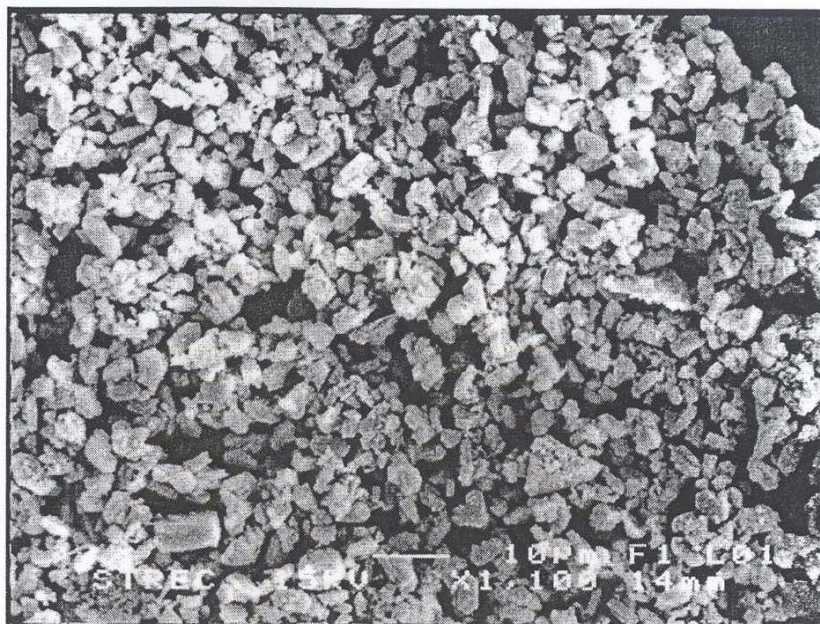
(a)



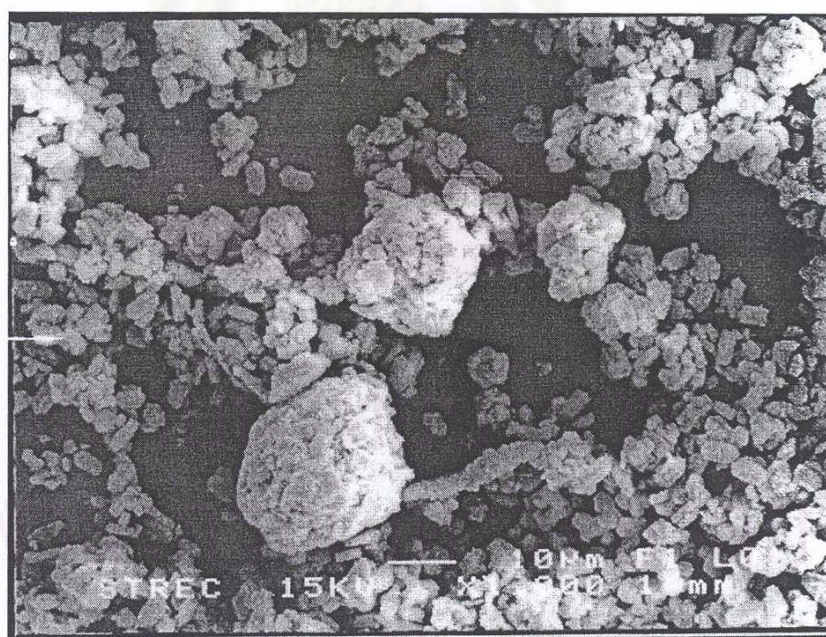
(b)

Figure 5.26 Scanning electron micrograph of catalysts. (a) fresh 0.8%Pd/Cu/HZSM-5
 Figure 5.25 Scanning electron micrograph of catalysts. (a) fresh 0.8%Pd/Cu/HZSM-5

(b) severely steamed 0.8%Pd/Cu/HZSM-5



(a)



(a)

Figure 5.26 Scanning electron micrograph of catalysts. (a) fresh 1.0%Pd/Cu/HZSM-5
(b) severely steamed 1.0%Pd/Cu/HZSM-5

5.1.3.2 Transmission Electron Microscopy (TEM)

Copper ion exchanged H-ZSM-5 is known as an effective catalyst for NO removal even in the presence of excess oxygen [18]. Many researchers have pointed out that the deterioration of Cu/HZSM-5 may be attributed to the sintering of active copper into inactive phases, such as CuO, Cu₂O [29-31]. For Pd/ZSM-5 catalyst, Raman, XRD and TEM measurements indicated that PdO is formed on deactivated catalysts. The deactivation of Pd-zeolite is caused by PdO resulted from the Pd agglomeration which can be promoted by water vapor [60,61]. In order to present that Pd ion exchanged Cu/HZSM-5 inhibits the agglomeration of ZSM-5, TEM measurement is then examined.

Figures 5.27 to 5.34 shows TEM image of the pretreated catalyst. For fresh catalysts, there is no observation of large dark spot, which is attributed to the agglomeration. In the case of pretreated catalysts, dark spots implying metal agglomerates exhibit on the zeolite crystal.

Most pretreated catalysts show metal particle size (dark spot) at approximately 50 nm, except for 0.2-0.3 %Pd/Cu/HZSM-5, whose metal particle sizes are ca. 8 nm. From the results it is concluded that 0.2-0.3%PdCu/HZSM-5 promotes the metal particle agglomerates with the smallest size.

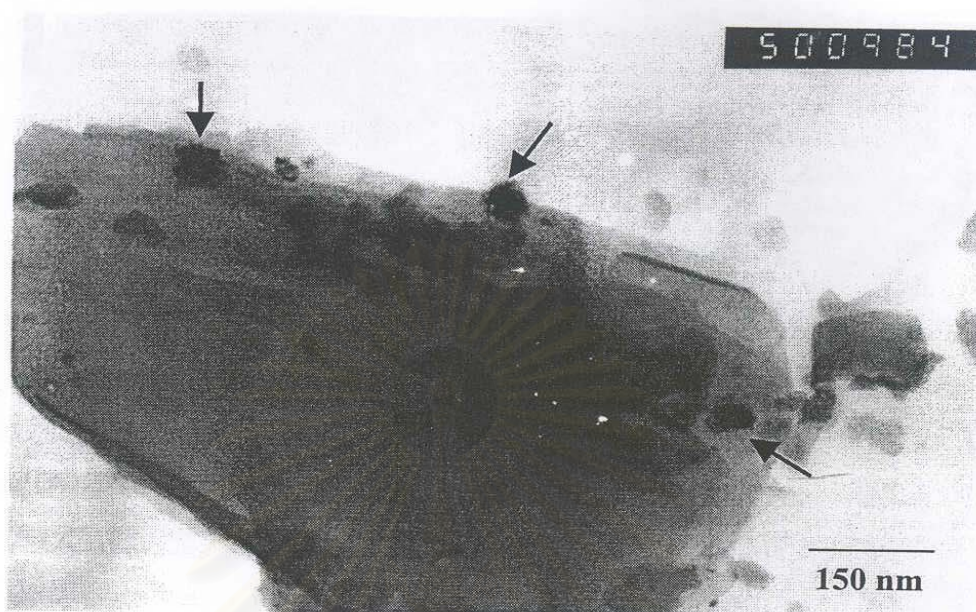


Figure 5.27 TEM image of severe steamed Cu/HZSM-5

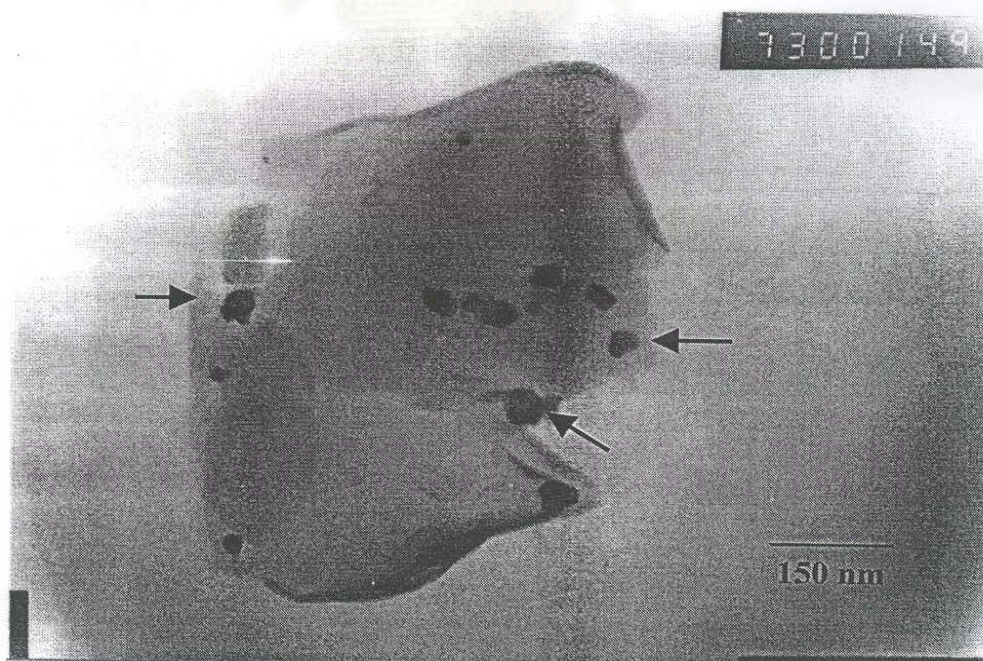


Figure 5.28 TEM image of severe steamed 0.1%Pd/Cu/HZSM-5

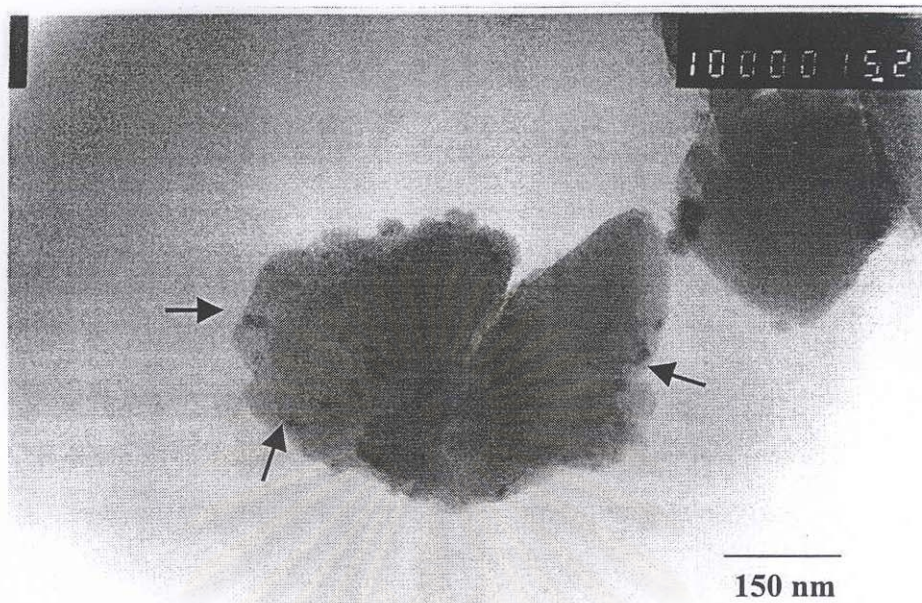


Figure 5.29 TEM image of severe steamed 0.2%Pd/Cu/HZSM-5

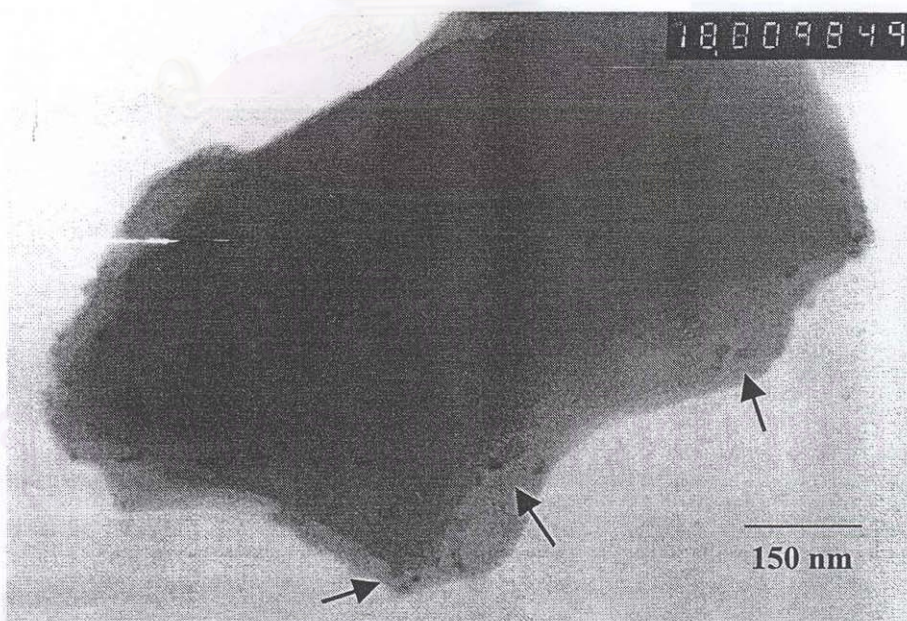


Figure 5.30 TEM image of severe steamed 0.3%Pd/Cu/HZSM-5

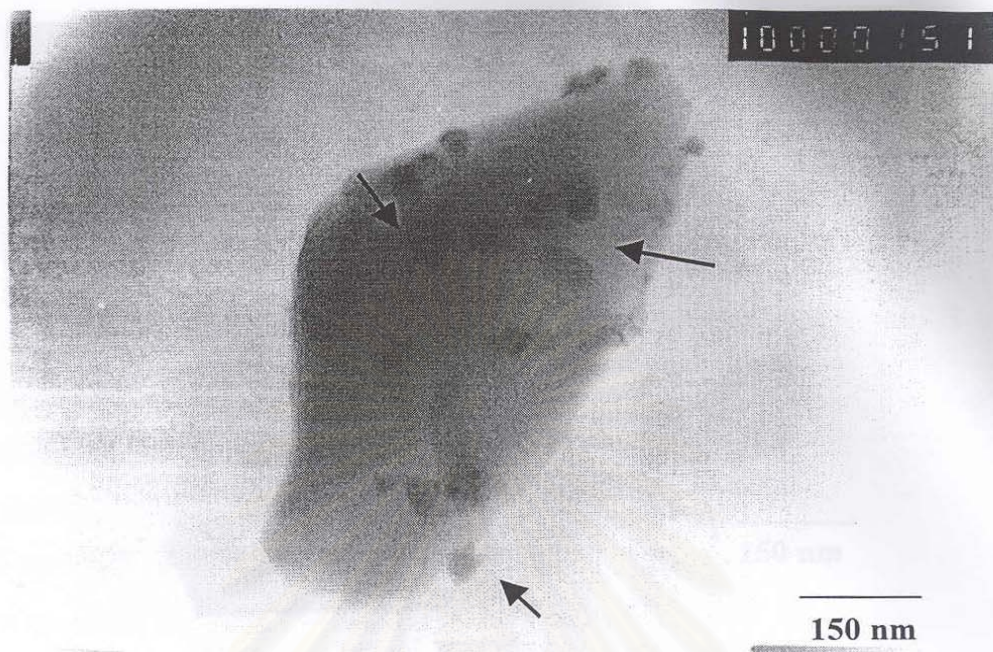


Figure 5.31 TEM image of severe steamed 0.4%Pd/Cu/HZSM-5

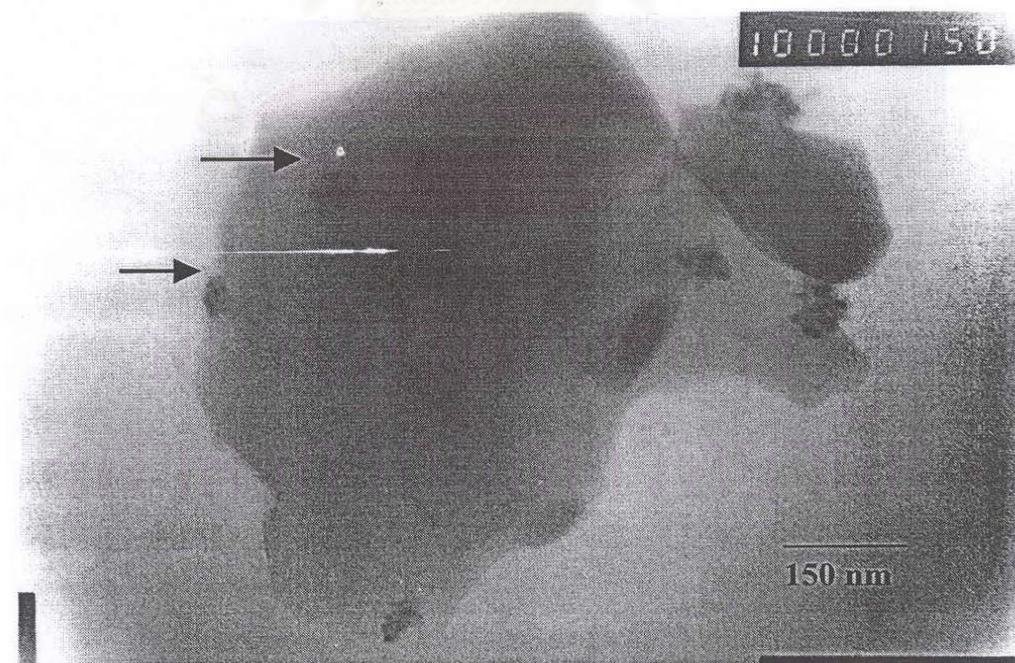


Figure 5.32 TEM image of severe steamed 0.6%Pd/Cu/HZSM-5

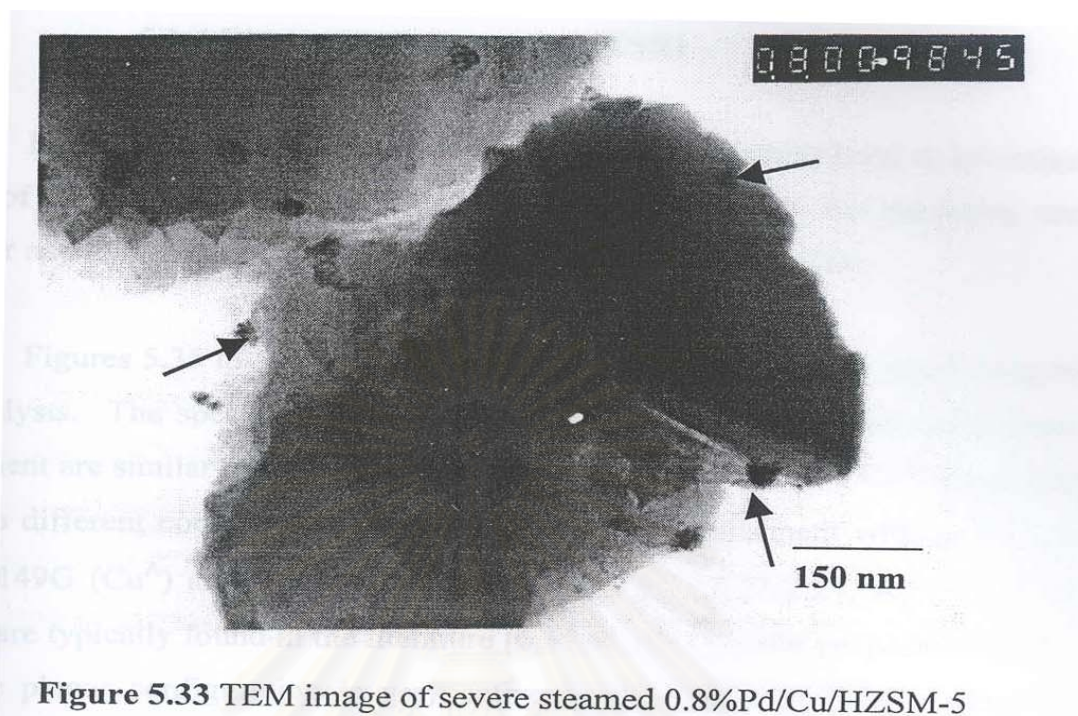


Figure 5.33 TEM image of severe steamed 0.8%Pd/Cu/HZSM-5

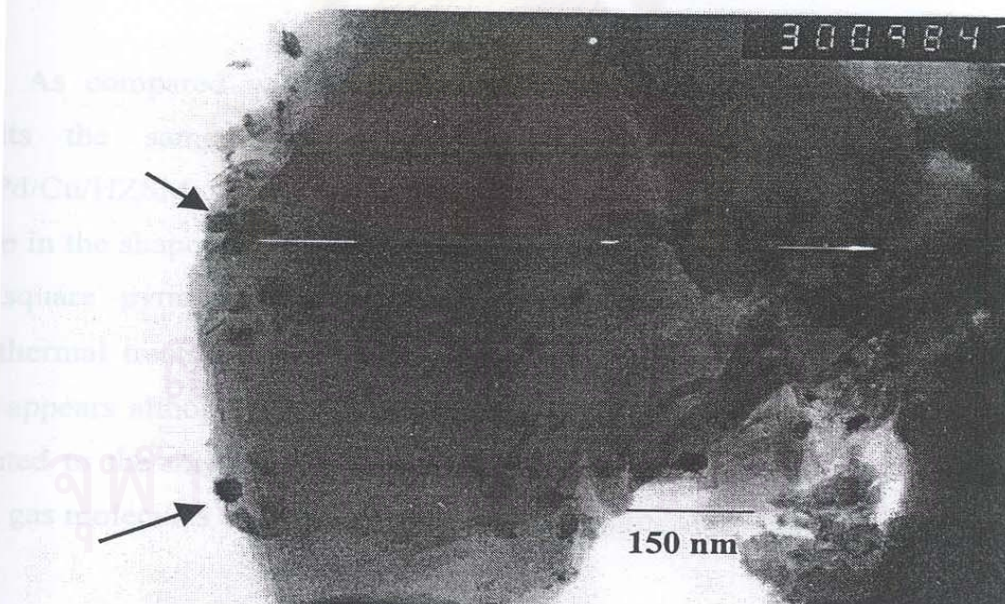


Figure 5.34 TEM image of severe steamed 1.0%Pd/Cu/HZSM-5

5.1.4 Electron spin resonance (ESR)

Electron spin resonance (ESR) experiments were carried out to investigate the state of Cu^{2+} . The ESR results provide information about the oxidation states of copper and the coordination structure of Cu^{2+} in Cu/HZSM-5 [36].

Figures 5.35 to 5.42 show the ESR spectra of Cu/HZSM-5 and Pd/Cu/HZSM-5 catalysts. The spectra of Cu/HZSM-5 and Pd/Cu/HZSM-5 without hydrothermal treatment are similar in shape which indicate the presence of two Cu^{2+} species located in two different coordination (a square pyramidal environment with $g_{\parallel} = 2.31-2.33$, $A_{\parallel} = 149\text{G}$ (Cu^{A}) and a square planar one with $g_{\parallel} = 2.27-2.29$, $A_{\parallel} \sim 157\text{G}$ (Cu^{B}). They are typically found in the literature [6,35,48,62]. Shelef proposed that Cu^{2+} in a square planar configuration is very active for NO removal [17]. Iwamoto et al. suggested that Cu ions migrated to 5-member oxygen ring due to the thermal treatment, which causes the deactivation of the catalyst [36]. It can be suggested that Pd dose not have an impact on the configuration of Cu.

As compared with fresh catalysts, 0.3%Pd/Cu/HZSM-5 after pretreatment exhibits the same features. Nevertheless, the pretreated Cu/HZSM-5 and 0.1%Pd/Cu/HZSM-5 not only loses the intensity of ESR spectra, but also have a change in the shape of the signal. This means that the amount of two Cu^{2+} species in both square pyramidal and square planar coordination are diminished due to hydrothermal treatment. In additions, a new spectrum with $g_{\parallel} = 2.30$, $A_{\parallel} = 160\text{G}$ (Cu^{C}) appears although part of two Cu^{2+} species remained. This new signal may be attributed to the migration of Cu ions to the location near 5-member oxygen rings which gas molecules cannot penetrate, as suggested by Iwamoto et al. [36],

On the other hand, the pretreated catalysts with 0.8-1.0 wt. % Pd loading did not show any change of coordinated Cu^{2+} species; however, some lost of the intensity of ESR spectra has been observed. This means that the amounts of two Cu^{2+} species in both square pyramidal and square planar coordination are diminished due to some change in Pd and Cu on H-ZSM-5 such as alloying and/or oxides formation.

The above ESR results suggested that change in state of copper ions in Cu/HZSM-5 with hydrothermal treatment, causes the deactivation of Cu/HZSM-5 [35]. In ref.[35], Matsumoto et al. suggested that the deactivation of Cu/ZSM-5 be due to change of copper ions into inactive forms. According to ESR spectra of pretreated in figure 5.35, ESR results can be the direct evidence of those inactive copper species.

The location of the copper ions can be determined by the interaction between copper ions and an Al site in zeolite lattice. In this study, NMR result showed that dealumination occurred in the Cu/HZSM-5 with hydrothermal treatment. It is suggested that 0.3%Pd/Cu/ZSM-5 can preserve most parts of active Cu^{2+} species even after pretreatment at 800°C and 10 mol% H_2O .



สถาบันวิทยบริการ
จุฬาลงกรณ์มหาวิทยาลัย

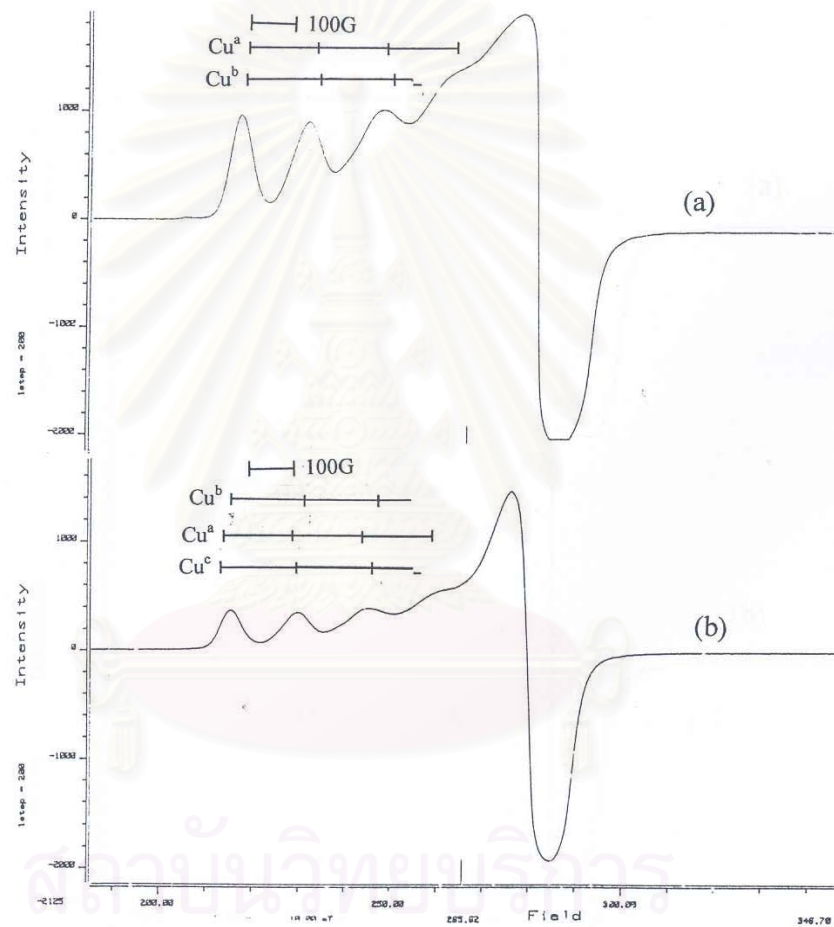


Figure 5.35 ESR spectra of high spin Cu^{2+} of Cu/HZSM-5 with and without hydrothermal treatment at 800°C 10 mol% H_2O
 (a) fresh Cu/HZSM-5, (b) severely steamed Cu/HZSM-5

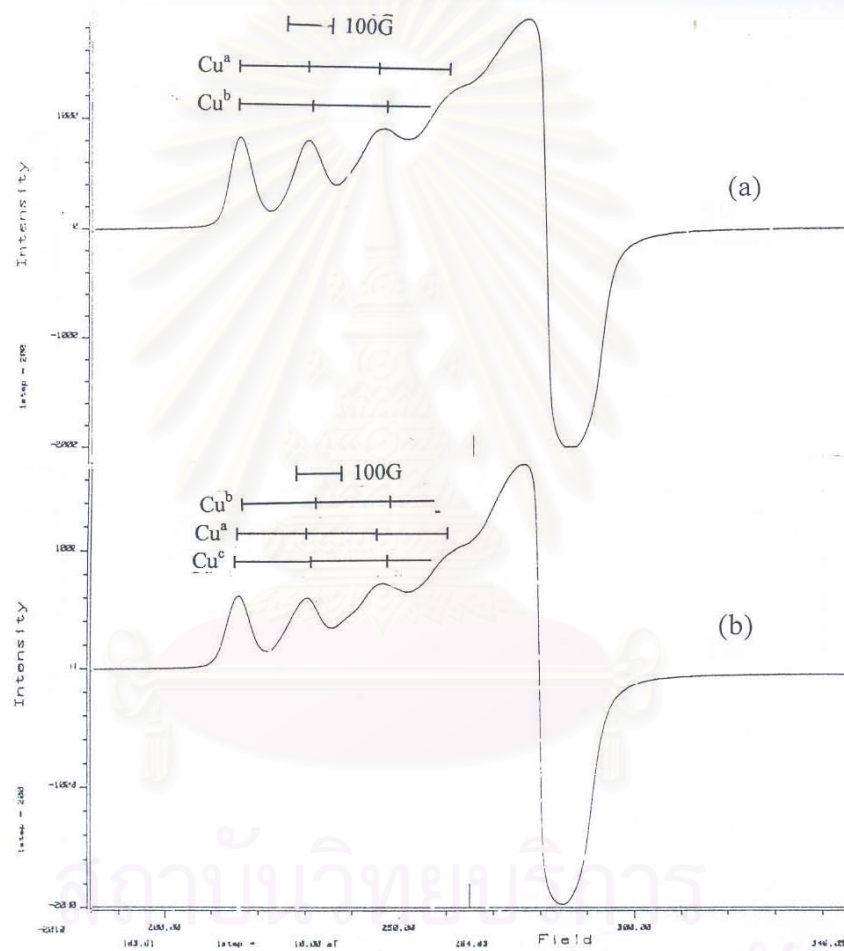


Figure 5.36 ESR spectra of high spin Cu^{2+} of Pd/Cu/HZSM-5 with and without hydrothermal treatment at 800°C 10 mol% H_2O
 (a) fresh 0.1%Pd/Cu/HZSM-5, (b) severely steamed 0.1%Pd/Cu/HZSM-5

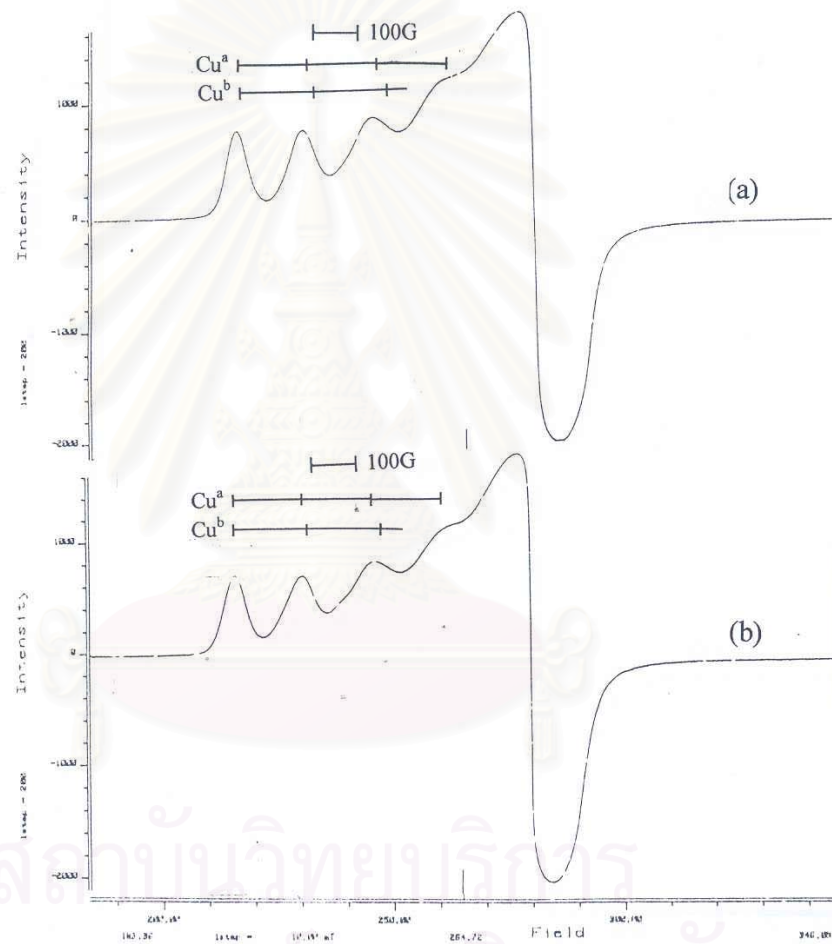


Figure 5.37 ESR spectra of high spin Cu^{2+} of Pd/Cu/HZSM-5 with and without hydrothermal treatment at 800°C 10 mol% H_2O
 (a) fresh 0.2%Pd/Cu/HZSM-5, (b) severely steamed 0.2%Pd/Cu/HZSM-5

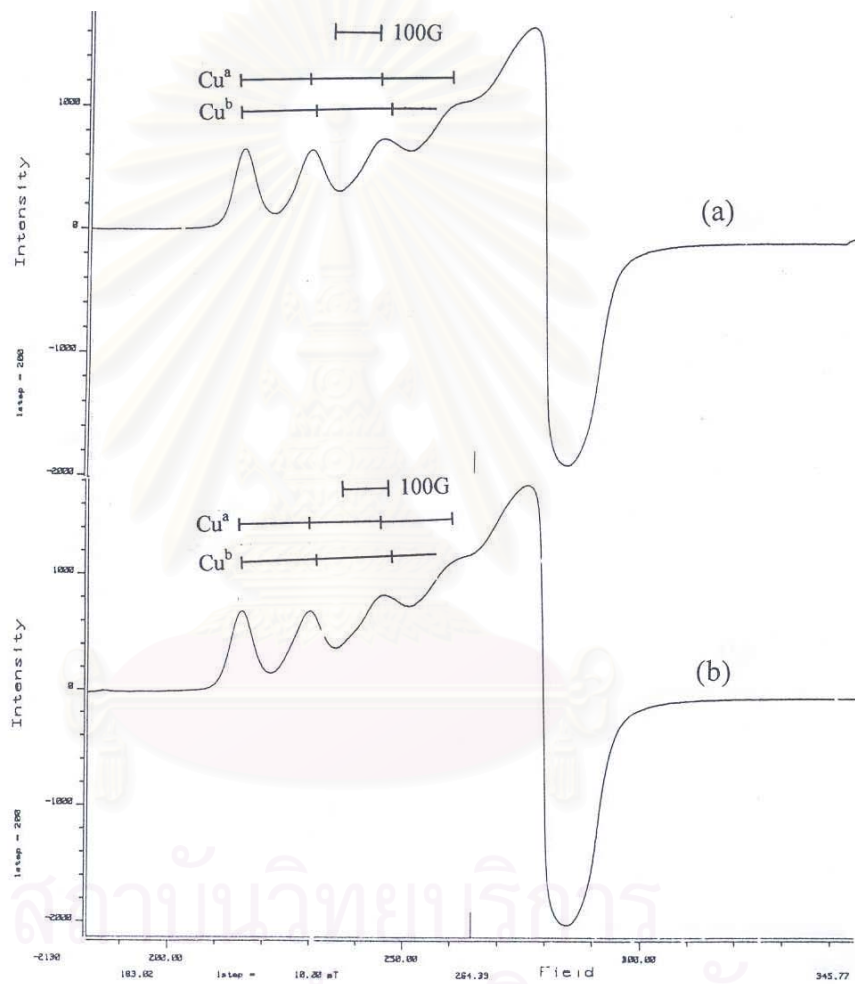


Figure 5.38 ESR spectra of high spin Cu^{2+} of Pd/Cu/HZSM-5 with and without hydrothermal treatment at 800°C 10 mol% H_2O
 (a) fresh 0.3%Pd/Cu/HZSM-5, (b) severely steamed 0.3%Pd/Cu/HZSM-5

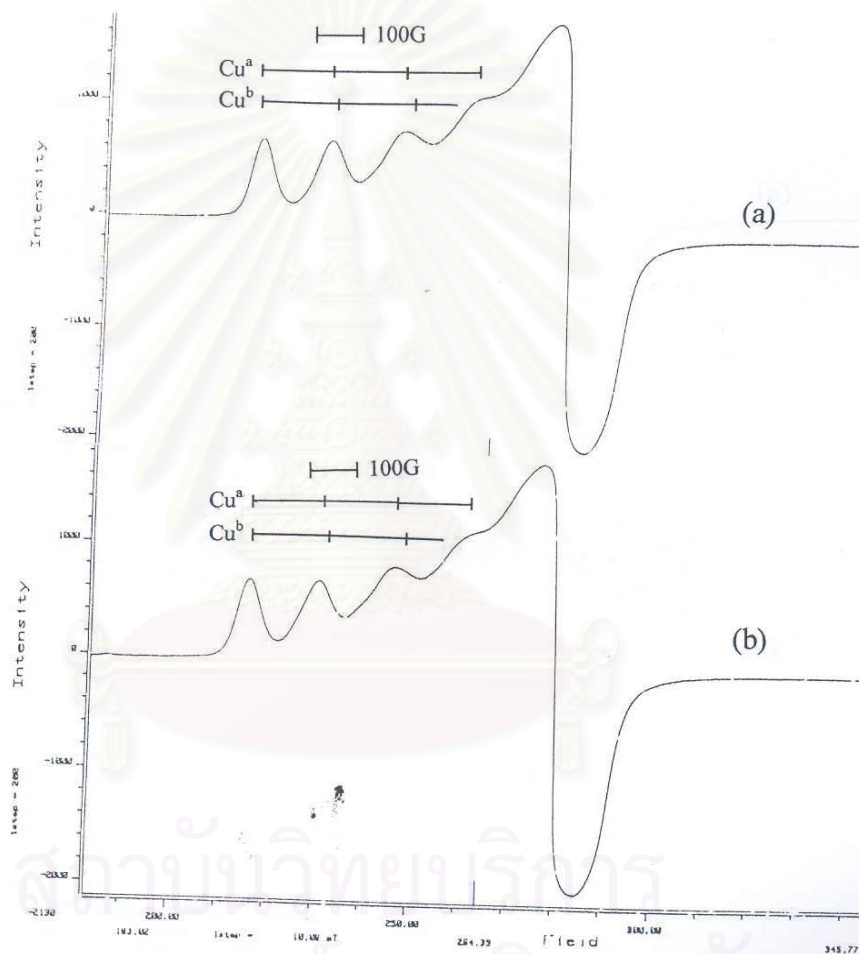


Figure 5.39 ESR spectra of high spin Cu^{2+} of Pd/Cu/HZSM-5 with and without hydrothermal treatment at 800°C 10 mol% H_2O
 (a) fresh 0.4%Pd/Cu/HZSM-5, (b) severely steamed 0.4%Pd/Cu/HZSM-5

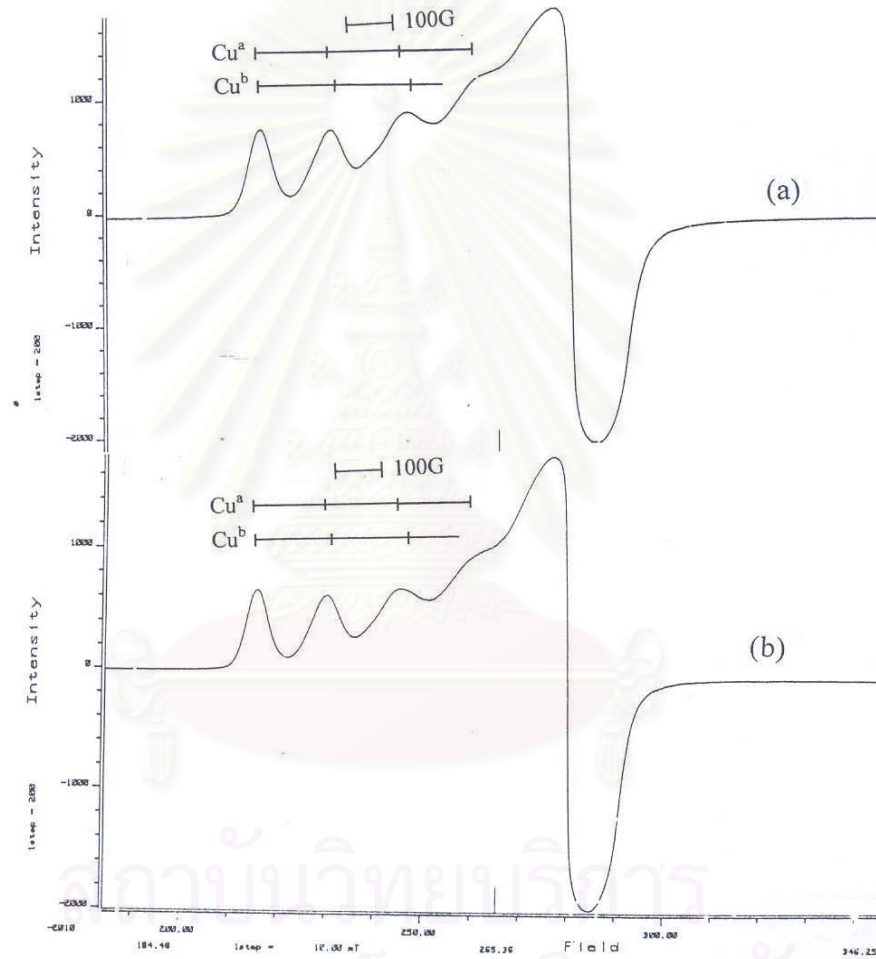


Figure 5.40 ESR spectra of high spin Cu^{2+} of Pd/Cu/HZSM-5 with and without hydrothermal treatment at 800°C 10 mol% H_2O
 (a) fresh 0.6%Pd/Cu/HZSM-5, (b) severely steamed 0.5%Pd/Cu/HZSM-5

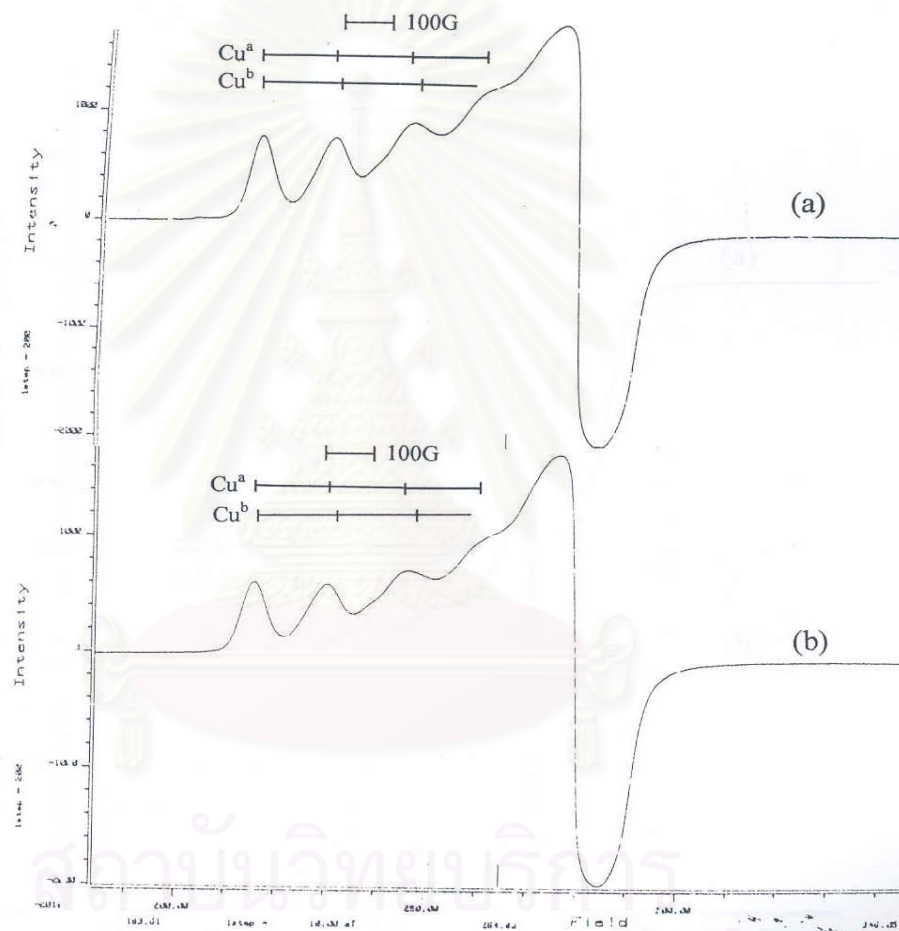


Figure 5.41 ESR spectra of high spin Cu^{2+} of Pd/Cu/HZSM-5 with and without hydrothermal treatment at 800°C 10 mol% H_2O
 (a) fresh 0.8%Pd/Cu/HZSM-5, (b) severely steamed 0.8%Pd/Cu/HZSM-5

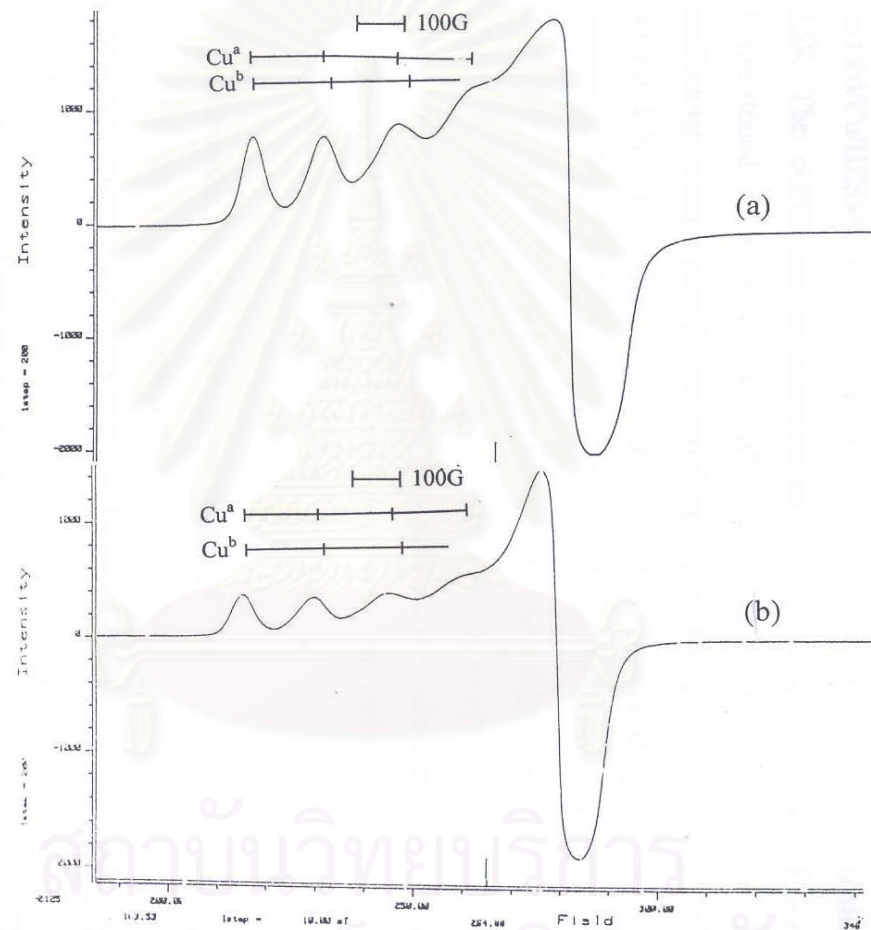


Figure 5.42 ESR spectra of high spin Cu^{2+} of Pd/Cu/HZSM-5 with and without hydrothermal treatment at 800°C 10 mol% H_2O
 (a) fresh 1.0%Pd/Cu/HZSM-5, (b) severely steamed 1.0%Pd/Cu/HZSM-5

5.2 Catalytic performance

NO conversion reactions were carried out on the catalysts both with and without pretreatment.

The effect of reaction temperature on NO conversion to N_2 for Cu/HZSM-5 and Pd/Cu/HZSM-5 with different amount of Pd loading are shown in figures 5.43 to 5.58. The conversion of n-octane to carbon oxides (CO and CO_2) is also demonstrated. It has been found that the conversion of NO markedly decreased at any reaction temperature after hydrothermal treatment. However, the margin difference in activity before and after pretreatment was alleviated with the presence of a certain amount of Pd (ca. 0.2-0.3 wt. % loading). When the amount of Pd was loaded at higher than 0.3 wt. %, such beneficial effect on the stabilization of Cu/HZSM-5 was surprisingly lost. As for the conversion of n-octane to carbon oxides, Cu/HZSM-5 also exhibited a substantial decrease in n-octane conversion upon pretreatment. The presence of Pd improved the n-octane conversion of the pretreated catalysts similar to NO conversion.

Nevertheless, while the improvement of NO conversion for the pretreated catalysts is limited by a certain amount of Pd presence, the n-octane conversion was almost continuously improved with the increasing amount of Pd. Pd/Cu/HZSM-5 catalysts with 0.8 wt. % and 1.0 wt. % loading of Pd, in particular, exerted more or less conversion of n-octane at the reaction temperatures higher than 400°C after hydrothermal treatment. This indicates that n-octane would not be effective for use in NO conversion on Pd/Cu/HZSM-5 with the high loading amount of Pd. Therefore, this should be one of the reasons for the limitation of NO conversion improvement on Pd/Cu/HZSM-5 after hydrothermal treatment by an optimum amount of Pd.

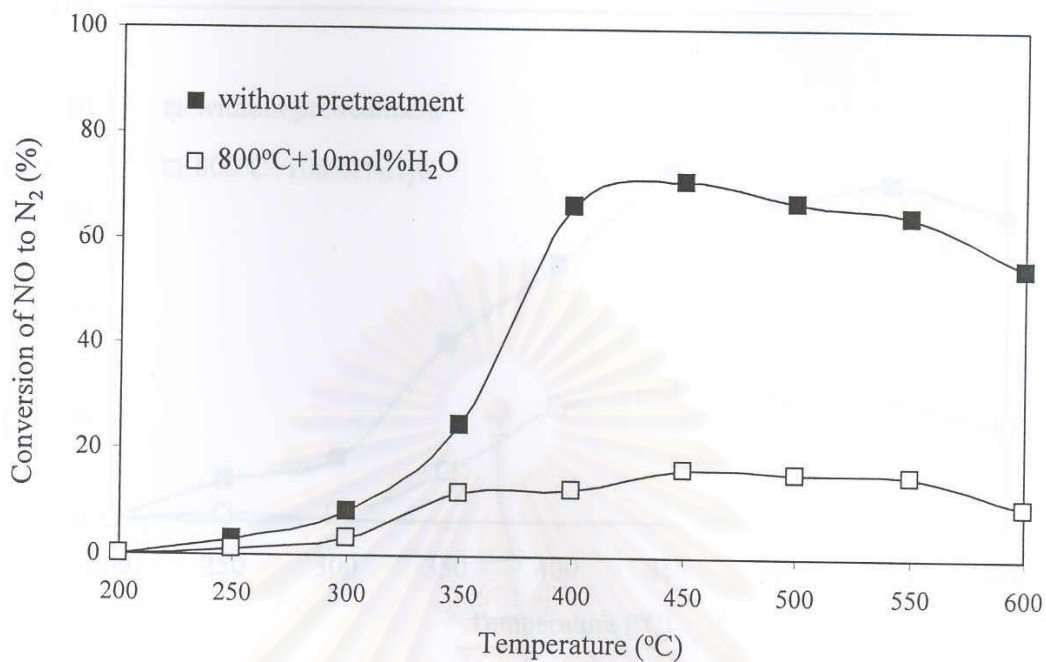


Figure 5.43 The effect of hydrothermal-treatment on the activity of NO conversion of Cu/HZSM-5. Feed gas: NO 1,000 ppm, n-octane 1,000 ppm, O₂ 2 mol%, H₂O 10 mol%, He balance, GHSV 30,000 h⁻¹.

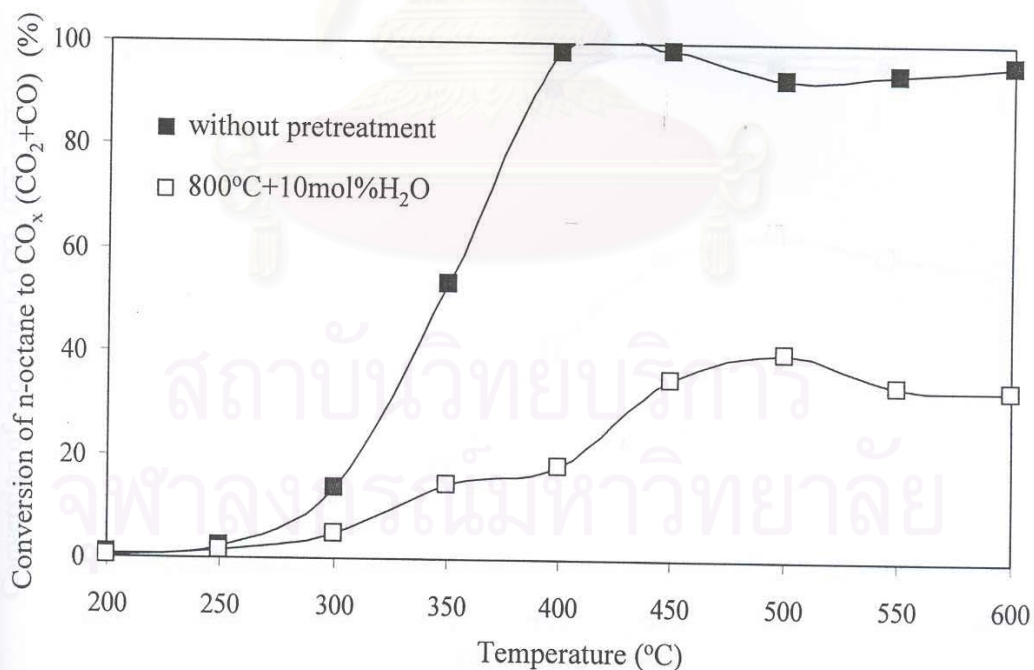


Figure 5.44 The effect of hydrothermal-treatment on the activity of n-octane conversion of Cu/HZSM-5. Feed gas: NO 1,000 ppm, n-octane 1,000 ppm, O₂ 2 mol%, H₂O 10 mol%, He balance, GHSV 30,000 h⁻¹.

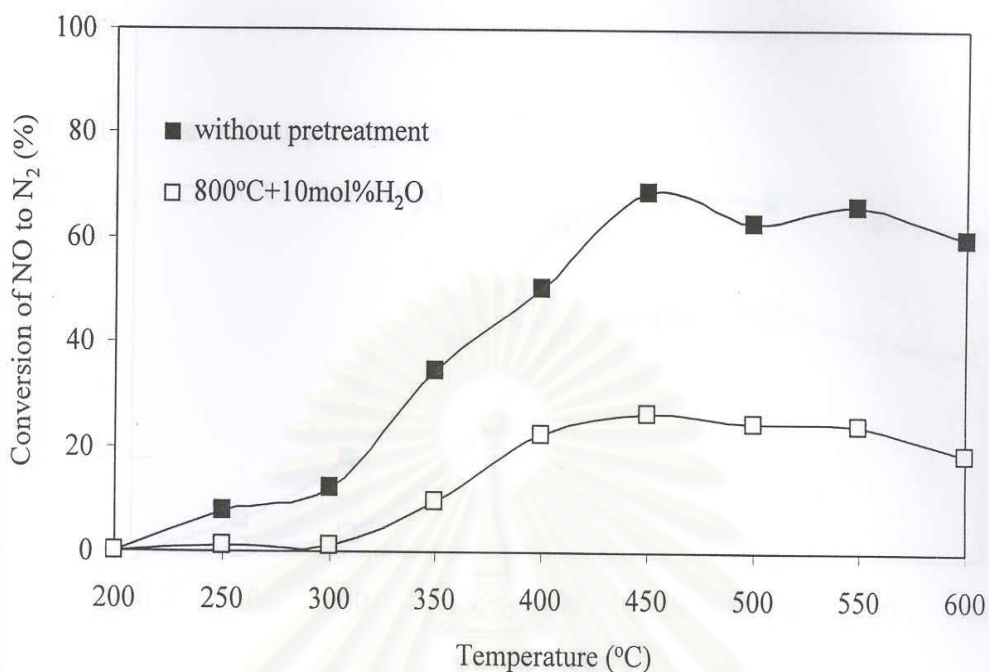


Figure 5.45 The effect of hydrothermal-treatment on the activity of NO conversion of 0.1%Pd/Cu/HZSM-5. Feed gas: NO 1,000 ppm, n-octane 1,000 ppm, O₂ 2 mol%, H₂O 10 mol%, He balance, GHSV 30,000 h⁻¹.

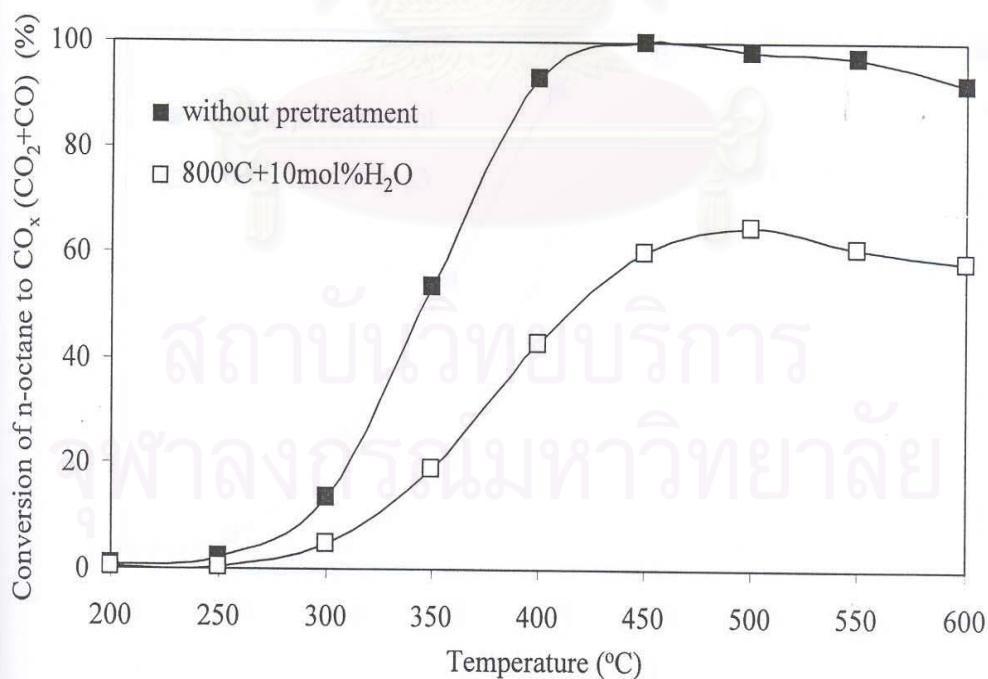


Figure 5.46 The effect of hydrothermal-treatment on the activity of n-octane conversion of 0.1%Pd/Cu/HZSM-5. Feed gas: NO 1,000 ppm, n-octane 1,000 ppm, O₂ 2mol%, H₂O 10mol%, He balance, GHSV 30,000 h⁻¹.

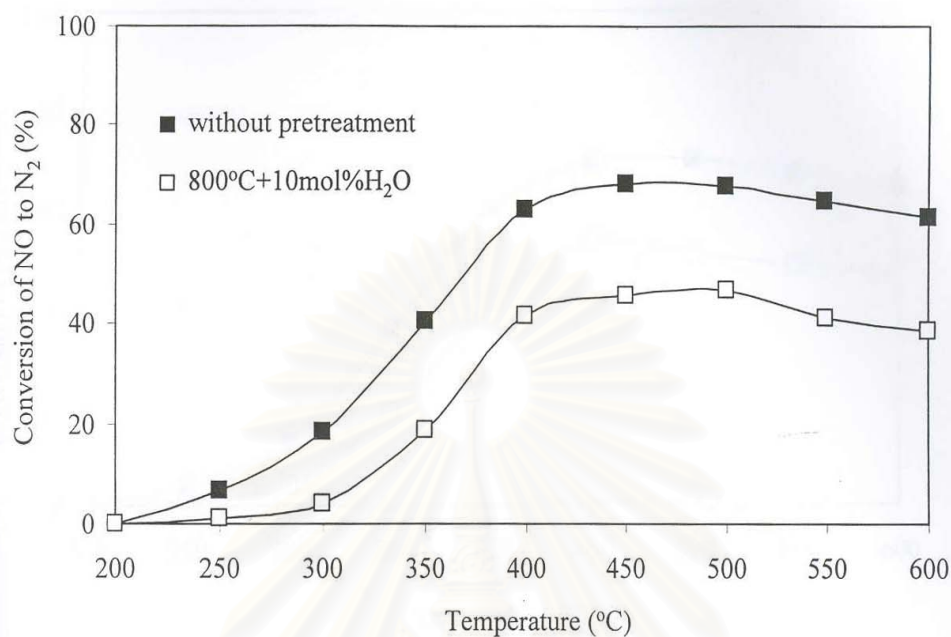


Figure 5.47 The effect of hydrothermal-treatment on the activity of NO-conversion of 0.2%Pd/Cu/HZSM-5. Feed gas: NO 1,000 ppm, n-octane 1,000 ppm, O₂ 2 mol%, H₂O 10 mol%, He balance, GHSV 30,000 h⁻¹.

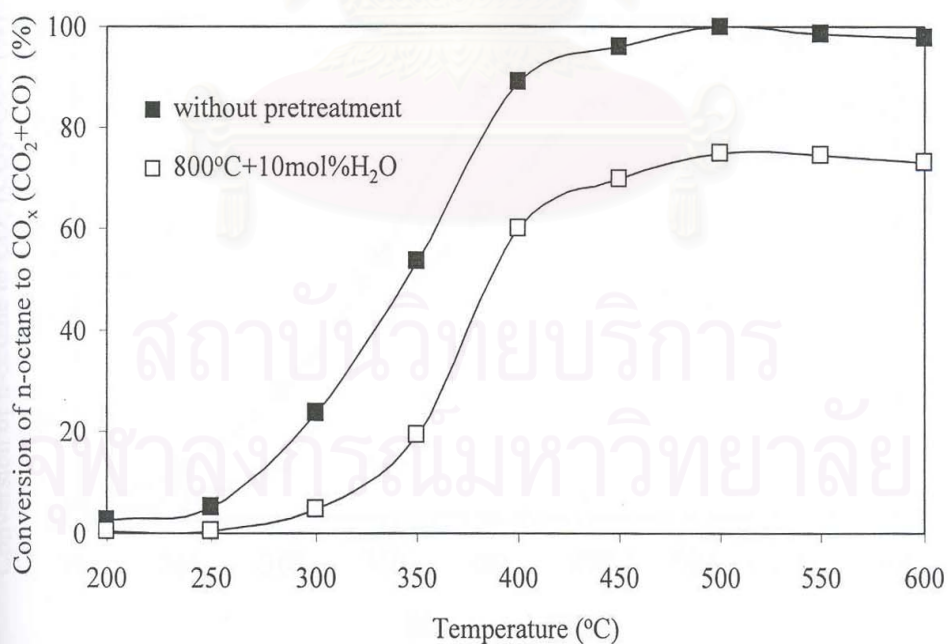


Figure 5.48 The effect of hydrothermal-treatment on the activity of n-octane conversion of 0.2%Pd/Cu/HZSM-5. Feed gas: NO 1,000 ppm, n-octane 1,000 ppm, O₂ 2 mol%, H₂O 10 mol%, He balance, GHSV 30,000 h⁻¹.

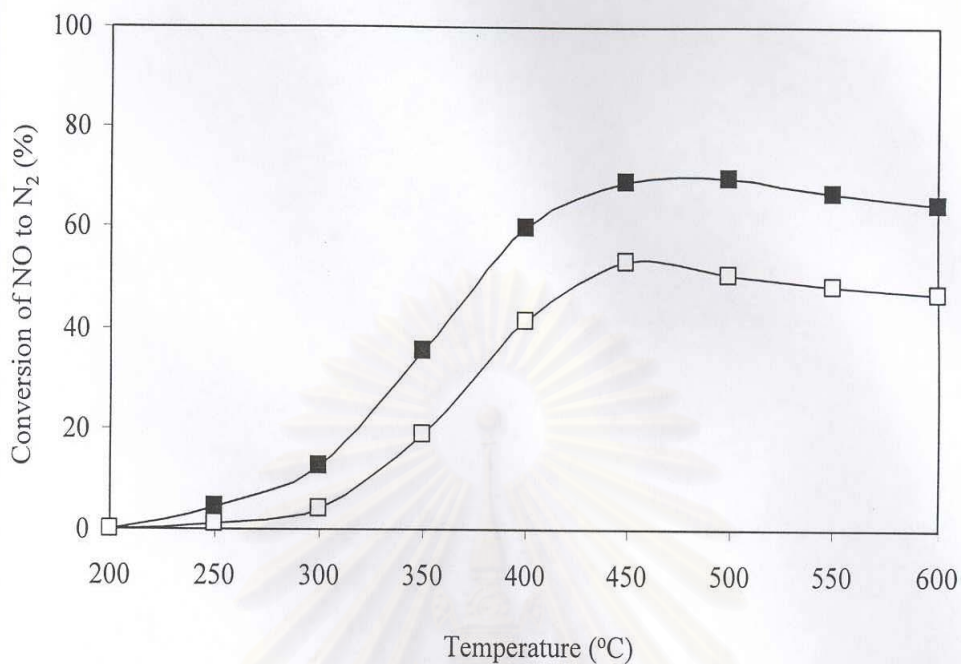


Figure 5.49 The effect of hydrothermal-treatment on the activity of NO conversion of 0.3%Pd/Cu/HZSM-5. Feed gas: NO 1,000 ppm, n-octane 1,000 ppm, O₂ 2 mol%, H₂O 10 mol%, He balance, GHSV 30,000 h⁻¹.

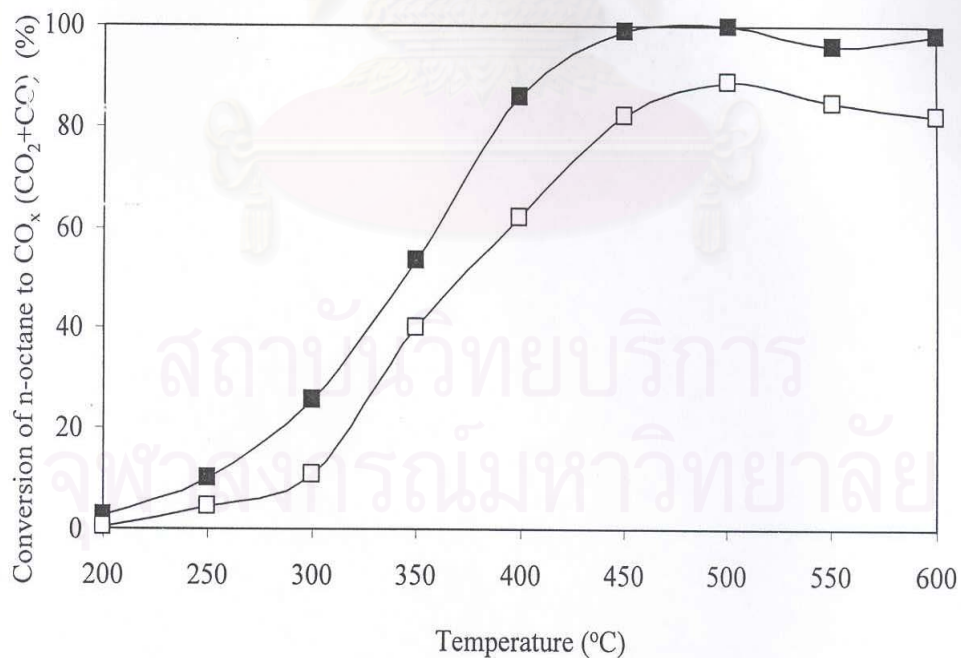


Figure 5.50 The effect of hydrothermal-treatment on the activity of n-octane conversion of 0.3%Pd/Cu/HZSM-5. Feed gas: NO 1,000 ppm, n-octane 1,000 ppm, O₂ 2 mol%, H₂O 10 mol%, He balance, GHSV 30,000 h⁻¹.

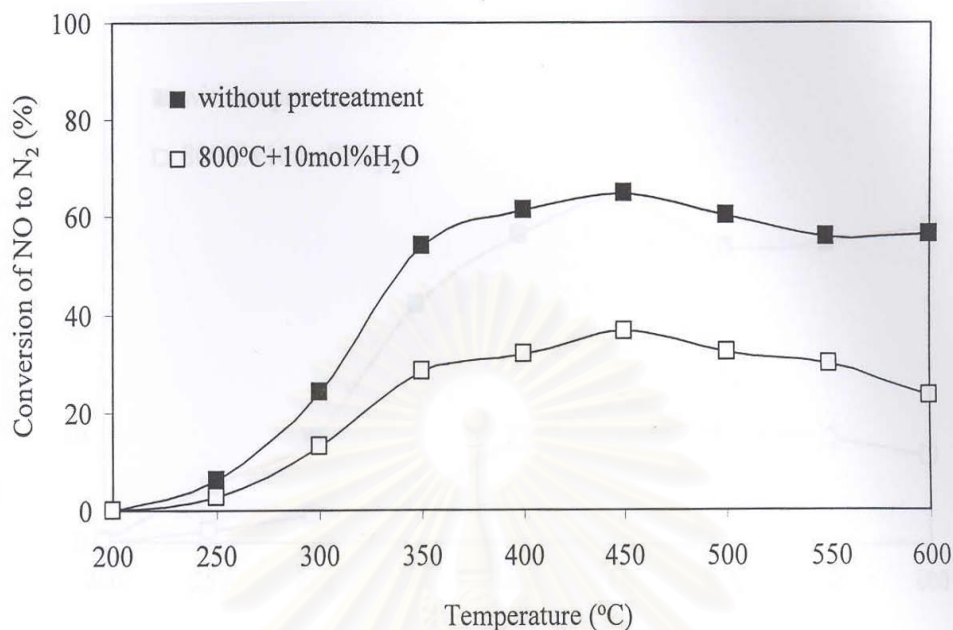


Figure 5.51 The effect of hydrothermal-treatment on the activity of NO conversion of 0.4%Pd/Cu/HZSM-5. Feed gas: NO 1,000 ppm, n-octane 1,000 ppm, O₂ 2 mol%, H₂O 10 mol%, He balance, GHSV 30,000 h⁻¹.

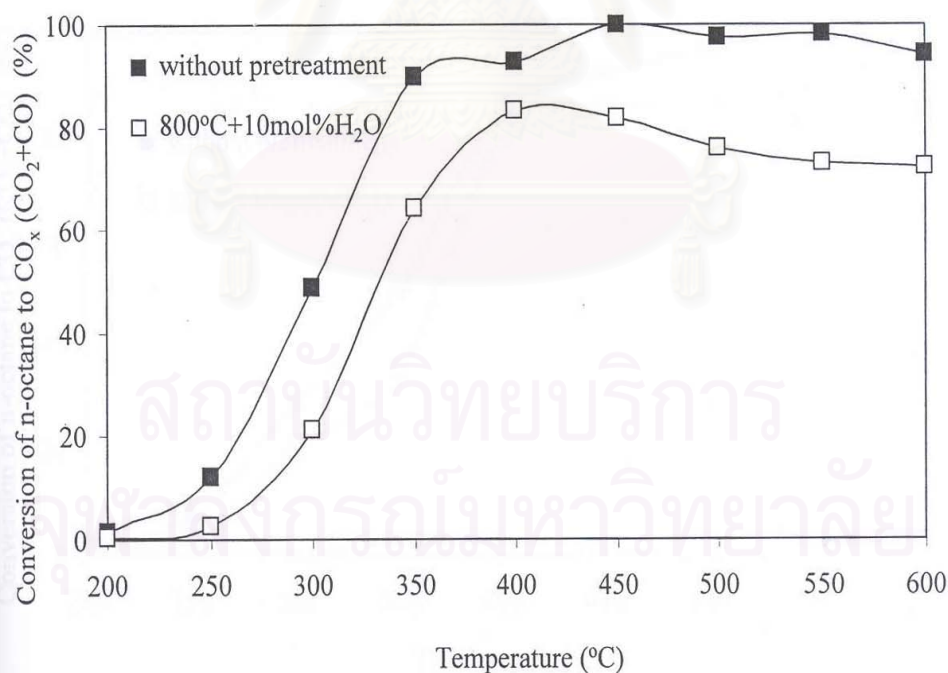


Figure 5.52 The effect of hydrothermal-treatment on the activity of n-octane conversion of 0.4%Pd/Cu/HZSM-5. Feed gas: NO 1,000 ppm, n-octane 1,000 ppm, O₂ 2 mol%, H₂O 10 mol%, He balance, GHSV 30,000 h⁻¹.

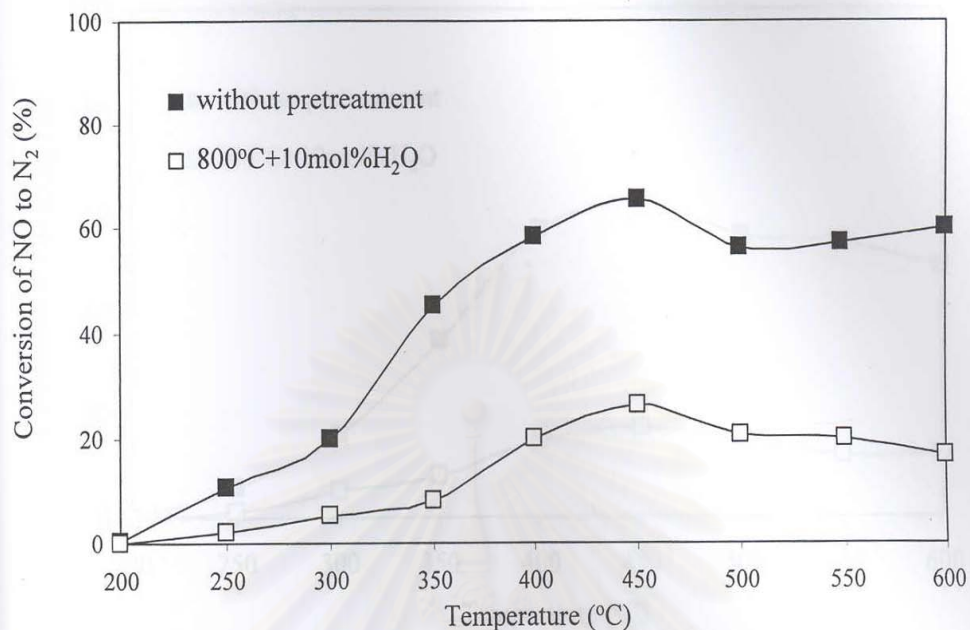


Figure 5.53 The effect of hydrothermal-treatment on the activity of NO conversion of 0.6%Pd/Cu/HZSM-5. Feed gas: NO 1,000 ppm, n-octane 1,000 ppm, O₂ 2 mol%, H₂O 10 mol%, He balance, GHSV 30,000 h⁻¹.

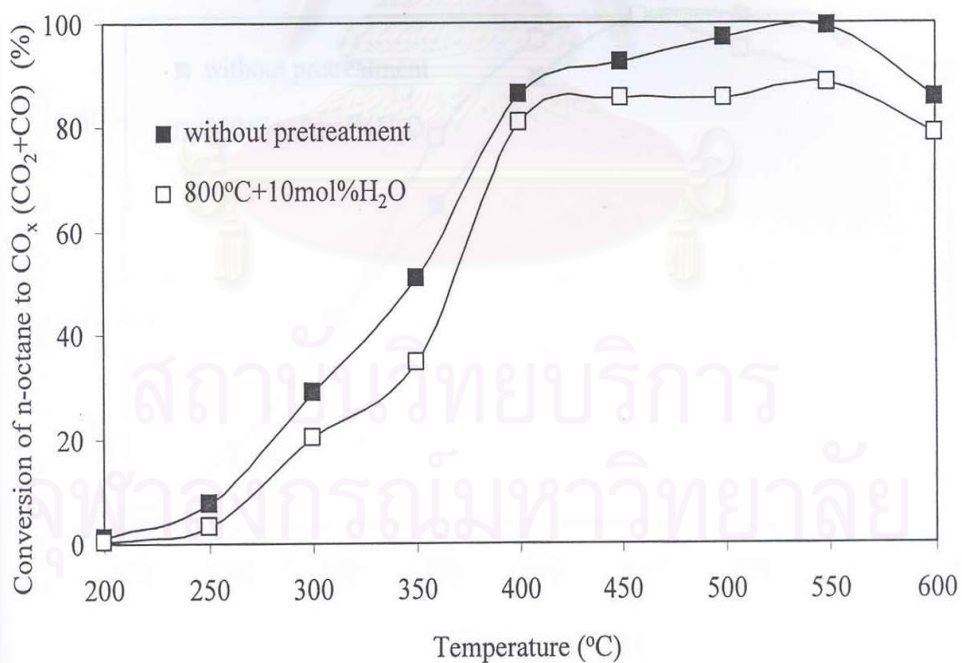


Figure 5.54 The effect of hydrothermal-treatment on the activity of n-octane conversion of 0.6%Pd/Cu/HZSM-5. Feed gas: NO 1,000 ppm, n-octane 1,000 ppm, O₂ 2 mol%, H₂O 10 mol%, He balance, GHSV 30,000 h⁻¹.

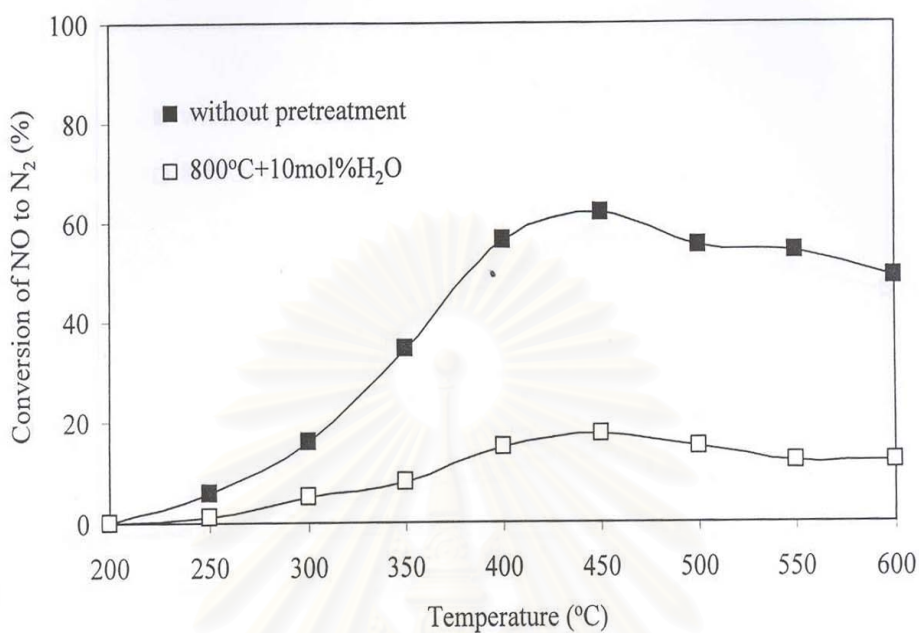


Figure 5.55 The effect of hydrothermal-treatment on the activity of NO conversion of 0.8%Pd/Cu/HZSM-5. Feed gas: NO 1,000 ppm, n-octane 1,000 ppm, O₂ 2 mol%, H₂O 10 mol%, He balance, GHSV 30,000 h⁻¹.

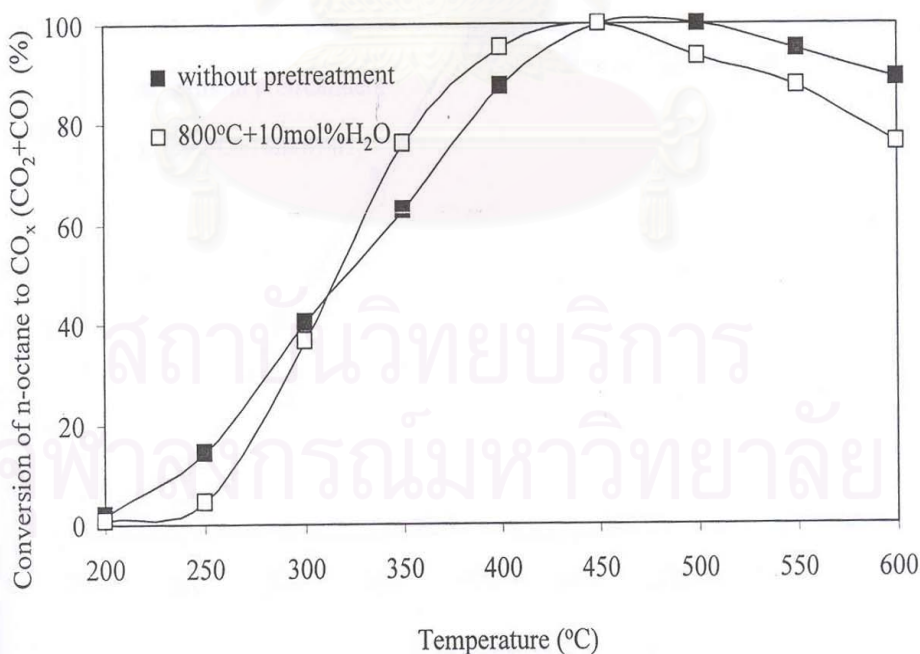


Figure 5.56 The effect of hydrothermal-treatment on the activity of n-octane conversion of 0.8%Pd/Cu/HZSM-5. Feed gas: NO 1,000 ppm, n-octane 1,000 ppm, O₂ 2 mol%, H₂O 10 mol%, He balance, GHSV 30,000 h⁻¹.

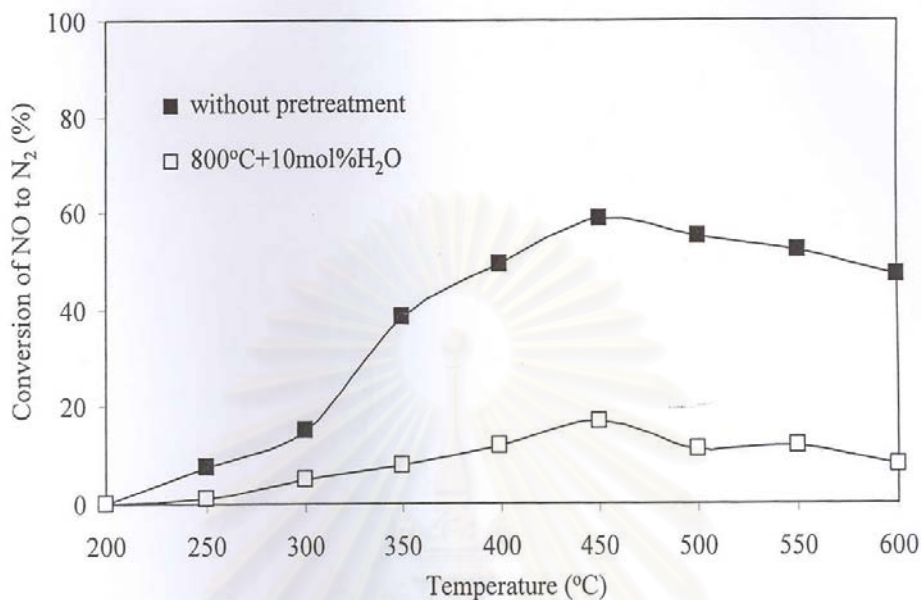


Figure 5.57 The effect of hydrothermal-treatment on the activity of NO conversion of 1.0%Pd/Cu/HZSM-5. Feed gas: NO 1,000 ppm, n-octane 1,000 ppm, O₂ 2 mol%, H₂O 10 mol%, He balance, GHSV 30,000 h⁻¹.

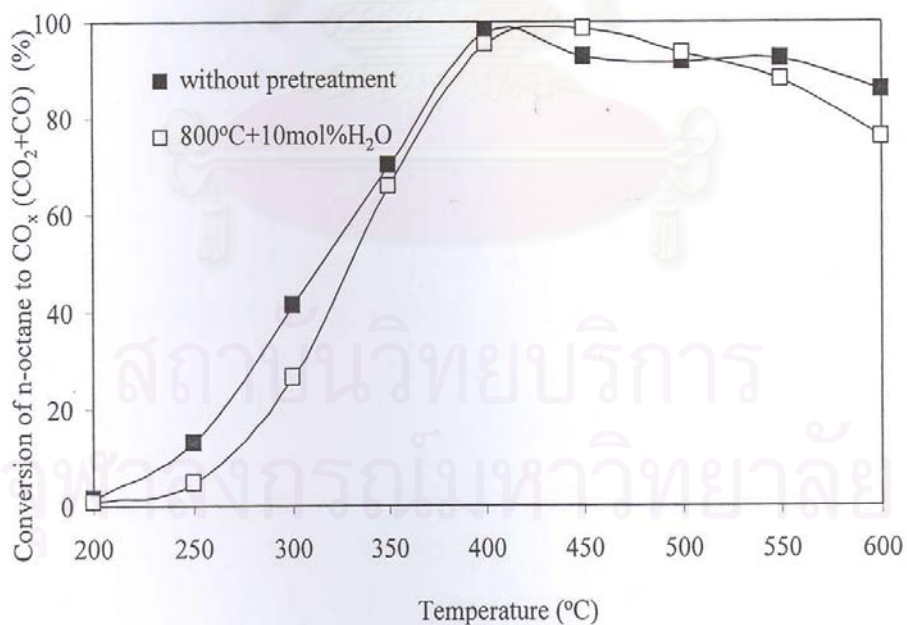


Figure 5.58 The effect of hydrothermal-treatment on the activity of n-octane conversion of 1.0%Pd/Cu/HZSM-5. Feed gas: NO 1,000 ppm, n-octane 1,000 ppm, O₂ 2 mol%, H₂O 10 mol%, He balance, GHSV 30,000 h⁻¹.

CHAPTER VI

CONCLUSIONS AND RECOMMENDATIONS

6.1 CONCLUSIONS

The conclusions of the present research are as following:

1. Pd group metals can maintain the active Cu^{2+} species for NO conversion against hydrothermal treatment at 800°C with 10 mol% H_2O . Pd plays an important role to preserve active Cu^{2+} species for NO conversion in lean burn condition.

2. From ^{27}Al MAS-NMR results, it suggests that Pd/Cu/HZSM-5 since 0.3 wt. % Pd loading stabilized the Al tetrahedral in zeolite lattice even after being pretreated at 800°C with 10 mol% H_2O for 12 h.

3. The deterioration of Cu/HZSM-5 catalysts with hydrothermal treatment is due to the dealumination of the zeolite framework, causing migration of Cu^{2+} ions to inactive sites and the aggregation of metal components on the external surface of zeolite. As for 1.0%Pd/Cu/HZSM-5, the deterioration of catalyst is due to the formation large metal particle sitting outside the zeolite framework.

4. In our study, 0.3%Pd/Cu/ZSM-5 catalyst is the most effective catalyst for NO removal under severe condition

5. Regarding Pd/Cu/HZSM-5 with Pd loading higher than 0.3 wt. % especially 0.8-1.0 wt. %, their catalytic performances did not show as high as that 0.3%Pd/Cu/HZSM-5. It has been suggested that there may be some changes in Pd and Cu on H-ZSM-5, such as alloying and/or palladium oxides formation, leading to some loss of Cu^{2+} active species for NO removal.

6.2 RECOMMENDATIONS

From this research, the recommendations for further study are as follows:

1. With the real exhaust gases, the presence of a large amount of oxygen and sulfur dioxide is inevitable; therefore, it is extremely interesting, from a practical point of view, to clarify their effect on the catalytic activity.
2. The actual location of Cu and Pd in ZSM-5 should be studied.
3. Study palladium species in ZSM-5 for selective catalytic reduction of NO with hydrocarbon before and after pretreatment. Should be determined.



สถาบันวิทยบริการ
จุฬาลงกรณ์มหาวิทยาลัย

REFERENCES

1. Shelef, M., "Selective catalytic reduction of NO_x with N-free reductants", *Chemical Review*, **95** (1995): 209-225.
2. Bosch, H., and Jansen, F., "The selective catalytic reduction (SCR) use for NO_x removal from stationary facilities", *Catalysis Today*, **2** (1988): 369-372.
3. Inui, T., Kojo, S., Shibata, M., Yoshida, T., and Iwamoto, S., "Study zeolite catalyst for the selective catalytic reduction (SCR) of NO_x using hydrocarbons as reductant in the presence of excess oxygen", *Studies in Surface Science and Catalysis*, **69** (1991): 355-360.
4. Kikuchi, E., Kojo, K., Tanaka, S., and Abe, M., "Promotive effect of additives to In/H-ZSM-5 catalyst for selective reduction of nitric oxide with methane in the presence of water vapor", *Chemistry Letters*, (1991): 1063-1065.
5. Iwamoto, M., Yashiro, H., Tanda, K., Mizuno, N., Mine, Y., and Kagawa, S., "Removal of nitrogen monoxide through a novel catalytic process. 1. Decomposition on excessively copper ion exchanged ZSM-5 zeolites", *Journal of physical chemistry*, **95** (1991): 3727-3730.
6. Grunert, W., Hayes, N.W., Joyner, R.W., Shpiro, E.S., Siddiqui, M.R.H., and Baeva N., "Structure, Chemistry, and Activity of Cu-ZSM-5 catalysts for selective reduction of NO_x in the presence of oxygen", *Journal of physical chemistry*, **98** (1994): 10832-1046.
7. Yan, J.Y., Lei, G.D., Sachtler, W.H.M., and Kung, H.H., "Deactivation of Cu/ZSM-5 catalysts for lean NO_x reduction: Characterization of changes of Cu state and zeolite support", *Journal of Catalysis*, **161** (1996): 43-54.
8. Inui, T., Iwamoto, S., Kon, S., Sakimon, T., and Kagawa, K., "Evidently advantageous features of metallosilicates as the catalyst for elimination of NO in the exhaust gases containing a large excess of O₂ and H₂O", *Catalysis Today*, **38** (1997): 169-174.
9. Burch, R., and Scire, S., "Selective catalytic reduction of nitric oxide with ethane and methane on some metal exchanged ZSM-5 zeolites", *Applied Catalysis B: Environmental*, **3** (1994): 295-318.

10. Burch, R., and Ramli, A., "A comparative investigation of the reduction of NO by CH₄ on Pt, Pd, and Rh catalysts", *Applied Catalysis B: Environmental*, **15** (1998): 49-62.
11. Hirabayashi, H., Yahiro, H., Mizuno, N., and Iwamoto, M., "Study platinum group metal catalyst for NO removal in the presence of water vapor", *Chemistry Letters*, (1992): 2235-2240.
12. Amiridis, M.D., Zhang, T., and Farrauto, R.J., "Selective catalytic reduction of nitric oxide by hydrocarbon", *Applied Catalysis B: Environmental*, **10** (1996): 203-227.
13. Iwamoto, M., Yashiro, H., Tanda, K., Mizuno, N., Mine, Y., Kagawa S., "Contribution of acidic properties of metallosilicate catalysts to NO decomposition reaction", *Studies in Surface Science and Catalysis*, **84** (1994): 1523-1530.
14. Iwamoto, M., Yashiro, H., Tanda, K., Mizuno, N., Mine, Y., Furukawa, H., and Kagawa, S., "Removal of nitrogen monoxide through a novel catalytic process. 2. Infrared study on surface reaction of nitrogen monoxide adsorbed on copper ion-exchanged ZSM-5 zeolites", *Journal of physical chemistry*, **96** (1992): 9360-9366.
15. Iwamoto, M., Misono, M., *Proceeding of Meetings of Catalytic Technology for Removal of Nitrogen Monoxide*, Univ. of Tokyo, Tokyo, Japan, (1990): 17-25.
16. Held, W., Koenig, A., Richter, T., and Puppe, L., "Catalytic NO_x reduction in net oxidizing exhaust gas", *SAE Paper 900496*, (1990): 13-18.
17. Shelef, M., "On the mechanism of nitric oxide decomposition over Cu-ZSM-5", *Catalysis Letters*, **15** (1992): 305-310.
18. Kintaichi, Y., Hamada, H., Tabata, M., Sasaki, M., and Ito, T., "Selective reduction of nitrogen oxides with hydrocarbons over solid acid catalysts in oxygen-rich atmospheres", *Catalysis Letters*, **6** (1990): 239-244.
19. Hamada, H., Kintaichi, Y., Sasaki, M., Ito, T., and Tabata, M., "Highly selective reduction of nitrogen oxides with hydrocarbons over H-form zeolite catalysts in oxygen-rich atmospheres", *Applied Catalysis B: Environmental*, **64** (1990): L1-L4.

20. Campbell, S.M., Bibby, D.M., Coddington, J.M., Howe, R.F., and Meinhold, R. H., "Dealumination of HZSM-5 zeolites: Calcination and hydrothermal treatment", *Journal of Catalysis*, **161** (1996): 338-349.
21. Sato, S., Yu, Y., Yahiro, H., Mizuno, N., and Iwamoto, M., "Cu-ZSM-5 zeolite as highly active catalyst for removal of nitrogen monoxide from emission of diesel engines", *Applied Catalysis*, **70** (1991): L1-L5.
22. Sato, S., Hirabayashi, H., Yahiro, H., Mizuno, N., and Iwamoto, M., "Iron ion-exchanged zeolite: the most active catalyst at 473 K for selective reduction of nitrogen monoxide by ethene in oxidizing atmosphere", *Catalysis Letters*, **12** (1992): 193-200.
23. Iwamoto, M., "High potential of novel zeolitic materials as catalysts for solving energy and environmental problem", *Studies in Surface Science and Catalysis*, **84** (1994): 1395-1401.
24. Li, Y., Slager, T.L., Armor, J.N., "Catalytic combustion of methane over palladium exchanged zeolite", *Journal of Catalysis*, **150** (1994): 338-345.
25. Chajar, Z., Primet, M., Praliaud, H., Chevrier, M., Gauthier, C., and Mathis, F., "Influence of the preparation method on the selective reduction of nitric oxide over Cu-ZSM-5. Nature of the active sites", *Applied Catalysis B: Environmental*, **4** (1994): 199-211.
26. Campa, M. C., Indovina, V., Minelli, G., Moretti, G., Pettiti, I., Porta, P., and Riccio, A., "The catalytic activity of Cu-ZSM-5 and Cu-Y zeolites in NO decomposition: dependence on copper concentration", *Catalysis Letters*, **23** (1994): 141-149.
27. Iwamoto, M., Mizuno, N., and Yahiro, H., "Selective catalytic reduction of NO by hydrocarbon in oxidizing atmosphere", *Proceeding of the 10th International Congress on Catalysis*, (1992): 1286-1298.
28. Iwamoto, M., Yahiro, H., Torikai, Y., Yoshioka, T., and Mizuno, N., "Novel preparation method of highly copper ion-exchanged ZSM-5 zeolites and their catalytic activities for NO decomposition", *Chemistry Letters*, (1990): 1967-1970.

29. Martinez, A., Gomez, S.A., and Fuentes, G.A., "Deactivation of Cu-ZSM-5 during selective catalytic reduction of NO by propane under wet condition", *Catalyst Deactivation*, (1997): 225-230.
30. Kharas, K.C.C., Robota, H.J., and Lui, D.J., "Deactivation in Cu-ZSM-5 lean-burn catalysts", *Applied Catalysis B: Environmental*, **2** (1993): 225-237.
31. Abreu, C.T., Ribeiro, M.F., Henriques, C., Ribeiro, F.R., and Delahay, G., "Deactivation of CuMFI catalysts under NO selective catalytic reduction propane: influence of zeolite form, Si/Al ratio and copper content", *Catalysis Letters*, **43** (1997): 31-36.
32. Kucherov, A.V., Hubbard, C.P., and Shelef, M., "Rearrangment of cationic sites in CuH-ZSM-5 and reactivity loss upon high-temperature calcination and steam aging", *Journal of Catalysis*, **157** (1995): 603-610.
33. Budi, P., Hyde, E.C., and Howe R.F., "Steam deactivation of transition metal MFI zeolite catalysts for NO_x reduction", *Studies in Surface Science and Catalysis*, **105** (1997): 1549-1556.
34. Tanabe, T., Iijima, T., Kaiwai, A., Mizuno, J., Yokota, K., and Isogai, A., "ESR study of the deactivation of Cu-ZSM-5 in a net oxidizing atmosphere", *Applied Catalysis B: Environmental*, **6** (1995): 145-153.
35. Matsumoto, S., Yokota, K., Doi, H., Kimura, M., Sekizawa, K., and Kasahara, S., "Research on new DeNo_x catalysts for automotive engines", *Catalysis Today*, **22** (1994): 127-133,
36. Iwamoto, M., Wang, J., Sperati, K.M., Sajaki, T., and Misono, M., "Migration of copper ions in Cu-MFI without destruction of zeolite lattice or dealumination upon hydrothermal treatment at 923K", *Chemistry Letters*, (1997): 1281-1282.
37. Pentunchi, J.O., and Hall, W.K., "Effect of selective reduction of nitric oxide on zeolite structure", *Applied Catalysis B: Environmental*, **4** (1994): 239-257.
38. Correa, C.M., Villa, A.L., and Zapata, M., "Decomposition of nitrous oxide in excess oxygen over Co- and Cu- exchanged MFI zeolites", *Catalysis Letters*, **38** (1996): 27-32.
39. Armor, J.N., Farris, T.S., "The unusual hydrothermal stability of Co-ZSM-5", *Applied Catalysis B: Environmental*, **4** (1994): L11-L17.

40. Sano, T., Suzuki, K., Shoji, H., Ikai, S., Okabe, K., Murakami, T., Shin, S., Hagiwara, H., and Takaya, H., "Dealumination of ZSM-5 zeolites with water", *Chemistry Letters*, (1987): 1421-1424.
41. Li, Y., Battavio, P.J., and Armor, J.N., "Effect of water vapor on the selective reduction of NO by methane over cobalt-exchanged ZSM-5", *Journal of Catalysis*, **142** (1993): 561-571.
42. Hirabayashi, H., Yahiro, H., Mizuno, N., and Iwamoto, M., "High catalytic activity of platinum-ZSM-5 zeolite below 500 K in water vapor for reduction of nitrogen monoxide", *Chemistry Letters*, (1992): 2235-2236.
43. Rokosz, M.J., Kucherov, A.V., Jen, H.W., Shelef, M., "Spectroscopic studies of stability of zeolitic deNO_x catalysts", *Catalysis Today*, **35** (1997): 65-73.
44. Kucherov, A.V., Hubbard, C.U., Kucherous, T.N.K., and Shelef, M., "Modification and stabilization of Cu-ZSM-5 by introduction of a second cation", *Studies in Surface Science and Catalysis*, **105** (1997): 1469-1476.
45. Teraoka, Y., Ogawa, H., Furukawa, H., and Kagawa, S., "Influence of cocations on catalytic activity of copper ion-exchanged ZSM-5 zeolite for reduction of nitric oxide with ethene in the presence of oxygen", *Catalysis Letters*, **12** (1992): 361-366.
46. Budi, P., Hyde, E.C., and Howe, R.F., "Stabilization of CuZSM-5 NO_x reduction catalysts with lanthanum", *Catalysis Letters*, **41** (1996): 47-53.
47. Dangsawai, T., *Effect of severe condition on activity of copper ion-exchanged MFI and cobalt-silicate in nitric oxide removal*. Doctor of Engineering thesis, Department of Chemical Engineering, Faculty of Engineering, Chulalongkorn University, 1999.
48. Dangsawai, T., Praserttham P., Kim, J.B., Inui, T., "Pd-modification of Cu-H-ZSM-5 catalyst for NO removal under hydrothermal pretreatment conditions", *Advances in Environmental Research*, **3** (2000): 450-458.
49. Misono, M., and Kondo, K., "Catalytic removal of nitrogen monoxide over rare earth ion-exchanged zeolites in the presence of propene and oxygen", *Chemistry Letters*, (1991): 1001-1002.
50. Misono, M., "Catalytic reduction of nitrogen oxides by bifunctional catalysts", *CATTECH*, **3**, **2** (1998): 183-196.

51. Hamada, H., Kintaichi, Y., Sasaki, M., Ito, T., and Tabata, M., "Selective reduction of nitrogen monoxide with propane over alumina and HZSM-5 zeolite", *Applied Catalysis*, **70** (1991): L15-L20.
52. Burch, R., and Millington, P.J., "Role of propane in the selective reduction of nitrogen monoxide in copper-exchanged zeolites", *Applied Catalysis B: Environmental*, **2** (1993): 101-116.
53. Breck, D.W., *Zeolite Molecular Sieves*. New York: Robert E. Krieger Publishing Co., 1984.
54. Satterfield, C.N., *Heterogeneous Catalysis in Practical*. New York: McGraw-Hill Book Co., 1980.
55. Flanigen, E.M., Zeolite and Molecular sieves: an historical perspective. In H. V. Bekkum (ed.), *Studies in Surface Science and Catalysis*, **58**: Introduction to Zeolite Science and Practice, 13-34. Netherlands: Elsevier, 1991.
56. Gate, B.C., *Catalytic Chemistry*, Singapore: John Wiley & Sons, 1992.
57. Kokotailo, G.T., Zeolite crystallograph. In F. R. Ribeiro et al. (eds.), *Zeolites: Science and Technology*, 83-108. Netherlands: Martinus Nijhoff Publishers, 1984.
58. Cilambelli, P., Corbo, P., Gambino, M., Minelli, G., Moretti, G., and Porta, P., "Lean NO_x reduction CuZSM-5 catalysts: evaluation of performance at the spark ignition engine exhaust", *Catalysis Today*, **26** (1993): 33-39.
59. Descorme, C., Gelin, P., Lecuyer, C., and Primet, M., "Palladium-exchanged MFI-type zeolites in the catalytic reduction of nitrogen monoxide by methane. Influence of the Si/Al ratio on the activity and the hydrothermal stability", *Applied Catalysis B: Environmental*, **13** (1997): 185-195.
60. Tabata, T., Kokitsu, M., Okada, O., Nakayama, T., Yasumatsu, T., and Sakane, H., "Deterioration mechanism of Cu/ZSM-5 as a catalyst of selective reduction of NO_x by hydrocarbons from the exhaust of stationary natural gas-fuelled engine", *Studies in Surface Science and Catalysis*, **88** (1994): 409-416.
61. Ohtsuka, H., Tanabe, T., "Effect of water vapor on the deactivation of Pd-zeolite catalysts for selective catalytic reduction of nitrogen monoxide by methane", *Applied Catalysis B: Environmental*, **21** (1999): 133-139.

62. Kucherov, A.V., Shigapov, A.N., Ivanov, A.A., and Shelef, M., “Stability of the square-planar Cu^{2+} sites in ZSM-5: Effect of preparation, Heat treatment, and Modification”, *Journal of Catalysis*, **186** (1999): 334-344.
63. Ogura, M., Hayashi, M., Kage, S., Matsukata, and M., Kikuchi, E., “Determination of active palladium species in ZSM-5 zeolite for selective reduction of nitric oxide with methane”, *Applied Catalysis B: Environmental*, **23** (1999): 247-257.
64. Gmehling, J., Onken, U., *Vapor-Liquid Equilibrium Data Collection. Chemistry Data Series*. Frankfurt: DECHEMA, 1977.
65. Hirata, M., Ohe, S., Nagama, K., *Computer Aided Data Book of Vapor-Liquid Equilibria*. Amsterdam: Elsevier, 1975.



สถาบันวิทยบริการ
จุฬาลงกรณ์มหาวิทยาลัย



APPENDICES

สถาบันวิทยบริการ
จุฬาลงกรณ์มหาวิทยาลัย

APPENDIX A

SAMPLE OF CALCULATIONS

A-1 Calculation of Metal Ion-exchanged ZSM-5

The example of calculation shown below is for Pd/Cu/HZSM-5 catalyst. The content of palladium was varied in the range 0.1-1 wt.% Pd.

For Pd/H-ZSM-5 catalysts: NH₄-ZSM-5 catalysts was ion exchanged in an aqueous solution of [Pd (NH₄)₄]Cl₂.H₂O 99.99%, it is molecular weight 263.44, and the molecular weight of palladium is 106.4.

Example: Determine the amount of Pd into catalyst = 0.3 wt.%

$$\begin{aligned} \text{The catalyst used} &= x \text{ g} \\ \text{so that } \text{Pd}/(x+\text{Pd}) &= 0.3/100 \\ 100-\text{Pd} &= 0.3 \times (x+\text{Pd}) \\ (100-0.3) \times \text{Pd} &= 0.3 \times x \\ \text{thus } \text{Pd} &= 0.3 \times x / (100-0.3) \text{ g} \\ \text{weight of } [\text{Pd} (\text{NH}_4)_4] \text{Cl}_2 \cdot \text{H}_2\text{O} &= [0.3 \times x / (100-0.3)] \times [(263.44/106.4) \\ &\quad \times (99.99/100)] \end{aligned}$$

For Cu/H-ZSM-5 catalysts: NH₄-ZSM-5 catalysts was ion-exchanged in an aqueous solution of Cu (CH₃COO)₂.H₂O 95.5%, it molecular weight is 199.546, and the molecular weight of copper is 63.546.

Example: Determine the amount of Cu into catalyst = 2.0 wt.%

$$\begin{aligned} \text{The catalyst used} &= x \text{ g} \\ \text{so that } \text{Cu}/(x+\text{Cu}) &= 2.0/100 \\ 100-\text{Cu} &= 2.0 \times (x+\text{Cu}) \\ (100-2.0) \times \text{Cu} &= 2.0 \times x \\ \text{thus } \text{Cu} &= 2.0 \times x / (100-2.0) \text{ g} \\ \text{weight of } \text{Cu} (\text{CH}_3\text{COO})_2 \cdot \text{H}_2\text{O} &= [2.0 \times x / (100-2.0)] \times [(199.546/63.546) \\ &\quad \times (99.99/100)] \end{aligned}$$

A-2 Calculation of reaction flow rate.

This study uses flow rate of stream gas by using the formula of GHSV (gas hourly space velocity) as follows:

$$\begin{aligned} \text{The catalyst used} &= 0.25 \text{ g} \\ \text{quartz reactor diameter} &= 0.6 \text{ cm} \end{aligned}$$

$$\text{GHSV} = \frac{\text{Volumetric flow rate}}{\text{Volume of Catalyst}}$$

$$\text{Volumetric flow rate} = 30,000 \times \text{Volume of catalyst.}$$

$$\text{at STP: Volumetric flow rate} = \frac{\text{Volumetric flow rate} \times (273.15+t)}{273.15}$$

where t = room temperature, °C

สถาบันวิทยบริการ
จุฬาลงกรณ์มหาวิทยาลัย

APPENDIX B

VAPOR PRESSURE OF n-Octane

Set the partial vapor pressure of the reactants to the requirement by adjusting the temperature of saturator according to the antoine equation [64,65];

$$\log P = A - \frac{B}{(T+C)}$$

When P = vapor pressure of reactant, mbar

T = temperature, °C

A, B and C is constants

Range of temperature that applied ability -20 – 126 °C

The values of constants are in table B-1

Table B-1 The values of constants.

Reactant	A	B	C
Water	8.19625	1730.630	233.426
n-Octane	7.05636	1358.800	209.855

สถาบันวิทยบริการ
จุฬาลงกรณ์มหาวิทยาลัย

VITA

Mr. Jakrit Rungsimanop was born in KhonKaen, Thailand, on June, 1975. He received his Bachelor degree of Engineering from the Department of Chemical Engineering, KhonKaen University in 1998. He continued his Master's Study at Chulalongkorn University in June, 1998.



สถาบันวิทยบริการ
จุฬาลงกรณ์มหาวิทยาลัย